INTELLIGENT ADAPTIVE CONTROL ALGORITHMS FOR DISTRIBUTED GENERATION SYSTEMS

BY

NEZAR MOHAMMED ABDULRAB AL-YAZIDI

A Dissertation Presented to the

DEANSHIP OF GRADUATE STUDIES

KING FAHD UNIVERSITY OF PETROLEUM & MINERALS

DHAHRAN, SAUDI ARABIA

In Partial Fulfillment of the

Requirements for the Degree of

DOCTOR OF PHILOSOPHY

In

SYSTEMS AND CONTROL ENGINEERING

NOVEMBER 2016

KING FAHD UNIVERSITY OF PETROLEUM & MINERALS
DHAHRAN 31261, SAUDI ARABIA

DEANSHIP OF GRADUATE STUDIES

This thesis, written by **NEZAR MOHAMMED ABDULRAB AL-YAZIDI** under the direction of his thesis adviser and approved by his thesis committee, has been presented to and accepted by the Dean of Graduate Studies, in partial fulfillment of the requirements for the degree of **DOCTOR OF PHILOSOPHY IN SYSTEMS AND CONTROL ENGINEERING** .

Dissertation Committee

Dr. Magdi S. Mahmoud (Adviser)

Dr. Mohammed Abouheaf (Co-adviser)

Dr. Lahouari Cheded (Member)

Dr. Mohammad A. Abido (Member)

Dr. Azzedine Zerguine (Member)

Dr. Hesham K. Al-Fares
Department Chairman

Dr. Salam A. Zummo
Dean of Graduate Studies

3/1/17
Date

To my parents and my family

ACKNOWLEDGMENTS

In the name of ALLAH (SWT), the Entirely Merciful, the Especially Merciful.

All praise and thanks belongs to ALLAH (SWT), the LORD of the entire existence. It is HIM alone we worship and submit, and HIM alone we ask for help.

Peace and blessings be upon the beloved Prophet Muhammad (SAW), the mercy unto the worlds.

I extend my deepest gratitude to my academic and research advisor Dr. Magdi S. Mahmoud for his continuous support, patience and encouragement. He stood by me in all times and was the greatest support I had during my tenure in the university and most importantly during my thesis. He sets high goals for my research. He gives me flexibility to work on any problem that interests me, makes me question theories which I took for granted, and challenges me to seek breakthroughs.

Also, I would like to think my co-advisor Mohammed I. Abouheaf who has a wide range of research interests and sharp insights, he always was available to help and always was motivating me to do better, which truly helped me.

I would also like to thank my thesis committee Dr. M. A. Abido, Dr. Lahouari Cheded and Dr. Azzedine Zerguine for their time and valuable comments. Also, especial thanks to Dr. Abido for his course Intelligent Control that introduced me to the exciting topic of intelligent and evaluation algorithms.

I am grateful to King Fahd University of Petroleum and Minerals (KFUPM) for providing a great environment for education and research.

I would also like to thank the deanship for scientific research (DSR) at KFUPM for financial support through research group project **RG-1316**.

A very special thanks goes out to Hadhramout establishment for human development (HEHD) for the scholarship which enabled me to undertake M.Sc. and Ph.D. programs at KFUPM. I am truly thankful to all of the Hadhramout establishment members and supporters especially Eng. Abdullah A. Bugshan and Dr. Saleh Arm.

I would like to acknowledge my parents for their everlasting love, trust and faith in me for providing me the finest things I ever needed. I could never have pursued my higher education without their encouragement and support. To my beloved wife, my daughter Renad, my son Mohammed, my sisters, and my brothers, Walid, Abdullrab , Zuhair, and Omar. Also I am thankful to all my family who have always loved and supported me in all forms of life, their love gives me immense strength to keep moving ahead.

Last but not the least, I would like to thank all my friends and colleagues back at home and at KFUPM whose presence and discussions were the biggest support

during times of loneliness and despair namely Dr. Muhammad Sabih and Dr. Azhar M. Memon. Things would not have been better if not for their continuous support.

TABLE OF CONTENTS

ACKNOWLEDGMENTS ..... **V**

TABLE OF CONTENTS ..... **VIII**

LIST OF TABLES ..... **XII**

LIST OF FIGURES ..... **XIII**

LIST OF ABBREVIATIONS ..... **XIV**

ABSTRACT (ENGLISH) ..... **XVXV**

ABSTRACT (ARABIC) ..... **XV**

1 CHAPTER 1 INTRODUCTION **1**

1.1 Background **2**

1.2 Distributed Generation Systems **5**

1.3 Grid-Connection Operation Mode **6**

1.3.1 PQ control **7**

1.4 Islanded Operation Mode **7**

1.4.1 Droop control **8**

1.5 Networked control systems **9**

1.5.1 Time delays **10**

1.5.2 Packets dropout 10
1.5.3 Quantization 11
1.6 Research Objectives 12
1.7 Organization of The Dissertation 13

2 CHAPTER 2 ADAPTIVE INTELLIGENT TECHNIQUES 16
2.1 Introduction 17
2.2 Distributed Generations systems 18
2.3 Microgrids Control Techniques 23
2.3.1 PI/PID controller 26
2.3.2 Model predictive controller (MPC) 27
2.3.3 Linear quadratic regulator (LQR) 28
2.3.4 Sliding mode control (SMC) 29
2.3.5 Robust control 51
2.4 Intelligent Techniques 34
2.4.1 Particle swarm optimization (PSO) 57
2.4.2 Fuzzy logic control 58
2.4.3 Neural networks 40
2.5 Adaptive Techniques 42
2.5.1 Adaptive PI/PID controller 45
2.5.2 Adaptive sliding mode controller 44
2.5.3 Reinforcement learning 46
2.6 Conclusions 48

3 CHAPTER 3 QUANTIZED H∞ ESTIMATOR 49

3.1 Introduction 49

3.2 Microgrid System Modeling 52

3.3 Networked Control Modeling 57

3.4 Control Design 62

3.5 Main Results 64

3.6 Simulation Results 71

3.6.1 Hold input scheme 71

3.7 Conclusions 87

4 CHAPTER 4 $\mathcal{L}_1$ ADAPTIVE NETWORKED CONTROLLER 92

4.1 Introduction 93

4.2 Microgrid System Modeling 98

4.2.1 Case of three distributed generation units 104

4.3 Distributed Generation Network Model 107

4.4 L_1 Adaptive Controller 109

4.4.1 Adaptation law 111

4.4.2 Control law 112

4.4.3 Performance analysis 114

4.5 Simulation Studies 118

4.6 Conclusions 121

5 CHAPTER 5 A MULTI-AGENT CONTROL SCHEME 128

5.1 Introduction 129

5.2 Dynamical Model of Photovoltaic Cell 132

5.3 Dynamic Graphical Games (DGGs) 135

5.3.1 Graph notations 135

5.3.2 Problem formulation 136

5.4 Graphical Kalman Filter 137

5.4.1 Bellman equations for the DGGs 141

5.4.2 Nash equilibrium solution for DGGs 142

5.5 Online Adaptive Reinforcement Learning 142

5.6 Critic Neural Network Implementation for The Adaptive Learning Algorithm 148

5.6.1 Online learning of CNWs in realtime 150

5.7 Simulation examples 151

5.8 Conclusions 157

6 CHAPTER 6 CONCLUSIONS AND FUTURE DIRECTIONS 164

6.1 Main Contributions 164

6.2 Future Directions 166

REFERENCES 168

VITAE 202

LIST OF TABLES

2.1 PID Control Techniques 24
2.2 Predictive Control Techniques 24
2.3 Linear Quadratic Control Techniques 25
2.4 Sliding Model Control 25
2.5 Robust Control Techniques 26
2.6 Particle Swarm Optimization Applications 36
2.7 Evaluation and Optimization Techniques 36
2.8 Fuzzy Logic Applications 36
2.9 Neural Network Applications 37
2.10 PI/PID Adaptive Techniques 43
2.11 Adaptive Sliding Mode Control Techniques 43
2.12 Reinforcement Learning Techniques 47

3.1 Parameters of the DGs [177],[178]. 56

4.1 Parameters of the DGs connected to MG [177]. 104

LIST OF FIGURES

2.1 A typical microgrid system. 19
2.2 Distributed generation systems. 27
2.3 Hierarchical microgrid structure. 28
2.4 Droop controller of current loop. 32
2.5 Adaptive PI droop control. 45

3.1 A typical Microgrid System. 52
3.2 MG associated with n DGs 53
3.3 Structure of the standalone microgrid comprises of numerous DGs 53
3.4 Membership functions of four rule models. 72
3.5 Fuzzy state trajectories state 1 74
3.6 Fuzzy state trajectories state 2 74
3.7 Fuzzy state trajectories state 3 75
3.8 Fuzzy state trajectories state 4 75
3.9 Fuzzy state trajectories state 5 76
3.10 Fuzzy state trajectories state 6 76
3.11 Fuzzy state trajectories state 7 77
3.12 Fuzzy state trajectories state 8 77
3.13 Fuzzy state trajectories state 9 78
3.14 Fuzzy state trajectories state 10 78
3.15 Fuzzy state trajectories state 11 79
3.16 Fuzzy state trajectories state 12 79
3.17 Fuzzy state trajectories state 13 80

3.18 Fuzzy state trajectories state 14 80
3.19 Fuzzy state trajectories state 15 81
3.20 Fuzzy state trajectories state 16 81
3.21 The controller gain in terms of rule-1 83
3.22 The estimator gain in terms of rule-1 83
3.23 The controller gain in terms of rule-2 84
3.24 The estimator gain in terms of rule-2 84
3.25 The controller gain in terms of rule-3 85
3.26 The estimator gain in terms of rule-3 85
3.27 The controller gain in terms of rule-4 86
3.28 The estimator gain in terms of rule-4 86
3.29 Fuzzy state trajectories of wind turbine state 1 87
3.30 Fuzzy state trajectories of wind turbine state 2 88
3.31 Fuzzy state trajectories of wind turbine state 3 88
3.32 Fuzzy state trajectories of wind turbine state 4 89
3.33 Fuzzy state trajectories of wind turbine state 5 89
3.34 Fuzzy state trajectories of wind turbine state 6 90
3.35 The controller and estimator gains for WT model in terms of rule-1 90
3.36 The controller and estimator gains for WT model in terms of rule-2 90
3.37 The controller and estimator gains for WT model in terms of rule-3 90
3.38 The controller and estimator gains for WT model in terms of rule-4 91

4.1 A typical microgrid system under $\mathfrak{L}_1$ adaptive control. 99
4.2 Single line diagram of the islanded system consisting of multiple DGs 100
4.3 $\mathfrak{L}_1$ adaptive controller with uncertainties. 109
4.4 Lab. scale distributed generations architecture. 119
4.5 d and q component of load voltage. 122
4.6 d and q component of DG1 current. 123
4.7 d and q component of load current. 124
4.8 d and q component of DG2 current. 125

4.9 d and q component of DG2 current. 126

5.1 Photovoltaic Cell Electrical Model. 133
5.2 PV cell with DC boost converter. 135
5.3 The directed graph structure. 151
5.4 Phase plot using Kalman filtering. 152
5.5 The dynamics without Kalman filtering. 152
5.6 The dynamics using Kalman filtering. 153
5.7 Tracking error dynamics without Kalman filtering. 153
5.8 Tracking error dynamics using Kalman filtering. 154
5.9 Agent 1: Critic weights update in the presence of load variations. 154
5.10 Tracking error dynamics using Kalman filtering in the presence of load variations. 155
5.11 Critic weights trajectories. 156
5.12 Actor weights trajectories. 157
5.13 The states trajectories and error dynamics of agent-1. 158
5.14 The states trajectories and error dynamics of agent-2. 159
5.15 The states trajectories and error dynamics of agent-3. 160
5.16 The Tracking error dynamics and error dynamics of agent-4. . . . 162
5.17 Phase plot of the agents. 163
5.18 Tracking error dynamics in the presence of load variations. . . . 163

$\triangleq$	**Abbreviations**
$\bigotimes$	Kronecker product
$\|...\|$	The 2-norm
$\lambda(D)$	An eigenvalue of matrix D
AC	Alternating Current
ARE	Algebraic Riccati equation
CNN	Critic neural network
DC	Direct Current
DER	Distributed energy resource
$DFIG$	Doubly fed induction generator
$diag(...)$	Diagonal matrix
DG	Distributed generation
$DGGs$	Dynamic graphical games
DGs	Distributed generation systems
DP	Dynamic programming
$\mathfrak{E}(.)$	Mathematical expectation
$FACTs$	A flexible alternating current transmission system
FLC	Fuzzy logic control
I_n	The $n \times n$ identity matrix
HJB	Hamiltonian-Jacobi-Bellman
KCL	Kirchhoff current law
KVL	Kirchhoff voltage law
LQR	Linear quadratic regulator
KW	Kilo Watts
L_{ti}	Inductance of VSI filtering in DG_i
MAs	Multi-agents
MG	Microgrid
$MIMO$	Multi-input multi-output
MPC	Model predictive control
MW	Mega Watts
$NCSs$	Networked control systems
NNs	Neural networks
PI	Policy iteration
$PI\ Controller$	Proportional-integral controller
PID	Proportional-integral-derivative
$Prob(.)$	Probability measure
PQ	Power quality

$\triangleq$	**Abbreviations**
PSO	Particle swarm optimization
PV	Photovoltaic
PWM	Pulse-width modulation
$\Re$	Real number
$\Re^n$	n-dementional real number vector space
RL	Reinforcement learning
R_{ti}	Resistance of VSI filtering in DG_i
$SISO$	Single-input single-output
$sgn(...)$	Sign function
SMC	Sliding mode control
$SSSC$	Static synchronous series compensator
VI	Value iteration
VSI	Voltage source inverters
x^{-1}	Inverse of a vector x
x^T	Transpose of a vector x

THESIS ABSTRACT

NAME:	Nezar Mohammed AbdulRab Al-Yazidi
TITLE OF STUDY:	Intelligent Adaptive Control Algorithms for Distributed Generation Systems
MAJOR FIELD:	Systems and Control Engineering
DATE OF DEGREE:	2016

Directed by further developments because of industrial revolution into human modern life, the need of continuous and reliable supply is immensely a big challenge. In addition due to increasing energy consumption, and new developments in distributed generation technologies, the energy sector is beneficially progressing into new architecture of power grid towards microgrids. Renewable energy resources namely wind turbines, fuel cells, and photovoltaic are effectively producing clean power energy to reduce CO_2 emissions. The aim of this dissertation is to implement appreciate control systems of DGs within standalone microgrids operation. As microgrids are becoming smart, MG control systems utilize communication networks to send information to enable cooperation among distributed generators. However, the communication constraints can degrade the control performance and

probably destabilize the entire microgrid system. Interestedly, the influence of time-delays, signals dropout, quantization have been immensely gained great considerations in vast control applications. The recently developed adaptive controller and intelligent algorithms and distributed generations measurement technologies make the integration of distributed generations into feedback control potentially promising. Firstly, we have applied adaptive H_∞ controller for three DGs based inverter. These DGs are integrated in centralized framework. It is assuming that MG networks are subjects to communication constraints. Case studies have been tested utilizing two different distributed generation models. Our attention is secondly focused on the implementation of an $\mathfrak{L}_1$ adaptive controller using MIMO output feedback. In this part, we have utilized a decentralized strategy to enhance the reliability of the control systems in the occurrence of communication constraints. The stability analysis and error performance have been satisfied. Then, a novel adaptive distributed controller for multi-agent photovoltaic system is developed based on online adaptive learning. In the distributed framework, DGs are exchanging information based on a communication network in the presence of disturbances. This is done using local neighborhood information and partial knowledge about the units dynamics. The methodology is that the dynamics of the open loop photovoltaic system is estimated by using Kalman filter (KF). Then, we utilize KF to build up our intelligent controller. The proposed methodology is designed in terms of reinforcement learning, and adaptive control techniques to study the stability and the performance of DGs in response to different constraints. The simulation

will be handled using Matlab. Case studies in, the most common distributed generation disturbances have been used to demonstrate the fault-ride-through capability as well as the adequate steady state and transient response.

ملخص الأطروحة

الاسم الكامل: نزار محمد عبدالرب اليزيدي

عنوان الرسالة: خوارزمات التحكم الذكي المتكيف لنظم التوليد المتوزعة

التخصص: هندسة نظم و التحكم

تاريخ الدرجة العلمية: نوفمبر 2016

من أهم تأثيرات الثورة الصناعية في الحياة العصرية للأنسان، وظهور الحاجة الماسة إلى إمدادات مستمرة و مضمونة بالطاقه الكهربائية. وبالإضافة بسبب زيادة استهلاك الطاقة، والتطورات الجديدة في تكنولوجيا دمج المولدات المتوزعة بالشبكة الرئيسية، فأن قطاع الطاقة يسير باتجاة الاستفادة من الهيكله الجديد للشبكة الكهرباء نحو الشبكه الصغيره الذكية. موارد الطاقة المتجددة مثل توربينات الرياح، وخلايا الوقود، والضوئية اللتي لها القدرة على أنتاج طاقة لكهربائية نظيفة بشكل فعال للحد من أنبعاثات ثاني أكسيد الكربون.

و الهدف من هذه الاطروحة هو تصميم أنظمة تحكم فعالة لادارة أنظمة التوليد الموزعة عندما تعمل الشبكات الصغيرة بوضع منعزل عن المنظومة الرئيسية لتوليد القدرة. و حيث أن الشبكات الصغيرة أصبحت ذكية، فأن أنظمة التحكم فيها تستخدم شبكات الاتصالات لنقل المعلومات بين المولدات الموزعة لتمكين التعاون الفعال بينها. غير ان قيود شبكات الاتصالات و التأثيرات السلبية ممكن أن تضعف اداء نظام التحكم أو تزعز الاستقرار التام للشبكة الصغيرة. ومن المثير للأهتمام تأثير التاخير الزمني خلال الارسال الحزم و كذلك فقدان الحزم أكتسبت أهتمامًا كبيرًا في مجالات تحكم واسعة. حديثًا أنظمة التكيف ذاتي والخوارزميات الذكية و المتطورة و كذلك تقنية المولادات الموزعة ساعدت في دمج المولات الموزعة في انظم التحكم الواعدة.

اولآ: لقد طبقنا نظام التحكم المتكيف H_∞ لثلاثة مولادات موزعة توفر حمل مشترك في نظام تحكم مركزي. في هذه الدراسه نحن نفترض وجود قيود على الاشارات و الحزم المرسلة خلال الشبكة. نحن نقدم كذلك مثالان محاكاه لتوضيح النتائج. وتركز انتباهنا ثانيًا على تنفيذ وحدة تحكم متكيف L_1 بأستخدام نمودج متعدد المدخلات و المخرجات مع نظام الأسترجاع الخلفي للمخرجات. و في هذا الجزء، نحن نطبق نظام التحكم اللا مركزي لتحسين الأداء في وجود آثار الشبكات السلبية. و هنا يتم تحقيق تحليل استقرار النظام و كذلك أداء في وجود الخطاء بين الخرج الفعلي و التقريبي. و أخيرًا يثم تطوير نظام تكييف متوزع لمتعددة الوكيل على أساس النظام التكييف المتعلم الفوري. في إطار هذا النظام الموزع، المولدات الموزعة تقوم بتبادل المعلومات خلال شبكة الاتصال في وجود اضطرابات. ويتم ذلك بأستخدام معلومات المحلية جزئية حول ديناميات المولدات المجاورة. في هذة الطريقة يثم تقدير ديناميك الخلايا الضوئية الموزعة باستخدام كلمان فلتر. يثم تصميم الطريقة المقترحة على أساس تعزيز التعليم و نظام التحكم التكييفي لدراسة أستقرار و أداء النظام في وجود القيود و التاثيرات السلبية. يثم محاكاة مثالان مختلفين لتوضيح النتائج و لنظهر فعالية و قدرة الطريقة التحكم المقترحة.

CHAPTER 1

INTRODUCTION

Due to ever increasing energy consumption and global climate change problems, distributed generations (DGs), smart grid and renewable energy technologies are earned more attention to solve these issues. In general, most of customers suffer from the gradually increased in the cost of generation electric power from the conventional station. Additionally, the power supply stations are possibly stopped due to the lack of fossil fuels. In conventional setting, the main power stations are usually located in remote areas due to their large sizes. As a result, the power transfers over very long-distances loss a significant amount of power. Also, in some regions, these lines may be dropped due to the influence of climate such as hurricanes, rains, and humidity. Distributed generation is predicted to replace the conventional centralized generations in the future, in forms of microgrid networks. It is worth knowing that DGs enhance the quality, reliability, performance and decrease losses for the electric power system. The distributed generations are principally implemented with bounded power range from 1 kilo Watts to 50

Mega Watts (MW) placed near to load site. Distributed energy sources namely photovoltaics PV, wind turbines, fuel cells, and engine-generators. Penetration of renewable sources improve DG systems because of its small scale capacity and environment friendly nature. Today, the use of renewable source energies grows rapidly, especially wind turbines, fuel cell, solar panels, and thermal power plants. However, interconnected distributed generation might inherently serve control and reliability challenges in the presence of disturbance and faults, especially in standalone operation mode. Consequently, reliable controllers have been definitely applied to sustain the stability, reliability and performance of the microgrids.

1.1 Background

With rapidly developments in human modern life from communications, transportation, education, financial, manufacturing architectures as well as the population of the world, the need of a sustainable supply of electric power is significantly rising up. In addition to recent claim hazards and pollution, the requirements of minimizing the CO_2 emissions in the global environment are discussed for times. One solution in a hand is reducing the use of fossil fuel by using renewable energy resource technology to provide clean electric power.

To sustain a continuous supply of electric power in shutdown, or peak load periods, back up systems are implemented to generate amount of power to feed the critical units in the absence of main power source. Microgrids or DG supply local loads in remote areas in distributed power networks and co-operate with

utility grid at the point of common coupling [1]–[5]. Microgrids exhibited marvelous promise as clean and efficient sources of energy compared to fossil fuels with a successfully facilitate the employment of renewable energy resources [6, 7]. Microgrids is a combination of local loads, energy storage units and distributed generation units such as micro-turbines, wind turbines, fuel cells, and photovoltaic cells. Energy storage units, such as bank of batteries, flywheels, and capacitors coexist with the distributed generation sources to maintain the active and reactive power at the nominal levels. The microgrids can intelligently operate in two modes of operation namely grid connected and islanded connected. In the former mode, the microgrids feed the power to local areas, and the voltage and frequency are regulated locally. While in the later mode, the utility grid along with the microgrids feed electric power to the network loads [7]. Energy storage units are taken leading positions as back up systems in islanded microgrid to maintain load variations by regulating active and reactive power. Microgrid is a secure, reliable, sustainable, and efficient local network. Thus grids can promote power quality, decrease transmission droops as well as decrease consumer costs. The essential note of microgrid was innovated by the Consortium for Electric Reliability Technology Solutions (CERTS) in 1998 [8].

The distributed generation units are usually low power, under 100 MW, and they can represent by a DC source situated at the side of the demands to provide a reliable electricity. In particular, distributed generation has ability to enhance the efficiency and reliability by locally generate the electrically power and to eliminate

complexity of the need of transmission and distribution of electric power in the distributed traditional network [5]. Basically, DGs can be classified into two types:

- The effective type is called dispatchable energy generators. In these type of DGs, the electric output power can be regulated to meet the local demands. The dispatchable resource involves several kinds on/off generators such diesel generator, micro turbines, energy storage devices.

- Non-dispatchable (discontinuous) generators are related to renewable energy sources such wind turbine, and photovoltaic cells. Their electric output are not regulated in the presence of environment constraints.

The existing microgrids are classified in terms of power type into three types: AC, DC, and Hybrid AC/DC. The first type of MG, is the most used configuration and is prescribed shortly a microgrid. In AC microgrid, DGs and their local load are interfaced to AC bus through an appropriate inverter. This type has some disadvantages such, synchronization, reactive power management, and frequency phase. Recently, the second type of MG is applied widely to benefit from the rise of integrating DC sources (dispatchable and non-dispatchable) by using an DC bus as a backbone. In this context, DC microgrids are established to expand the area of application of DC micro sources and have the capability to eliminate the reactive power and synchronization. The key feature of the third type is that it incorporates AC and DC distributed networks. The control of different components of hybrid microgrid is challenging due to the complexity of hybrid network.

DGs interface with local microgrid via DC/AC or AC/AC voltage source inverters (VSI). VSIs provide a convenient control topology, synchronism conditions and power management in islanded mode. In particular, voltage source inverters are powerful tools that determine the quality of microgrid voltage. In this sense, the inverter controller can compensate voltage and quality due to loads uncertainties. While in grid-connected mode, current-source inverters interface to inject adequate power to main grid. Besides, the inverters can be established in parallel in terms of droop control technique. These parallel inverter sustain synchronization without external set-points. The parallel inverters might be suffered from disturbance and over currents. Droop control schemes are effective methods to maintain voltage and frequency among parallel inverters without any wired communication architecture. In form of wired architecture, droop control technique will impact once at last one of the inverters fails.

1.2 Distributed Generation Systems

DG as referred to small generators than can implement in remote area to supply electric power to some consumers or to co-operate with main grid. In its literature, various definitions of DGs have been stated for the distributed generation unit. For instance, Anglo American civilizations, the expression embedded generation is utilized, while North American civilizations usually utilize the expression dispersed generation. Further, the expression decentralized generation is utilized by Europe civilizations [9, 10]. There are proposed several power scales of distributed

generations. For example, the Electric Power Research Institute determines the scale of DGs from a couple kilowatts to 50 Mega Watts (MW) [24]. While the Gas Research Institute, determines the scale between 10KW– 25 MW. Also, the power scale of DG is specified to be between a couple kilowatts–100 MW. [10]. In [23], DGs are proposed with a limited range from 500 kilowatts (kW) to 1 MW. The power supply of distributed generations are defined to under 50 MW to 100 MW. From other point of view, some government strictly determine the limitation of accepted used generator in their countries. For instance, England government mainly defines the range of DG to be under 100 Mega Watts. Swedish law determines the range of distributed generation to be less than 1.5 MW [10].

1.3 Grid-Connection Operation Mode

Microgrid or distributed generations are small scale power, in which they actually require the public main grid to feed some demands. The utility grid forces the nominal reference voltage at PCC and frequency of MG using a microgrid central controller (MGCC) or might be selected by the owner. Microgrids represent as a controllable load or DC-source, to provide the elementary need of the local demands with adherence with the main grid. Micro-sources and storage units will behave as PQ generators to sustain the active/reactive power and the voltage control will not be an option. In addition, the distributed generation units act at their maximum specified power.

1.3.1 PQ control

Without any faults or voltage dips at the utility main grid site, microgrids must work in grid-tied operation mode. In this case, MGs are obliged to meet some requirements of the local loads and the main grid as well. DGs and storage devices achieve PQ control by injecting or absorbing some of the powers into the bus to terminate disparity in the voltage/frequency output of inverters. The set points are directed by the utility grid. The power controller regulates the frequency droop property at a certain level to sustain the active output power at the nominal value. Likewise, the quality controller regulates the voltage droop property to sustain the reactive power at the nominal value.

1.4 Islanded Operation Mode

In case of any interruption, microgrid separates and shifts to an islanded (standalone) mode, the DG units provide an adequate power quality and reliability for the sensitive loads. Indeed, DGs maintain the value of the voltage and frequency of the microgrid to the standard values. Also they should be able to share the active-reactive power among the loads proportionally to their power rating. In fact, there are other issues should be taken in consideration within standalone mode like the harmonic-current sharing, voltage /frequency restoration, and reactive power. Regarding above aforementioned, control based inverters should be able to compensate these issues to meet all power managements during this mode[1, 3]. In particular, several control techniques based inverters have been

reported in standalone operation mode namely centralized and distributed techniques.

The MG is mostly hierarchically controlled by centralized control technique. Thus centralized controller can maintain the power quality of distributed generations and the local loads effectively. Moreover, this method considers less cost and depends of the communication architecture to perform the control system. The center controller MGCC is responsible only to send the control input signals to distributed generation units. However, once the centralized controller fails the whole control system will be down because of this single point of failure. The future trends are toward the design of droop controller in the forms of decentralized control techniques without any communication networks among inverters to overcome the problems of a single point of failure occur.

1.4.1 Droop control

Droop control technique is concerning to sustain the reliability and stability of voltage and frequency in a standalone microgrid and to tackle the influence of load uncertainties on the steady state dynamics. Thus droop control systems utilize wireless communications between the parallel inverters for a proper power sharing. Moreover, their flexibility utilizes to transition the microgrid between grid-connected and islanded operation using the static switch. The control methods of the inverter is comprise of voltage, current, power controllers. In particular, conventional controllers are implemented in current and voltage loops to track the

set value of the droop voltage.

1.5 Networked control systems

Over years, networked control systems (NCS) are extensively implemented to study the influence of communication limitations on the control performance. Thus feedback control systems are mostly performing in a spatially distributed to carry out remote control application. In these framework, NCSs have vast application areas such manufacturing plants, automobiles, and aircraft. Very recently, NCSs have been successfully utilized as one sort of distributed control methodologies of power electrical grids [63] [64]. Networked control systems comprise of remote sensing units, plants, and estimation/control algorithms. It is particularly proven that NCSs can improve the overall performance and stability of microgrid at local loops by eliminating voltage and frequency variations, and inaccuracy in power sharing mechanism. Furthermore, the system reliability is sustained in existence of network constraints [64, 65, 169]. In large wide area models, the challenges are increased due to the fact that the probability of the occurrence of time delays or signals dropout on the transferred information are raised. The issues of unreliable communication paths in presence of concentrate communication constraints namely, time delay, packet dropout, and quantization effects have been extremely reported and gained more attention.

1.5.1 Time delays

With the huge utilization of shared channels and the fallibility of several channels, the probability of the occurrence of different time-delays are definitely increased. Thus time delays may be existed in sensor/controller link or controller/plant link. In general, time delays are immensely produced by digitization/dedigitization processing of the continuous signals due to clocking mismatch or buffering issues [208] [176]. Additionally, in its literature, several sorts of time delays have been addressed namely constant, random, and time-varying delay and so on. The unreliable aspects of the links is formed by Bernoulli procedures β_k and α_k, wherever

$$Prob(\beta_k) = \begin{cases} m_k; & \text{if } \beta_k = 1; \\ 1 - m_k = \bar{m}_k; & \text{if } \beta_k = 0. \end{cases}$$

and

$$Prob(\alpha_k) = \begin{cases} p_k; & \text{if } \alpha_k = 1; \\ 1 - p_k = \bar{p}_k; & \text{if } \alpha_k = 0. \end{cases}$$

1.5.2 Packets dropout

Another problem to cope with NCSs are packets dropout. The packets dropout are possibly existing in the fallibility channels. In particular, long time delays can be commonly considered as packets dropped out. On other directions, the transferring packets may be dropped because of physically malfunctions of the networks and unsuitable buffering mechanism. There are two well known schemes to compensate of the lost control signals, hold input, zero input scheme. In the

former one, previous control signals are applied once the current one was lost. While, in the latter one, zero input is applied for the same case. In a parallel with time delays, both issues have negative influence on the control system performance and may cause instability [176].

The hold compensate input strategy is

$$u_k = \begin{cases} u_k; & \text{if } \alpha_k = 0, \ \textit{the signal was received successfully.} \\ u_{k-1}; & \text{if } \alpha_k = 1, \ \textit{the signal was dropped out.} \end{cases}$$

The zero compensate input strategy is

$$u_k = \begin{cases} u_k; & \text{if } \alpha_k = 0, \ \textit{the signal was received successfully.} \\ 0; & \text{if } \alpha_k = 1, \ \textit{the signal was dropped out.} \end{cases}$$

1.5.3 Quantization

Quantization effects on the communication network have been broadly studied. In particular, dynamic systems are modeled in a continuous time representations. However, in setting of digital communications, the transmitted signals are progressing through analog/digital conversation in one side and digital/analog conversation in the other side. The meter observations should be coded and transmitted via bounded communication channels. At the receiver site, the received signals are encoded within the same time synchronization. These approximated discrete signals due to A/D and D/A conversations are involving with some errors. There are two well known quantization schemes have been reported namely, logarithmic and uniform. The logarithmic quantizer has been widely experienced to sustain

slight errors. While the uniform qunatizer has been utilized to realize the lowest rates [208].

A logarithmic quantizer can be defined as :

$$\begin{aligned} \mathcal{V} &= \{\pm v_j,\ v_j = \sigma^j v_0,\ j = 0, \pm 1,\ \pm 2, ...\} \cup \{0\}, \\ & 0 < \sigma < 1,\ v_0 > 0 \end{aligned}$$

In which σ, $\mathbf{q}(.)$ denote the density and the logarithmic of the quantizer. The latter can be prescribed as:

$$\mathbf{q}(\eta) = \begin{cases} v_j, & if\ v_{mj} < \eta \leq v_{Mj}, \\ 0, & if\ \eta = 0, \\ -\mathbf{q}(-\eta), & if\ \eta < 0 \end{cases} \tag{1.1}$$

where η is the input signal, and $\omega = (1-\sigma)/(1+\sigma)$, $v_{mj} = v_j/(1+\omega)$, $v_{Mj} = v_{mj}/\sigma$. The quantizer impact is bounded for σ such that:

$$\mathbf{q}(\eta) - \eta = \mathbf{\Delta}\eta,\ ||\mathbf{\Delta}|| \leq \omega \tag{1.2}$$

1.6 Research Objectives

This work goals at mainly developing adaptive control algorithms for the distributed generation units into standalone microgrids that have capability to sustain stability and desired performance of the microgrid control system under the

occurrence of network disturbances and uncertainties. To fulfilled, the above objective needs to evolve and builds upon a number of tasks. Key tasks are:

1. Development of a powerful robust H_∞ controller for fuzzy system for standalone microgrid comprised of three DGs subject to load variations and communication constrains.

2. Development of an $\mathfrak{L}_1$ adaptive controller utilizing output feedback for decentralized distributed generators. It is assumed that the microgrid network is unreliable that may cause time delays at control–plant channels.

3. Development of a multi-agent control system for distributed DGs in the occurrence of disturbance. The open loop states are evaluated using Kalman filter. Additionally, the robustness of the proposed controller is tested in the presence of load variations.

1.7 Organization of The Dissertation

This dissertation consists of six chapters.

- Chapter 1, is an introductory chapter that describes the motivation, objectives and contributions through this dissertation. A review is also given in this chapter that considers definition, and some concepts of vast that mainly studied in this work.

- Chapter 2, is a survey gives the detailed power system component dynamic models and load models used in this research. We then introduce communi-

cation constraints, namely time delays, packets dropout, and quantization effects.

- Chapter 3, we investigate an intelligent quantized H_∞ control for a centralized microgrid based inverter structure that contains three distributed generations. Thus three generators are operating in standalone mode to provide an electric power to a common load. The intelligent fuzzy networked controller is mainly designed in terms of the hold input strategy and casting the design results in the framework of linear matrix inequalities (LMIs). To investigate the proposed controller, we test two different case studies. Practical challenges are studying namely time-delays, packet drop and quantization utilizing H_∞. Also, stability analysis and controller robustness are considered.

- Chapter 4, we tackle uncertainty and communication constraints using $\mathfrak{L}_1$ adaptive output feedback. A multi-input-multi output microgrid model has been simulated to check effectively the proposed method. Furthermore, the controller performance have been examined in the presence of load variation and varying time delays.

- Chapter 5, we study a novel distributed control scheme for islanded microgrids in the presence of disturbances. The information flow among the distributed energy sources is limited by a communication graph. Adaptive reinforcement learning technique uses a Kalman filter to estimate the dynamics distributed power network. The dynamics of the mutiagent systems

are susceptible to disturbances. Thus Kalman Filtering are introduced to rectify the stochastic behavior. The information flow between the PV cells is governed by a communication directed graph topology. Cooperative control ideas are used to maintain synchronization among the agents in which the PV cells will converge to a leader.

- Chapter 6, we summarize our work and several future research directions are also provided.

CHAPTER 2

ADAPTIVE INTELLIGENT TECHNIQUES

Nowadays, a compelling need has grown to understand the influence of greenhouse emissions on human existence on the earth as well as the effect of fossil fuel on the economy. An elementary idea of renewable energy resources is come to solve these global issues. This chapter introduces a survey on the adaptive and intelligent methods that has been applied microgrids systems. Adaptive control is a powerful technique capable of guaranteeing an excellent performance in presence of parametric uncertainties. Interestingly, the adaptive technique is effectively exercised in various control issues including stability, tracking error, and parameter uncertainties. Adaptive control has been extremely developed by using intelligent algorithms to automatically tune the control parameters namely fuzzy logic, particle swarm optimization, bacterial search algorithm, and etc. The objective is to evaluate and classify the design control methods and evaluation algorithms

of the microgrids to maintain stability and reliability, and to adjust controller parameters especially in standalone operation mode. The stability of islanded microgrids are constantly impacted by the related loads. Furthermore, the notion of microgrid in distributed networks is discussed in terms of distributed generation units and energy storage devices. A significant part of the research on an islanded microgrid involves droop control technique. In normal operation, distributed generation units and storage units provide power quality control. Once a shutdown or a problem has occurred at the utility grid, microgrid can be isolated from the main grid and operate in a local grid to support the local loads. Thus distributed generations co-operate with storage units to sustain the stability of the islanded microgrid.

2.1 Introduction

Lowering CO_2 emissions is a big challenge to keep life on our planet. DGs are effective resources to solve this challenge. Distributed generation is predicted to place of the conventional centralized generations in the future. It is worth to know that DGs enhance the quality, reliability, performance and decrease losses for the electric power system [1, 2, 3, 5, 6, 7]. The requirement for robustly reliable power supplies has raised day by day with the proliferation of sensitive loads like computers, hospitals, satellite systems, critical communications, and so on. The scope of distributed generations based on generated power have been bounded from 1 MW to 100 MW. Distributed energy sources are namely photovoltaic PV,

turbines, fuel cells, and engine-generators [4]. Penetration of renewable resources can improve the quality of distributed power generations because it is effective small scale units and environment friendly nature [7]–[24].

2.2 Distributed Generations systems

Distributed power generation is an emerging complementary infrastructure to traditional power systems in which, it is envisioned based on decentralized generation of electrical power in proximity of consumption sites. The distributed generations are connected usually to medium or low voltage grid within distributed systems. Normally DG units are categorized based on the applications by the utilized technology provides the most suitable support [11]. The need of an interconnected control scheme for DGs, local loads, and storage devices is bringing to the idea of microgrid (MG). Microgrid system might practice interconnected/ or isolated to/from the utility grid. Distributed generation systems have various advantages such enhance reliable, quality, two way cooperation, and reduce the power losses, power cost [12]–[22].

In Fig. 2.1, a typical microgrid MG configuration is defined as a host grid consists of distributed energy resource (DER) units to ensure reliability and power delivery with two distinct modes namely grid connected mode and island mode [12] [14] –[17].

A lot of work has been done in forms of AC grid, DC grid, and hybrid grid. Hybrid grid consider AC and DC components connected to a power electronic

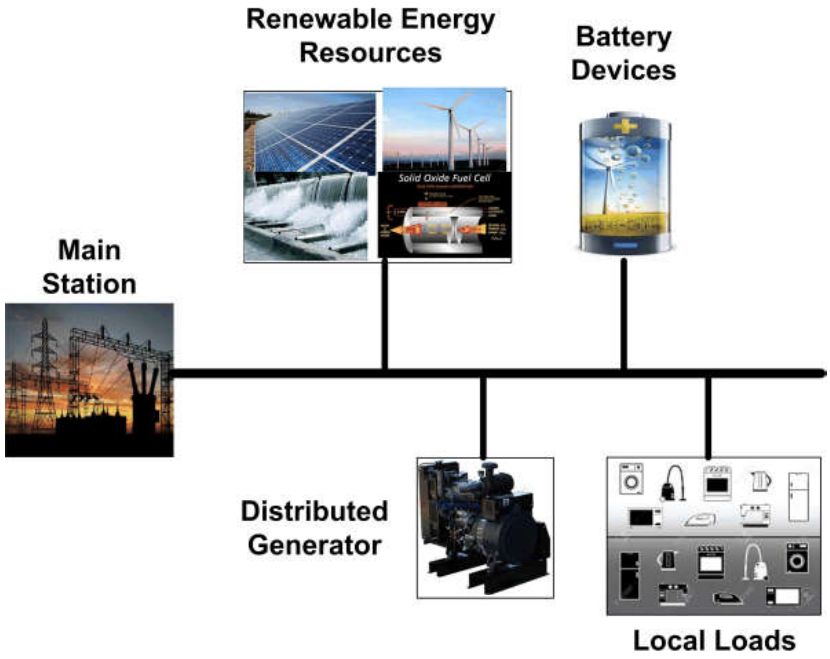

Figure 2.1: A typical microgrid system.

converter. Recently, using DC microgrid increases for the implementation of DC power sources such PVs and fuel cells with DC load. In spite of that, the need of conversion AC/DC and DC/AC is necessary when the DC microgrid connected to AC DGs or AC loads which make the system complex and lossy. Hybrid microgrid (HMG) can be used to connect AC-DC units but particularly HMG is still used in small scale grid to connecting DC resources such PVs to AC loads. The concept of smart grid is investigated to overcome the complexity and to promote connection between AC and DC units with high reliable and efficiency of power delivery [13].

As our world advances technologically, we are continuing to find a plethora of new applications for the devices we utilize. The demand of small scale distributed generation units can surpass the capabilities of renewable power generation. However, process control and management of the diverse distributed generation is a

big challenge. As the numerous of DGs significantly grow, an urgent need of splitting the control task among different units, which refer to using distributed control strategy. In particular, centralized scheme serve from disturbance and faults which regard the performance, reliability, and security of the power system. Non-centralized strategies including distributed and decentralized control were reported to deal with large scale systems. A simple structure namely decentralized control, where interactions between the DGs are ignored and the subsystems are totally independent. However, in the interconnected wide area, certain kinds of interactions among the different systems exist. On the other hand, the distributed generation technology offers data sharing among the subsystems through communication network. There were various distributed control methods including model predictive control, consensus based control, agent based control [12].

By utilizing modern technologies, smart distributed generations deliver power in efficient way. A sophisticated, smart communication technologies, real-time monitoring, control systems over distributed networks are essential for distributed elements, like generators, substations, and users. Smart power grid reacts to all episodes that happen over the grid like power generation, transmission, distribution, and consumption with smart metering and automatic control [25].

The concept of smart grid refers to the future of the intelligent power systems with two ways communication and energy transformation. Smart grid has integrated with different sorts of renewable energy systems, and flexible consumers [25]–[56]. This makes the smart grid framework to be an intelligent and a com-

plex system at the same time. In fact, various types of intelligent control strategies have been investigated to stabilize the distributed complex power systems [48, 49, 50, 51]. In addition, the whole distributed components of the power plant from the electric generators to the end users contributed the new improvements. The modernization of the electricity grid can benefit from the revolution technology that leaded by intelligent smart grids [38] [52].

Interestingly, integrating smart grid with several renewable distributed resources become a hot research area in academia and industrialized environment. Several authors studied the issues and the advantages of future power grid and many literature survives had been prepared concerning distributed generations, and microgrids [25] [29, 30, 31].

From a technical point of view, electric power grids are considered as cyber-physical systems, in which the electricity and the cyber architectures have been merged. Integration of cyber physical system (CPS) and power cloud computing for the power grid enhancing communication and self regulating. Furthermore, power smart grid applied self monitoring systems, and control applications in real-time exercised CPS. Cyber physical systems integrated the security of networking process in smart grid with microgrid framework [47, 57]–[62].

In recent years, networked control systems (NCS) are considered as one sort of different distributed control schemes of power electrical grids [63] [64]. It is worth noting that NCS improved the over all performance and stability for micro power grid at local loops by removing voltage and frequency variations, and

inaccuracy in power sharing mechanism. Furthermore, the system reliability is improved in the existence of network constraints namely time delay, data loss, quantization impacts, and bandwidth limited [64, 65, 169]. In particular, the hierarchical structure of the microgrid systems consist of primary, secondary, and tertiary control as shown in Fig. 2.3. The first level control, a so-called primary controller is concerning with the local layers in distributed generations DG unit. In the local loops such as voltage, current, virtual impedance, and droop loops, communications is not necessary with further distributed generation DG units for microgrids controllability. The key idea of implementing a secondary control is to compensate voltage and frequency variations in micro power grid result of primary control loop. Shafiee [63] developed a distributed secondary control in droop-controlled islanded microgrids. In contrary with primary control, the secondary control use feedback communication systems to transfer values of the MG parameters to each DG unit. In NCS closed loop system, sufficient conditions and the stability analysis have been investigated under limited tolerant packet loss. Linear quadratic Gaussian controller with output feedback has been designed for NCS to reduce the impact of data dropout on the system performance [66]–[67].

In particular, various types of heuristic algorithms had been applied to enhance the control and optimization for microgrids systems and distributed generation units namely particle swarm optimization, neural networks, fuzzy logic, and genetic algorithms. Thus intelligent and evaluation techniques are effectively applied in both microgrid operation modes tied and islanded mode. In the former,

which is the nominal operation, for instance, several intelligent algorithms have been proposed in order to study grid bus and to optimize electric power management online using battery storage systems and distributed energy resources. Indeed, the intelligent algorithms can be definitely determined how much power should be injected or took out or supplied.

This chapter focuses on discussing the adaptive and the intelligent techniques for power distributed generations. The integration of electronic devices with objectives to develop intelligent controllers can optimize the systems performance. The motivation of applying intelligent techniques is to enhance the control system performance, and the stability of DGs by tuning control system parameters in the whole operation points.

2.3 Microgrids Control Techniques

In general, various conventional control techniques have been used in the application of power system including proportional integral derivative (PI/PID), sliding mode, linear quadratic with fixed parameters for a certain operating point. The prescribed values of the control system parameters can provide a proper performance in steady state. However, these controllers may provide undesired performance once the operating points changed. As a result, the control parameters need to retune for the current case.

Table 2.1: PID Control Techniques

PI/PID Control Applications for Microgrids Systems	References
• PI/PID controller are utilized to control DFIG wind turbines, to sustain the systems performance under fault ride.	[68]
• To reduce the overshoot and steady state error, PI/PID controllers can be used for FACTS units.	[68]
• Under voltage and frequency fluctuations in the distributed networks PI controller for SSSC and battery systems used to enhance power flow in the network.	[71]
• Under faults and disturbance in the distributed network units, a fault tolerant scheme for SSSC has been implemented in PQ control systems using PI controller with a proper compensate scheme.	[72]
• Under highly harmonics in PWM converter systems, a sample design PI failed to compensate disturbed harmonics, instead of that a repetitive controller is applied.	[73]

Table 2.2: Predictive Control Techniques

MPC Control Applications for Microgrids Systems	References
• Using Standard MPC to eliminate the tracking error and overshoots in grid connected operation.	[74]
• A novel MPC to reduce the oscillations, together with a fuzzy logic control in order to remove the steady-state error and the impacts of time delays.	[75]
• A predictive direct estimation scheme for evaluate the critical parameters.	[76]
• Advanced predictive control technique demonstrated an enhancement in minimizing the interfaced harmonic of grid-current with a nonlinear filter.	[77, 78]
• An adaptive predictive current control for three-phase in normal operation mode.	[79]

Table 2.3: Linear Quadratic Control Techniques

Linear Quadratic Control Applications for Microgrids Systems	References
• Under the influences of disturbance and uncertainties optimal linear quadratic regulators has extremely utilized for a three-level inverter for photovoltaic systems based grid connected.	[80]
• A new scheme comprised of LQR and scheduling methodology has been used to eliminate any sort of disturbance in three-Level voltage source inverters.	[81]
• For each disturbance, an optimal LQR and attractive Gain -Scheduling are extremely utilized for the voltage inverter regulation subject to any type of disturbance. This control scheme is mainly implemented to balance DC-link and to optimize power support to distributed loads.	[82]
• Different type of models have been considered to study the steady-state and the small-noise model. Hence, a LQR was employed to regulate voltage and current of DC-link.	[83]
• Analyzes the performance of the three-level inverter that interfaces distributed generations with the main using a LQR.	[84]
• LQG based low voltage DC control is designed. With in this sense, Kalman filtering fusion is utilized to estimate unknown outputs to enhance the accuracy due to disturbance.	[85]

Table 2.4: Sliding Model Control

Sliding Model Control Applications for Microgrids Systems	References
• A review of control methodologies on microgrids networks. Thus chapter demonstrates different voltage schemes to sustain the stability and the reliability of distributed generations.	[86]
• An integral SMC with a fixed switching method for three-phase inverter based tied-grid to solve the chattering issue.	[90]
• An adaptive robust totally SMC has been introduced to ensure the reliability of a standalone microgrid subject to uncertainties and disturbance.	[92]
• Output feedback sliding mode control has been investigated for wind turbine with variable speed.	[93]
• A reliable second order SMC is employed for fault ride of wind turbine in the presences of disturbance.	[94]

Table 2.5: Robust Control Techniques

Robust Control Applications for Microgrids Systems	References
• An H_∞ controller with a voltage repetitive control are applied to handle current distortion into VSI and to sustain the system stability in grid mode.	[96]
• An H_∞ controller with a current repetitive control are established to sustain the equitable neutral point in the three phase inverter.	[97]–[98]
• H_∞ and repetitive voltage controllers for grid tied with a frequency adaptive mechanism to tackle frequency fluctuations.	[99]
• H_∞ repetitive controller for four-wire inverters.	[100]
• H_∞ repetitive controller for single and three phase inverters.	[101]–[102]
• Advanced structured H_∞ scheme of PI controllers for grid feeding interfaced with VSI using hinfstruct optimization tool.	[103, 104]

2.3.1 PI/PID controller

For decades, because of their simple structure, the PI/PID controller is utilized extensively in the industrial field and power systems. PID/PI is a robust, reliable, and provides near-optimal performance of the control system with appropriate tuning of gains. There are several strategies have been introduced to adjust the PID gains namely, Ziegler and Nichols, Cohen Coon, Chien, Hrones and Reswick method (CHR), Fine tuned and rule of thumb [68][69] [70]. However, the main disadvantage of PI/PID controllers is that their the capability of optimally tuning PID gain for nonlinear and complex systems. Within this framework, the PID performance substantially relies on the adequate values of the PID parameters. To overcome this drawback, a self-tuning PI/PID controller has been successfully developed to select the optimal values of the PID coefficients [69]. In [71], SSSC with/without battery devices have utilized to sustain power flow in standalone grid. Classic PI controller is implemented to regulate power flow by adjusting the SSSC and battery systems. Battery systems and SSSC are investigated as power quality PQ control is tied grid operation. Also, a PI controller for SSSC [72]. Author in [73] discussed bad performance of PI in the presence of a tremendous voltage harmonic.

Due to the simple structure and the weak gain of PI, it is unable to compensate harmonic frequencies because of disturbance. In this sense, repetitive control scheme are proposed to compensate the harmonic and disturbances in three-phase PWM converters. Table 2.1 illustrates some relevant references and their contributions for PI/PID controllers.

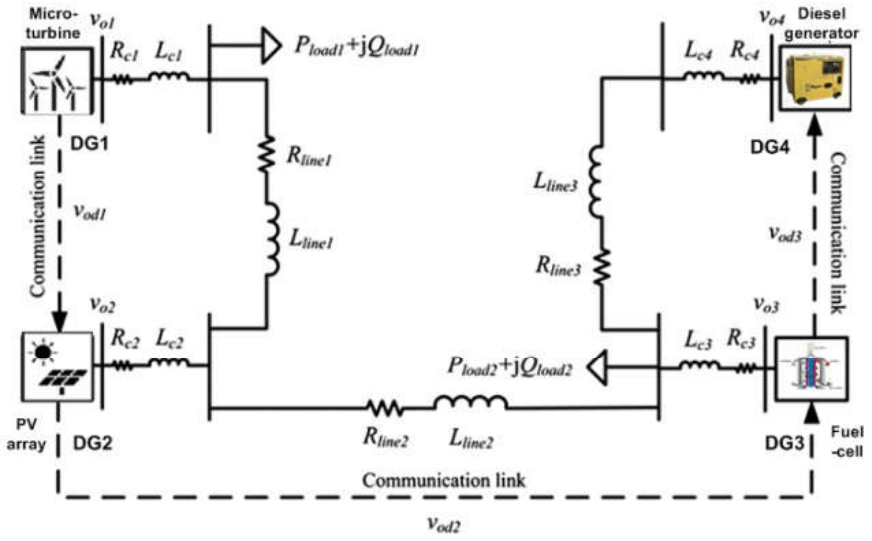

Figure 2.2: Distributed generation systems.

2.3.2 Model predictive controller (MPC)

Predictive control techniques are improved to forecast the reference signals. An interesting characteristic of these schemes is that they reduce the tracking error. In [74], a predictive active damping technique is associated with compensation method to reduce the oscillations behavior within the tied grid mode. [75] has introduced a predictive current control method with a fuzzy control for voltage regulator in the droop loop to remove the steady-state error and the impacts of time delays. In [76, 77], the authors proposed a predictive direct control scheme based on mathematical analytical. Further, an estimation method is applied to evaluate the critical parameters. New predictive

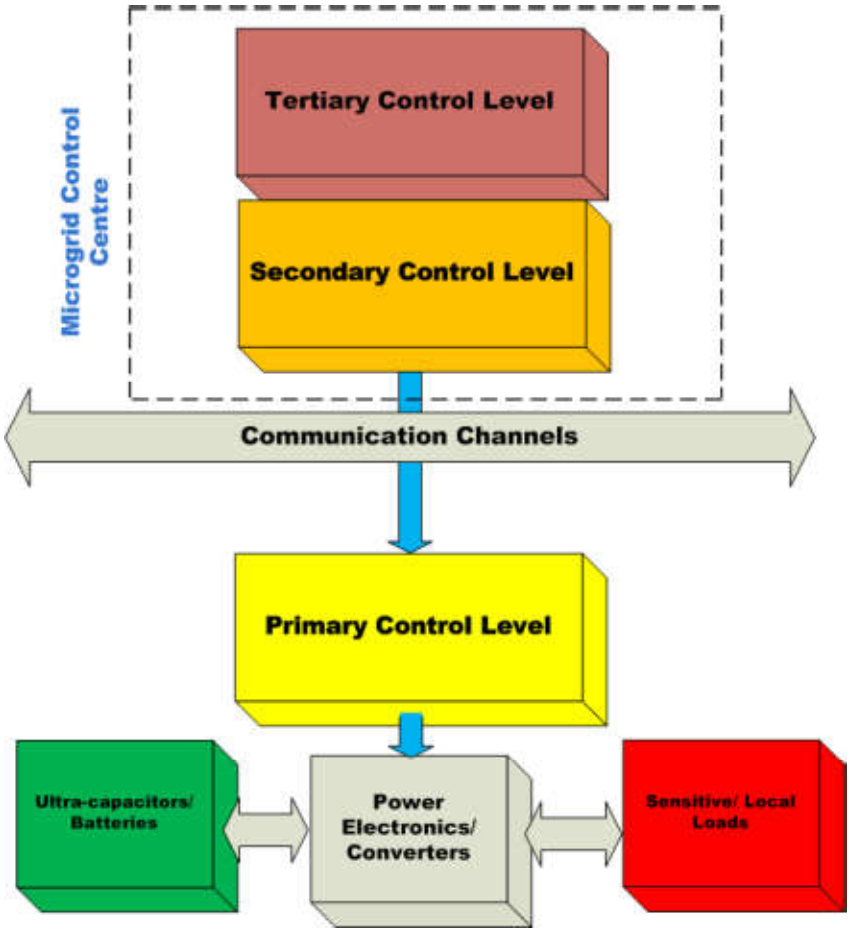

Figure 2.3: Hierarchical microgrid structure.

control technique demonstrated an enhancement in minimizing the interfaced harmonic of grid-current with a nonlinear filter [77, 78]. An adaptive predictive current control has been proposed for microgrid based three phase inverters in the normal operation mode [79]. Table 2.2 represents some applications of predictive controllers into power systems.

2.3.3 Linear quadratic regulator (LQR)

The concept of linear quadratic regulation(LQR) is to minimize/maximize the utility cost function to calculate the optimal control policy. The challenging with linear

quadratic regulator is the selection of the weighted matrices Q and R to sustain the proper response. Over the years, various classes of optimal control strategies have been designed for three level inverters to eliminate the steady state error [73]. In [82], a straightforward and powerful strategy have been investigated to control for the complete large-signal control of the Three-Level Neutral VSI. In this structure, LQR and Gain-Scheduling control methods were utilized for the voltage inverter subject to any type of disturbance. This control scheme is mainly implemented to balance DC-link and to optimize power sharing among loads.

Some results on the subject of LQRs and gain-scheduling control with disturbance and uncertainties are reported in [80]– [84]. Usually, a filtering algorithm (like Kalman filter) is integrated with linear quadratic regulator to estimate the state in the open loop systems in presence of disturbance. The concept of linear quadratic Gaussian is combination of LQR and Kalman filter, introduced to refine the influence of the disturbance [73], [85]–[86]. Thus, the linear quadratic regulation has been widely exercised for various applications, such voltage control of distributed generation units [86]. Several related works have been summarized in table 2.3.

2.3.4 Sliding mode control (SMC)

Sliding mode control has been intensively investigated for nonlinear robust control to ensure stability subject to parameter constraints. Once the sliding mode control (SMC) is applicable for variable structure problems, it can endure from chattering problem. In general, the sliding mode control has a couple of drawbacks such a proper transient and zero steady state error. However, by an appropriate design of the feedforward controller and sliding surface, the chattering can be tackled [87, 89]. In [90], authors

have introduced an integral SMC with a fixed switching method for three-phase inverter in tied grid operating mode. The chattering issue solved by optimizing the sliding mode coefficients of the ripple of the system output based on PWM with additional integral sliding surface to remove the tracking error. Practical application of sliding mode control is of voltage regulation for the inverter due to a fluctuation in tied operation. SMC is designed by means of direct power control to produce desired and smooth output power [89]. Moreover, direct power control and SMC had been worked together to remove inaccuracy in the evaluating of actual and useless power in the absence of current control scheme [91]. Recently, an adaptive robust totally SMC has been introduced for a standalone microgrid. The proposed controller was highly reliable against uncertainties and disturbance along with storage energy devices. Thus SMC can stabilize and support the local loads in both islanded and tied grid mode [92].

SMC for wind turbine variable speed has been implemented to maximize wind turbine with unknown wind speed measurements. Here, the output feedback SMC controller optimized angular velocity for the rotor [93]. In [7], authors developed a robust nonlinear SMC controller for distributed generations in the presence of parameters deviations. It was shown that, the sliding mode controller can guarantee better performance and the system stability. In [90] an integral resonant SMC has been implemented for grid-connected inverter. A proposed discrete feedforward SMC controller enhanced the tracking speed mechanism and the transient performance [87] [88]. In [89], Shang L. tackled the issue of transmission network fluctuating over grid connected inverters using a SMC. In addition, [94] introduced a robust second order SMC fault ride for a wind turbine with several disturbance. Design sliding surface is very important to investigate a robust controller. Table 2.4 demonstrates a snapshot of the control techniques in

power systems. Assuming the dynamics of a system is expressed as

$$\dot{x}_t = \Phi(x_t) + \Gamma(x_t)u_t; \quad y_t = \Theta(x_t) \tag{2.1}$$

where the state is $x_t \in \mathbb{R}^{n\times 1}$, $\Phi(x_t)$ and $\Gamma(x_t)$ are nonlinearities. $\Theta(x_t)$ smooth scalar and $u_t \in \mathbb{R}^n$ is called discontinuous [95]. The tracking error on variable x_t is

$$x_{terror} = x_t - x_{tdesired} \tag{2.2}$$

We can design the control law based on given surface such

$$\dot{s} = a_1\dot{x}_{t1} + a_2\dot{x}_{t2} + ...a_j\dot{x}_{tj} + \Phi(x_t) + \Gamma(x_t) \tag{2.3}$$

Where $a_1 > 0$ that sustain the states tend to zero. The candidate Lyapunov functional is assumed to be

$$\dot{V} = \frac{1}{2}s\dot{s} \tag{2.4}$$

Taking the control law is

$$u = \beta(\dot{x})\ sgn(s) \tag{2.5}$$

2.3.5 Robust control

Generally seeking, the problem of H_∞ schemes are been extremely utilized to synthesize control system stability and to satisfy the performance in presence of parametric uncertainties and external disturbance using linear matrix inequalities (LMIs) methods. LMIs is a powerful tool that is used to directly find a feasible and an optimal solution.

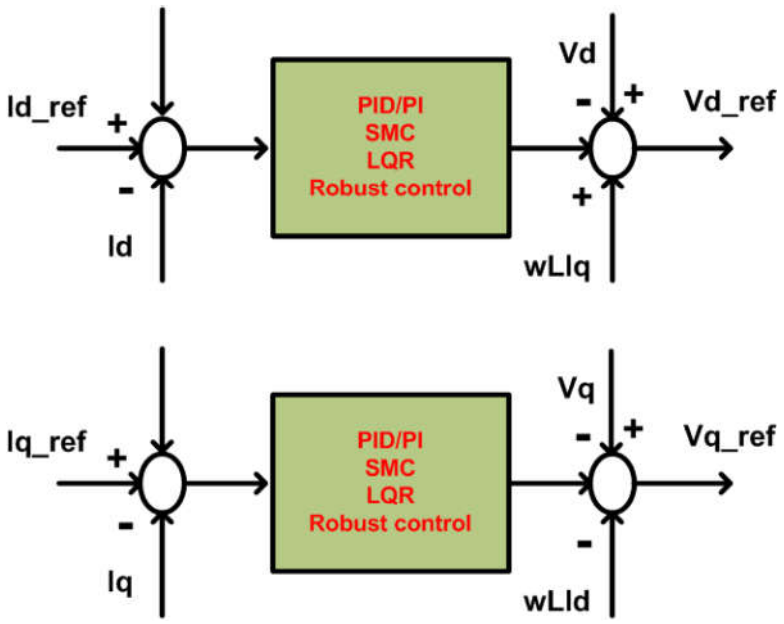

Figure 2.4: Droop controller of current loop.

In particular, The essential goal of H_∞ is that it has been employed to reduce the impacts of the uncertainties and the disturbance. Moreover, it is an effective strategy to enhance transient characteristic in spite of uncertainties.

Authors in [96], investigated an H_∞ current controller with a repetitive control to decline current distortion into voltage source inverter operating in tied mode. Also, an H_∞ current controller has been successfully used in order to sustain a balanced neutral point for the inverter and can terminate the current steeping towards the split capacitors [97]. Furthermore, a robust H_∞ current control topology is investigated to tackle a considerable current harmonics distortion by introducing an appropriate sinusoidal current to the main grid. Thus H_∞ current control is basically composed of internal model and a stabilizing compensator to sustain the system stability against system fluctuations due to nonlinear loads and voltage variations [98]. In [99], an integration of H_∞ and a repetitive controllers has been performed to regulate voltage in grid operation mode. Additionally, an adaptive is used to enhance the performance. These controllers formed

a robust control structure to handle current harmonics in inverters loops.

An H_∞ repetitive cascaded control scheme comprises of an inner voltage loop and an outer current loop to reinforce the power quality for the microgrid. Furthermore, thus control scheme supported the performance of the system dynamic against current harmonics. Besides, it provided a flexible shifting between both operation modes of the microgrid [99]-[102].

Recently, a structured H_∞ scheme of PI controllers for grid feeding interfaced with VSI. The outcome of a theoretical analytical on grid feeding control has been derived. In this frame, the PI gains is substantially calibrated using hinfstruct optimization Tool. Thus hinfstruct tool is an extension scheme While a synchronous reference PI control method is investigated for the current stabilization [103, 104]. Similarly, a developed structured H_∞ controller has been implemented for islanded microgrid. The control system consists of fast voltage, V-I droop, and current controllers, see Fig. 2.4. The voltage and current loop are constructed in terms of extended H_∞ controller. An Hinfstruct function is a strong optimization tool applied to adjust PI gains [104]. However, with any interruption, these parameters need to meet the variation. In order to optimally tune of the control system parameters, various techniques and tools have been adopted for uncertain microgrids. The utilization of intelligent computational and adaptive control techniques improve the over all performance of the distributed power systems by automatically tune the control parameters. There are various of robust control methodologies have been reported in power systems, table 2.5 summarizes some relevant works.

2.4 Intelligent Techniques

Traditionally, trial and error strategy has been given appropriate droop performance in forms of few different DGs. Increasing the DGs in the microgrid causes a difficulty in tuning the parameters of the control system once different frequency signals are following [105]– [120].

An online cuckoo search technique has been applied for a suitable power sharing. Thus cuckoo technique automatically tunes the parameters of local controller. The authors proved the powerful of the proposed technique comparing it with the traditional evaluation techniques [121].

In the literature, several powerful techniques have been proposed to optimally adjust the values of controller parameters, see [122]–[138]. In [135], the colonial competitive algorithm is used to find the optimal of the controllers for parallel DGs, interconnected with energy storage devices, and local loads using game theory. A centralized neural network microgrid controller is assigned to provide the nominal values frequency and voltage for the local loops.

One classic solution was exercised a particle swarm optimization method to automatically tune gains of the microgrid control system. A conventional PI controller is used in the droop control loops [136]. Hybrid intelligent control scheme comprises of fuzzy logic and particle swarm are implemented to optimize parameters of the PI control in islanded microgrid MG. The idea of using particle swarm PSO was to tune the fuzzification membership function in terms of frequency variations. Then, the PI gains was adjusted to satisfy the frequency regulation [122]. Furthermore, particle swarm PSO is applied to optimize the PI control gains of voltage source inverter in islanded MG [124].

In [123], a differential evolution algorithm is reported in order to sustain the stability of parallel inverters based microgrid. The differential evolution provided a proper response by realize the parameters of active power P, frequency ω and reactive power Q, and voltage V operation of inverters without any complement between the local controllers. An intelligent central controller is utilized to adjust the droop and PI controller parameters of controllable DGs within a smart standalone microgrid using bacterial foraging optimization[125].

In particular, power stations are located away from consumer loads for safety reasons due to fact that they are large scale plant, CO_2 emissions, waste generation and high-voltage transmission lines. However, the fuel costs of the operation and transmission are different. Conventionally, the power generated by the utility grid is designed to be larger than the power consumption by consumers and over transmission lines. The primary aim in power operation strategy is reduction of the total operation costs [127].

Economic load dispatch technique has been investigated to organize the power supply to meet demands with minimum cost. Thus economic dispatch technique, is employed to accomplish the optimal active and reactive power programming using evolution algorithms. A rich body of literature has been evolved on economic dispatch schemes for load sharing to minimize the operation cost [127]–[132]. The distributed generators are mainly classified in dispatch and non-dispatch. The scope of non-dispatch generators includes uncontrollable plants namely nuclear, wind turbine, and solar which is a less reliable and less secure. Dispatch (controllable) generators can be tuned on/off includes hydro-power, fuel cell, natural gas, diesel engine. The management of power supply can be enhanced by site a dis-patchable, nonrenewable sources near local loads to reduce power loss and to provide a sustainable electric power[127]–[129].

Table 2.6: Particle Swarm Optimization Applications

Particle Swarm Optimization Applied for Microgrids	References
• PSO automatically tune gains of PI controller in the droop control loops. To sustain the desired performance and power quality when faults and disturbance occur.	[124][136]
• A novel methodology comprises of PSO and Clonal Selection Algorithm provided an optimized placement of DGs.	[106]
• PSO algorithm determines the optimal position and the scale of DGs and DSTATCOM to enhance power quality.	[107]

Table 2.7: Evaluation and Optimization Techniques

Evaluation and Optimization Techniques Applied for Microgrids	References
• An online cuckoo search utilized to optimize the parameters of control systems to sustain suitable power sharing.	[121]
• Under faults and disturbance in the distributed network units, a differential evolution algorithm is utilized to sustain the stability of parallel inverters based microgrids.	[123]
• A colonial competitive algorithm is employed to optimize the controllers gains for parallel DGs by means of game theory.	[135]
• Within a standalone grid operation, an intelligent controller is designed using bacterial foraging optimization to tune PI controllers of DGs.	[125]

Table 2.8: Fuzzy Logic Applications

Fuzzy Logic Control Applied for Microgrids	References
• Fuzzy logic control is utilized to find the required performance of four area systems with proportional integral control.	[140]
• A hybrid FLC and tabu search algorithm is designed for load frequency control. TSA is utilized to optimize the fuzzy rules.	[141]
• Fuzzy control employed for self-adjusting PI gains of automatic generator control.	[142]
• Two eliminate errors in wide area system, a genetic algorithm optimize FLC functions to select required parameters of interconnected control systems.	[145]
• A neuro-fuzzy methodology with PSO algorithms had been implemented to enhance the stability of distributed system with less power consumption.	[154] [155]

Table 2.9: Neural Network Applications

Neural Network Applied for Microgrids	References
• Under the influence of disturbance, an NN identifier employed to identify and predict the dynamic parameters of parallel inverters.	[150] [151]
• A novel adaptive control algorithm for MPPT of islanded microgrid in wind turbine system.	[152]
• Subject to harmonic current, NNs are applied and studied to enhance the performance of active power filtering.	[153]

2.4.1 Particle swarm optimization (PSO)

The Particle Swarm Optimization has been a topic of interest for a while due to it is contributory in optimizing uncertain parameters for vast optimization problems.

In PSO mechanism, a velocity is computed for each particle to deduce individual position. The position is updated in each iteration in terms of behavior of individuals. Tables 2.6 and 2.7 demonstrate several applications of particle swarm and evaluation and optimization techniques. The algorithm of PSO can be written as:

1. Initialize individuals, velocity vector, and position vector.

2. Compute the velocity.

3. Compute the position.

4. Update velocity vector. [133].

The updating position vector is computed as

$$x_{P_{k+1}^i} = x_{P_k^i} + v_{P_{k+1}^i} \tag{2.6}$$

where $x_{P_k^i} \in \mathbb{R}^{n^i \times 1^i}$, is position vector, $x_{P_{k+1}^i}$ is velocity. where

$$v_{P_k^i} = v_{P_{k-1}^i} + g_1 * R_{n1} * (lbest_k - x_{P_k^i}) + g_2 * R_{n2} * (gbest_k - x_{P_k^i}) \tag{2.7}$$

where g_1, g_2 are constants, R_{n1} and R_{n2} are uniformly distributed random number. The best previous local position and global position $lbest_k$ and $gbest_k$ respectively. The initial swarm is deduced as:

$$x_{P_0}^i = x_{Pmin} + rand()(x_{Pmax} - x_{Pmin}) \tag{2.8}$$

$$v_{P_0}^i = v_{Pmin} + rand()(x_{Pmax} - x_{Pmin}) \tag{2.9}$$

The fitness function adopt according the associated problem [134].

In the later case [105], a power flow control using self-tuning strategy was investigated to optimize electric power flow in grid connected mode with varying load. The proposed controller was tested when the load is greater or smaller than prescribed power of DGs. PSO was applied to tune the controller parameters. An advanced optimal placement of distributed generation units is investigated for distribution power systems such as in Fig. 2.2. This location scheme was based on power losses and voltage derivations. A new technique base on combination of PSO and Clonal Selection Algorithm provided an optimized placement of DGs [106]. In [107], PSO algorithm using to determine the optimal position and the scale of DGs and DSTATCOM to degrading power loss. Furthermore, performance analysis was studied in terms of radial distribution.

2.4.2 Fuzzy logic control

Fuzzy logic control (FLC) is extensively utilized in a variety of challenge fields. FLC is considered as on of leading intelligently shots of distributed power optimization problems. Critical developments have been mainly investigated of FLC functions in order to provide more capability to handle issues of expert systems. Nowadays, hybrid intelligent

algorithms have been rapidly gained in popular to have the optimum use of distributed generation units, battery storage systems in distributed networks [139].

The fuzzy logic framework can be commonly combined with distributed control systems to select appropriate parameters of distributed controllers for load frequency control (LFC) , voltage control, and power sharing within microgrids. For example, FLC was presented a proper performance of four area systems with proportional integrate control [140]. In [141], the researchers implemented a hybrid FLC and tabu search algorithm (TSA) by means of LFC. In this manner, TSA is utilized to decide the fuzzy rules. Three area control was introduced based on FLC. Fuzzy control employed for self-adjusting integral gain automatic generator control [142]. Furthermore, the applications of FLC to two thermal power plants were proposed in [143][144]. In [145], a hybrid approach, genetic algorithm (GA) based FLC, have been immensely implemented to regulate two interconnected systems. In its literature, GA is being widely investigated to automatically tune and optimize the gains of the classic controller and determine the FLC function and the FLC rules. [146] used TSA algorithms with FLC to adjust the proportional integral gains in the LFC. In particular, the implementations of fuzzy logic function is in general a big challenge due to the fact that it depends based on the well knowledge of the systems. These problems can be definitely raised in complex and large scale systems. To deal with these situations, some intelligent algorithms have been commonly reported to enhance the performance of FLC by finding the near optimum solutions namely, genetic algorithm, particle swarm optimization, and differential evolution, and bacterial foraging algorithm and so on [147]. Table 2.8 lists some applications of fuzzy logic control.

2.4.3 Neural networks

The idea of neural networks are essentially coming from human brain. Neural networks have been immensely attracted in wide range of research fields. These neural networks (NNs) are effectively utilized to identify, control, optimize the system parameters in offline/online or real-time applications. Table 2.9 illustrates several applications of neural networks for control systems. Plenty of powerful functions of neural networks have been increasingly investigated to solve the problems of nonlinear and large scale systems due to their significant influence on microgrid control systems. The scope of neural networks applications include fault-tolerance, stability, parametric optimization and identification, self-learning, load sharing, and so on. Numbers of excellent results have been gained based NNs of distributed power generations [148][149]. Roughly speaking, islanded microgrids are subject to imbalance between generation units and load demands. In the grid tied operation, the main utility grid mainly determines and sustains the nominal voltage and frequency in the entire grid. However, when the microgrid is isolated, the microgrid takes an authority to adjust the voltage and frequency values to meet the attracted loads. In particular, it is tough to fix these problems with appropriate control systems or backup systems such batteries. NNs can be fruitfully used to train the system parameters by injecting enough active power from the battery system in the microgrid network to eliminate load fluctuations. Also, thus NNs function are extremely utilized to train and optimize the classical control gains in online or real-time application. An adaptive voltage sensorless technique was reported for microgrid in grid tied mode. In this technique, an NN identifier employed to identify and predict the dynamic parameters of parallel inverters. The utilization of NN identifier was associated with NN estimator to enhance the performance of microgrid system subject to

disturbance impact [150] [151].

In [152], a new adaptive control algorithm for maximum power point tracking (MPPT) of islanded minigrid composed of PMSG wind turbine was proposed. A neural network identifier developed to identify the parameters of turbine torque. In wind turbine environment, the speed can be determined by real time optimization of torque parameter using NNs. Additionally, backstepping controller was introduced to settle the speed at the desired values. Neural networks are widely applied and studied for waiving harmonic current. NNs has been strongly proposed to to enhance the performance of active power filtering against harmonic current deformity [153].

In [154] and [155], a neuro-fuzzy technology and PSO had been investigated to enhance the stability of distributed system with less power consumption. In instability case, ANFIS used to optimize power capacity of DG in micro power grid. On the other hand, particle swarm technology explored the best bus for transmission. Authors in [156] proposed an optimal control problem using adaptive continuous modulation without noise subject to time delay and packet dropout. Networked controller enable bidirectional communication in which sensing devices forward sensing data back to the control unit where the decision is take place. The controller unit transmits an actuation signal to the actuator at the plant side. ANFIS and PSO schemes are investigated to enhance the stability of DGs with less power consumption [156]. In particular, elements of the fuzzy controller are regulated on the concerning of the performance. Assuming the objective function is

$$J_k = \frac{1}{2}[y_k^2 + pfu_k^2] \tag{2.10}$$

Where f denotes the finding model, u_k is a weights, y_k is the output, and p is an

activation element. If disturbance or fault occurs, a set of input–output pairs generate from the training pattern for the suggested fuzzy controller. The selection of the sets of operating points and disturbances reflects the following:

1. The training of the controller covers the maximum change in frequency (or voltage in the case of the fuzzy voltage regulator);

2. The training data contains as much information as possible about the plant behavior for the operating wind speed velocities.

lets the applied neural network is

$$y_{k+1} = \theta_k \varphi_k + e_k \tag{2.11}$$

where θ_k is updated vector, φ_k is the variable vector, and $e(k)$ is the error.
Basically, the first and fourth layers are comprised of adaptive nodes and the second and third layers are fixed nodes [157].

2.5 Adaptive Techniques

Adaptive control techniques have been extremely studied and received more attention over decades. Adaptive control strategies are being mainly used to tackle parametric uncertainties and disturbances. Beyond any doubt, thus adaptive control strategies can be definitely sustained stability, robustness convergence, and tracking of the system dynamics. It is noted that the operating conditions of the system may be changed. As result of that the regulator performance in the plant might not be optimal. To avoid such challenges, vital adaptive solutions are extensively implemented to find near

Table 2.10: PI/PID Adaptive Techniques

Intelligent Adaptive PI/PID Techniques Applied for Microgrids	References
• Under voltage variations in islanded microgrids, NNs have been extremely utilized to implement an adaptive and distributed secondary control to adjust voltage variations.	[16]
• Neural Networks are utilized to adjust voltage and frequency variations of islanded microgrid by optimize PI gains. To achieve the desired goal, a differential evolution technique was successfully determined the training sets of NNs.	[158]

Table 2.11: Adaptive Sliding Mode Control Techniques

Intelligent Adaptive SMC Techniques Applied for Microgrids	References
• Subject to uncertainties and disturbance, a centralized adaptive SMC sustains the stability, the reliability, the performance of the standalone microgrid.	[92]
• Within a standalone grid operation, an advanced adaptive SMC is implemented with a backstepping control technology to tackle load fluctuations of wind turbine.	[159]
• An inner adaptive three-order SMC for a three-phase four-wire inverter is designed.	[160]
• An adaptive sliding mode observer tackles uncertainties of gas turbine dynamics. Also, sliding observer can enhance fault monitoring by real-time handling and detecting any deterioration.	[161]
• A nonlinear adaptive SMC is developed to sustain the stability and power propagation of the fuel cell system.	[163]

optimal operation conditions. This chapter introduces a couple the most remarkable topics of adaptive control in microgrids distributed systems namely adaptive PI/PID controller, adaptive sliding mode controller, and reinforcement learning. Figure 2.5 demonstrates some of adaptive PI droop control methodologies.

2.5.1 Adaptive PI/PID controller

In typical PID technique, the parameters of this controller have mostly selected using trial and error or some of the classic methodologies like Ziegler and Nichols, etc and

for more information can see [70]. PID with fixed gains can be strongly employed in a variety of control problems. However, when the operation condition changes due to any external disturbance or uncertainties or load variations. The PID gains definitely need to be automatically regulated to figure out these problems. To avoid such these events, various of evaluation algorithms have been extensively applied to adjust the gains of the classical control systems such PID, and sliding mode control, etc. Thus evaluation algorithms enable online and self tune of PID parameters over the maximum operating points. In [158], the voltage and frequency problems of standalone microgrid were tackled using NNs based distributed secondary control. Certainly, neural networks is a powerful utilized to train and to identify PID parameters over every possible conditions. To achieve the desired goal, a differential evolution technique was successfully determined the optimal values of PID control before training them. Furthermore, Neural networks have been extremely utilized to implement an adaptive and distributed secondary control to adjust voltage variations. NNs are mainly investigated to compensate for the uncertainties due to the unknown parameters of distributed generations. The NN weights are the control parameters [16]. Table 2.10 shows some of relevant works concerning adaptive PI/PID controllers.

2.5.2 Adaptive sliding mode controller

[92] demonstrated a significant improvement in the stability, reliability, performance of standalone microgrid using a centralized stabilizer control system. This controller is actually an adaptive robust total sliding-mode control. Microgrid is beneficial from this reliable and effective controller to handle the issues that might occur due to uncertainties and disturbances. In normal operation mode of microgrid, the SMC was utilized as

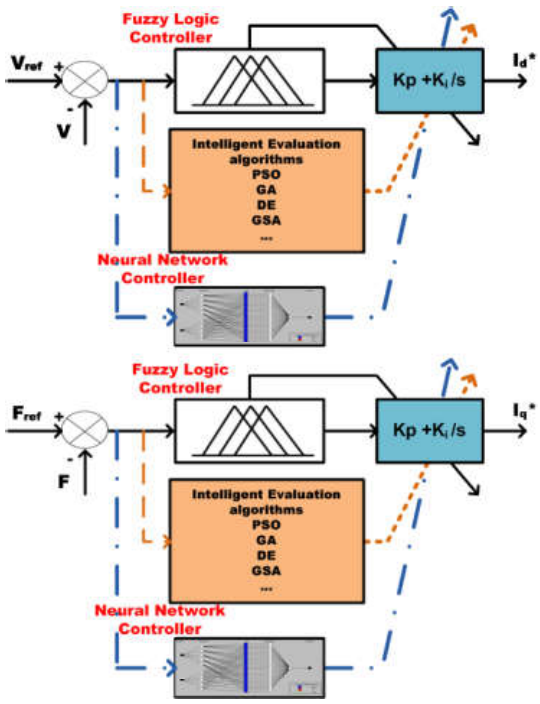

Figure 2.5: Adaptive PI droop control.

power quality (PQ) controller to regulate actual and reactive power in the main bus. Once an interruption occur, the microgrid separated for the main feeder to meet the demand of the related loads. In this sense, the SMC controller is frequently used to adjust the value of the frequency and voltage. A novel adaptive SMC (ASMC) associated with a back-stepping stroke piston controller to exactly track the pitch angle of wind turbine system and to decrease the load variations. First and foremost, ASMC was primarily implemented to control the pump displacement and enabled a seamless transit between microgrid operation modes. While the second part, the backstepping systems was in general declining the tracking error between the pitch angle and the reference one [159].

One of the significant challenges in renewable resource technology is the existence of electronic devices especially parallel inverters which consider as reason of dynamic uncertainties as well as disturbance. In [160], four-wire inverter interfaced to standalone

microgrid through three-phase wire. A high order SMC in presence of virtual output-impedance is presented. Within this architecture, the virtual output-impedance which can be employed for corresponding among impedance of the connected inverters. Thus adaptive SMC provided a powerful tool to solve voltage/frequency fluctuations and the changes of customer demands. Recently, an adaptive sliding mode observer (SMO) is investigated in order to tackle uncertainties for gas turbine system. This SMO can improve fault monitoring mechanism by real-time handling and detecting any deterioration in the system dynamics [161]. In [162], a voltage regulation technique has been developed for inverter based microgrid using an adaptive sliding mode. This adaptive controller was successfully experienced to eliminate the influence of external disturbance and parametric fluctuation. This technique needs to be executed with an appropriate tuning of the switching gain of the controller. Authors in [163], presented a nonlinear adaptive control in forms of SMC. This controller developed to maintain the stability and power propagation of an actual fuel cell system. For better performance of fuel cell, it integrated with a suitable boost converters. Also, the adaptive controller has predicted the bus impedance of the boost converter. Furthermore, it achieved appropriate voltage management and fairly current distribution. We have summarized some recent reports and their contributions in table 2.11.

2.5.3 Reinforcement learning

Heuristic dynamic programming algorithms have been extensively studied and exercised in vast fields. The theoretical developments and applications can prove that dynamic programming algorithms are vital techniques to control and to stabilize multiagents systems, complex systems, external disturbance, and uncertain systems. Within

Table 2.12: Reinforcement Learning Techniques

Adaptive Reinforcement Learning Techniques Applied for Microgrids	References
• Under load variations, a reinforcement learning based actor-critic networks is implemented for autonomous microgrid.	[164]
• To regulate frequency and voltages for islanded agents, RL is utilized to select the optimal police decisions to enhance the required system performance.	[165]
• RL algorithm can estimate wind turbine in grid connected mode to optimize battery use.	[166]

standalone operation mode, the distributed islanded microgrids can be certainly represented as multi-agents with some interactions among them. Reinforcement learning (RL) methodology has been introduced to control of standalone microgrids. Authors investigated RL in terms of actor-critic networks. In this chapter, RL based on value iteration was employed to handle load fluctuations [164]. Reinforcement learning was effectively utilized to reduce electricity prices by enhancing management process of the electric power in tied operations mode and performed to regulate frequency and voltages in the operation of islanded agents. Thus RL has the capability to determine the optimal policy decisions and the best objective function to improve the system performance [165].

Based on machine learning, reinforcement learning RL algorithm proposed to achieve customer goals for battery scheduling. This algorithm is significantly increased in the utilization of the battery in the peak load demand. RL mechanism estimate wind turbine grid connected to take good decision for better battery scheduling [166]. Table 2.12 lists several implementations of reinforcement learning with their references.

2.6 Conclusions

The above discussion highlights the need for intelligent optimization algorithms and adaptive control techniques to handle critical issues in the classical control systems due to the change of the operating points in MGs. Power electric manufacture plays a vital role in the developments of human life. The developments and techniques definitely require a constant power supply to serve the growth of customers demands. It well known that, a standalone operation of the microgrid is a big challenge due to stability issues, load variations, and communication constraints. In particular, the parameters of conventional controllers have been selected for certain operating conditions. However, in standalone operating, these parameters definitely require to retune for new operating conditions. In this spirit, we intend to use intelligent adaptive control algorithms by using fuzzy H_∞ in chapter 3, and online adaptive reinforcement learning for distributed DGs in chapter 5.

CHAPTER 3

QUANTIZED H_∞ ESTIMATOR

DG technology arises in several applications of power supply to tackle the issues of increasing energy demands. The concept of microgrids is introduced to integrate the distributed generation technology into utility power networks. This chapter introduces a fuzzy control scheme for networked systems utilizing a quantized H_∞ estimator over communication networks for distributed generations subject to random constraints. The developed estimation algorithm is worthy for ensuring the network stability and enduring any sort of quantization, time delay, and packet drops. In these senses, adequate conditions have been mainly derived by means of linear matrix inequalities. Illustrative examples are demonstrated to confirm the effectiveness of the design procedure.

3.1 Introduction

Day by day, networked control systems are being frequently utilized as a novel control for distributed generation units due to their remarkable characteristics, such as flexible, less wiring, ease maintenance and diagnosis. Distributed power generation is an emerg-

ing infrastructure predicted to rule off traditional central power plants. Thus energy resources by now include diesel motors, turbines, fuel cells, photovoltaic, and so on [11]. In particular, the DG units can be commonly associated with local loads and storage elements to make local network called microgrid. MG can perform to feed power to the utility grid, or as a standalone grid [12].

In particular, the hierarchical structure of microgrid systems consist of primary, secondary, and tertiary control. The primary control is concerning with the local layers in DGs for voltage, current, virtual impedance, and droop loops. The key idea of implementing a secondary control is to compensate voltage and frequency variations in micro power grid result of primary control loop. In contrary with primary control, the secondary control use feedback communication systems to transfer values of the MG parameters to each DG unit [66]–[67]. Shafiee et al. [63] developed a novel secondary control in droop-loop islanded microgrids.

In recent years, NCSs are introduced as one sort of successful distributed control strategies of power electrical grids [63], [64]. It is worth noting that NCSs improve the over all performance and stability for micro power grid at local loops by removing voltage and frequency variations, and inaccuracy in power sharing mechanism. Furthermore, the system reliability is sustained in existence of network constraints [64, 65, 169].

In closed loop NCS system, the stability sufficient condition and analysis have been investigated under limited tolerant packet loss. Linear quadratic Gaussian controller with output feedback has been designed for NCS to reduce the influence of data dropout on the controller performance [170].

Sufficient stability conditions and subsequent analysis of microgrids should take into consideration different communication network constraints, disturbance or faults.

In such operating conditions, the networked controller is implemented to sustain the stability of MGs. The issue of NCSs stability is being widely handled in the attendance of networks effects namely transmission delay, signals loss, and quantization [168]–[174].

A practical hold-input (HI) methodology has been used to compensate the failure in packet delivery of control signal. In this methodology, the former available input action is basically utilized by the plant [175, 176]. Unreliable characteristics of channel have been investigated by employing various compensation methodologies [175, 179, 180]. Fig. 3.1 demonstrates the influence of communication constraints on the microgrid network namely, random time delays, packets dropped and logarithmic quantization.

A dynamic output-feedback controller has been introduced for nonlinear stochastic in terms of subsequent signal lost and uniform quantization impacts [181]. In [182], an H_∞ filtering design for fuzzy model with incomplete observing premise variables. In this sense, novel line integral fuzzy Lyapunov functions has been successfully introduced to sustain a convex condition for implementing H_∞ filters. Recently, [183] reported a state estimation scheme for nonlinear cyber-physical systems in which a Takagi–Sugeno fuzzy systems were utilized to model the nonlinear dynamical systems. The cyber networked assumed to be subject to sensor saturation, quantization, signal lost.

In this chapter, we study a fuzzy networked control system in the presence of communication constraints using hold input scheme to compensate for the control signals. Furthermore, we tackle the problem of communication networks constraints namely quantization, random time delay, and packet dropouts using a quantizer H_∞ to sustain the stability of a prescribed microgrid system with several distributed generation units. Accordingly, this study is concerning with the investigation of a fuzzy networked controller for standalone microgrid based on hold input strategy and casting the design

results in the framework of linear matrix inequalities (LMIs) [173], [174]. Evidently, it can be achieved that the proposed approach is well-delineated, and the prediction error system is asymptotically stable in the sense of performance measure γ.

The structure of this chapter is such that, a mathematical model is clearly defined in section 3.2. Secondly, the sufficient condition of steady state transient is in general developed. The simulation examples are utilized to demonstrate the effectively of our approach in 3.6 part. Lastly, concludes the chapter.

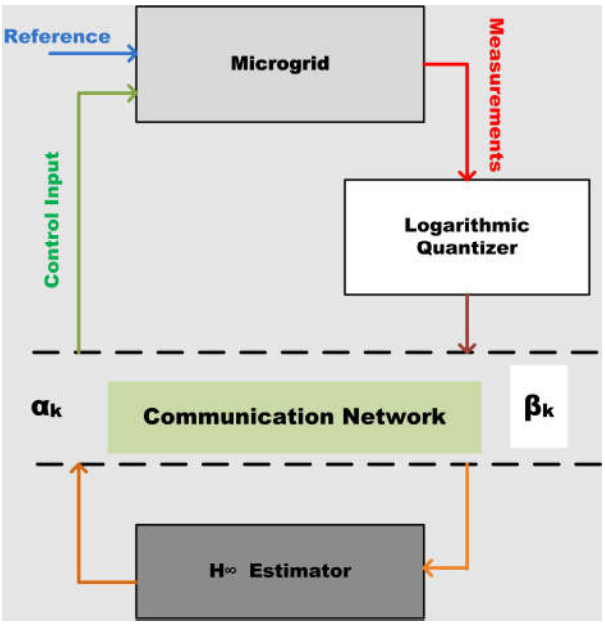

Figure 3.1: A typical Microgrid System.

3.2 Microgrid System Modeling

Microgrid (or minigrid) has capability to serve as small power sources supplying the utility grid, or to perform as standalone grid. Usually, MG operates in grid-connected mode but if any fault or disturbance occurs it is shifted to islanded operation mode. Microgrid has the ability to operate in interconnected, islanded, or transition operation

mode [2]. In this section, a mathematical model of microgrid operated in islanded operation mode is implemented. The configuration of a host microgrid integrates n distributed generations and related loads can be exhibited in Fig. 3.2.

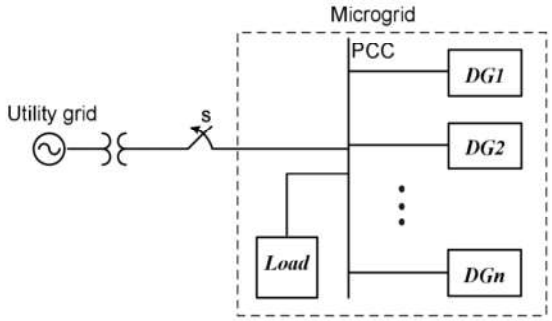

Figure 3.2: MG associated with n DGs

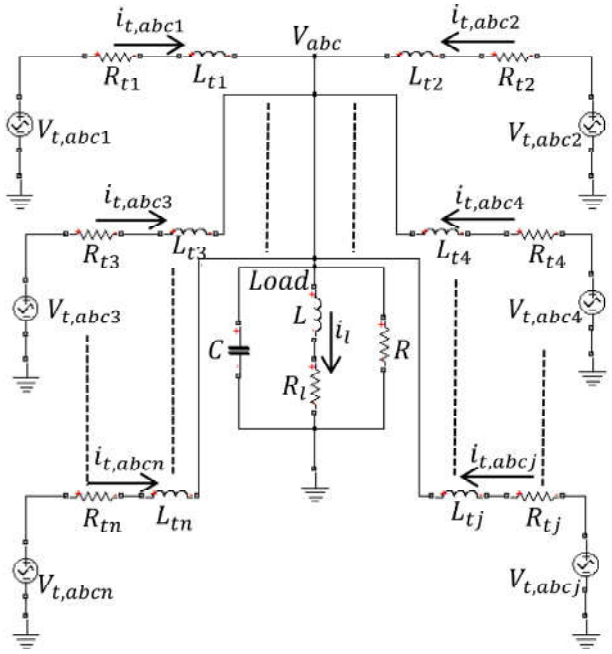

Figure 3.3: Structure of the standalone microgrid comprises of numerous DGs

To derive a linear model for microgrid system using Kirchhoffs voltage KVL and current KCL laws, every DG unit is represented by a directed current source attached with a voltage source inverter and an RL filter. The typically distributed systems of the microgrid incorporate three DGs, the following equations are deduced

$$
\begin{aligned}
v_{abc} &= L\frac{di_{L,abc}}{dt} + R_l i_{L,abc} \\
v_{t,abc_1} &= L_{t_1}\frac{di_{t,abc_1}}{dt} + R_{t_1} i_{t,abc_1} + v_{abc} \\
v_{t,abc_2} &= L_{t_2}\frac{di_{t,abc_2}}{dt} + R_{t_2} i_{t,abc_2} + v_{abc} \\
v_{t,abc_3} &= L_{t_3}\frac{di_{t,abc_3}}{dt} + R_{t_3} i_{t,abc_3} + v_{abc} \\
& i_{t,abc_1} + i_{t,abc_2} + i_{t,abc_3} \\
&= \frac{1}{R} v_{abc} + i_{L,abc} + C\frac{dv_{abc}}{dt}
\end{aligned} \tag{3.1}
$$

where a, b and c stand for the three stator phases, steady state equations (3.1), $v_{abc}, v_{t,abc_i}, i_{L,abc}, i_{t,abc_i}$, are essentially 3×1 vectors that contain the phase quantities, and $i = 1 : 3$. Using transformation ($abc\, to\, \alpha\beta$), the 3-phase arbitrary x_{abc} in (3.1) is transformed to a $\alpha\beta$ reference structure.

$$
x_{\alpha\beta} = x_a e^{j0} + x_b e^{j\frac{2\pi}{3}} + x_c e^{j\frac{4\pi}{3}} \tag{3.2}
$$

In this respect: $x_{\alpha\beta} \triangleq x_\alpha + jx_\beta$. The dynamics in the $\alpha\beta$ frame is expressed as

$$\begin{aligned}
&\frac{dv_{\alpha\beta}}{dt} = -\frac{1}{RC}v_{\alpha\beta} + \frac{1}{C}i_{t,\alpha\beta_1} - \frac{1}{C}i_{L,\alpha\beta} \\
&+\frac{1}{C}i_{t,\alpha\beta_2} + \frac{1}{C}i_{t,\alpha\beta_3} \\
&\frac{di_{t,\alpha\beta_1}}{dt} = -\frac{R_{t_1}}{L_{t_1}}i_{t,\alpha\beta_1} - \frac{1}{L_{t_1}}v_{\alpha\beta} + \frac{1}{L_{t_1}}v_{t,\alpha\beta_1} \\
&\frac{di_{L,\alpha\beta}}{dt} = \frac{1}{L}v_{\alpha\beta} - \frac{R_l}{L}i_{L,\alpha\beta} \\
&\frac{di_{t,\alpha\beta_2}}{dt} = -\frac{R_{t_2}}{L_{t_2}}i_{t,\alpha\beta_2} - \frac{1}{L_{t_2}}v_{\alpha\beta} + \frac{1}{L_{t_2}}v_{t,\alpha\beta_2} \\
&\frac{di_{t,\alpha\beta_3}}{dt} = -\frac{R_{t_3}}{L_{t_3}}i_{t,\alpha\beta_3} - \frac{1}{L_{t_3}}v_{\alpha\beta} + \frac{1}{L_{t_3}}v_{t,\alpha\beta_3}
\end{aligned} \tag{3.3}$$

By adapting (3.3) to its basis as:

$$x_{\alpha\beta} = x_{dq}e^{j\theta} = (x_d + jx_q)e^{j\theta} \tag{3.4}$$

$\theta(t) \triangleq \int_0^t \omega(\zeta)d\zeta + \theta_0$. $\theta(t)$ adapts the phase angle of a reference vector $(x_\alpha^{ref} + jx_\beta^{ref})$ in the $\alpha\beta$ frame. The directquadrature (dq) reference frame reduces the three AC quantities (abc frame) or rotating two phase (α β $gamma$) to two DC quantities. The dq-frame equations are represent as following:

$$\begin{aligned}
&\frac{dV_{dq}}{dt} + j\omega_0 V_{dq} = -\frac{1}{RC}V_{dq} + \frac{1}{C}I_{t,dq_1} - \frac{1}{C}I_{L,dq} + \frac{1}{C}I_{t,dq_2} + \frac{1}{C}I_{t,dq_3}, \\
&\frac{dI_{t,dq_1}}{dt} + j\omega_0 I_{t,dq_1} = -\frac{1}{L_{t_1}}V_{dq} - \frac{R_{t_1}}{L_{t_1}}I_{t,dq_1} + \frac{1}{L_{t_1}}V_{t,dq_1}, \\
&\frac{dI_{L,dq}}{dt} + j\omega_0 I_{L.dq} = \frac{1}{L}V_{dq} - \frac{R_l}{L}I_{L,dq}, \\
&\frac{dI_{t,dq_2}}{dt} + j\omega_0 I_{t,dq_2} = -\frac{1}{L_{t_2}}V_{dq} - \frac{R_{t_2}}{L_{t_2}}I_{t,dq_2} + \frac{1}{L_{t_2}}V_{t,dq_2} \\
&\frac{dI_{t,dq_3}}{dt} + j\omega_0 I_{t,dq_3} = -\frac{1}{L_{t_3}}V_{dq} - \frac{R_{t_3}}{L_{t_3}}I_{t,dq_3} + \frac{1}{L_{t_3}}V_{t,dq_3}
\end{aligned}$$

Table 3.1: Parameters of the DGs [177],[178].

Quantity	Value
R_{t1}	$15 \times e^{-4}\ \Omega$
L_{t1}	$0.3 \times e^{-3}\ H$
R_{t2}	$0.6 \times e^{-4}\ \Omega$
L_{t2}	$0.9 \times e^{-3}\ H$
R_{t3}	$9 \times e^{-3}\ \Omega$
L_{t3}	$1.2 \times e^{-3}\ H$
R	$76\ \Omega$
R_l	$1.35\ \Omega$
L	$0.112 \times e^{-3}\ H$
C	$0.0629 \times e^{-3}\ F$
q	120
f_0	$60\ Hz$

$$A_{mg} = \begin{bmatrix} -\frac{1}{RC} & -\omega_0 & \frac{1}{C} & 0 & -\frac{1}{C} & 0 & \frac{1}{C} & 0 & \frac{1}{C} & 0 \\ -\omega_0 & -\frac{1}{RC} & 0 & \frac{1}{C} & 0 & -\frac{1}{C} & 0 & \frac{1}{C} & 0 & \frac{1}{C} \\ -\frac{1}{L_{t1}} & 0 & -\frac{R_{t1}}{L_{t1}} & \omega_0 & 0 & 0 & 0 & 0 & 0 & 0 \\ 0 & -\frac{1}{L_{t1}} & -\omega_0 & -\frac{R_{t1}}{L_{t1}} & 0 & 0 & 0 & 0 & 0 & 0 \\ \frac{1}{L} & 0 & 0 & 0 & -\frac{R_l}{L} & \omega_0 & 0 & 0 & 0 & 0 \\ 0 & \frac{1}{L} & 0 & 0 & -\omega_0 & -\frac{R_l}{L} & 0 & 0 & 0 & 0 \\ -\frac{1}{L_{t2}} & 0 & 0 & 0 & 0 & 0 & -\frac{R_{t2}}{L_{t2}} & \omega_0 & 0 & 0 \\ 0 & -\frac{1}{L_{t2}} & 0 & 0 & 0 & 0 & -\omega_0 & -\frac{R_{t2}}{L_{t2}} & 0 & 0 \\ -\frac{1}{L_{t_3}} & 0 & 0 & 0 & 0 & 0 & 0 & 0 & -\frac{R_{t_3}}{L_{t_3}} & \omega_0 \\ 0 & -\frac{1}{L_{t_3}} & 0 & 0 & 0 & 0 & 0 & 0 & -\omega_0 & -\frac{R_{t_3}}{L_{t_3}} \end{bmatrix}$$

$$B_{mg} = \begin{bmatrix} 0 & 0 & 0 & 0 & 0 & 0 \\ 0 & 0 & 0 & 0 & 0 & 0 \\ \frac{1}{L_{t1}} & 0 & 0 & 0 & 0 & 0 \\ 0 & \frac{1}{L_{t1}} & 0 & 0 & 0 & 0 \\ 0 & 0 & 0 & 0 & 0 & 0 \\ 0 & 0 & 0 & 0 & 0 & 0 \\ 0 & 0 & \frac{1}{L_{t2}} & 0 & 0 & 0 \\ 0 & 0 & 0 & \frac{1}{L_{t2}} & 0 & 0 \\ 0 & 0 & 0 & 0 & \frac{1}{L_{t_3}} & 0 \\ 0 & 0 & 0 & 0 & 0 & \frac{1}{L_{t_3}} \end{bmatrix}; C_{mg} = \begin{bmatrix} 1 & 0 & 0 & 0 & 0 & 0 \\ 0 & 1 & 0 & 0 & 0 & 0 \\ 0 & 0 & 0 & 0 & 0 & 0 \\ 0 & 0 & 0 & 0 & 0 & 0 \\ 0 & 0 & 0 & 0 & 0 & 0 \\ 0 & 0 & 0 & 0 & 0 & 0 \\ 0 & 0 & 1 & 0 & 0 & 0 \\ 0 & 0 & 0 & 1 & 0 & 0 \\ 0 & 0 & 0 & 0 & 1 & 0 \\ 0 & 0 & 0 & 0 & 0 & 1 \end{bmatrix}^T$$

Reproducing the aforementioned equations, the states are $x = [V_d, V_q, I_{td_1}, I_{tq_1}, I_{Ld}I_{Lq}, I_{td_2}, I_{tq_2}, I_{td_3}, I_{tq_3}]$, the control vector $u = [V_{td_1}, V_{tq_1}, V_{td_2}V_{tq_2}, V_{td_3}, V_{tq_3}]$ and measurement vector is $y = [V_d, V_q, I_{td_2}, I_{tq_2}, I_{td_3}, I_{tq_3}]$. The state space model of standalone MG can be deduce as [177]

$$\dot{x}_{mg}(t) = A_{mg}x_{mg}(t) + B_{mg}u_{mg}(t)$$

$$y_{mg}(t) = C_{mg}x_{mg}(t)$$

where the state variable $x_{mg}(t) \in \Re^{n\times 1}$, $u_{mg}(t) \in \Re^{m\times 1}$; is the control input, and $y_{mg}(t) \in \Re^{m\times 1}$ is the output signal. The matrices of dynamic system can be qualified as the system $A_{mg} \in \Re^{n\times n}$, the input $B_{mg} \in \Re^{n\times m}$, and the observations $C_{mg} \in \Re^{m\times n}$. The parameter values are stated in Table 1 [177].

3.3 Networked Control Modeling

Consider the following class of NCSs with quantization and random packet dropped effects, this setup is summarized in Fig. (3.1). The dynamic discrete system of microgrid

is described by

$$
\begin{aligned}
& For \quad k = 1, 2, ..., n \\
& IF \ \ \theta_{k1} \ \ is \ \ M_{k1}^{l} \ \ and \ \ ...and \, \theta_{kp} \ \ is \ \ M_{kp}^{l} \ \ THEN \\
x_{k+1} &= A_{mg}^{l} x_k + \alpha_k^{l} B_{mg}^{l} u_k + (1 - \alpha_k^{l}) B_{mg}^{l} \xi_k + w_k \\
\xi_{k+1} &= \alpha_k^{l} \xi_k + (1 - \alpha_k^{l}) u_k; \\
y_k &= \beta_k^{l} (C_{mg}^{l} x_k + v_k) \\
z_k &= G^{l} x_k + v_k; \qquad k = 0, 1, 2..N
\end{aligned} \tag{3.5}
$$

Where $\theta_{k1}, ... \ \ and \ \ \theta_{kp}$, illustrate the premise variables, $M_{k1}^{l}, ... \ \ and \ \ M_{kp}^{l}$ $i = 1, 2..n$, illustrate the fuzzy rules. ξ_k denotes the tracking state, $x_k \ \in \Re^n$ is the actual state, $u_k \ \in \Re^m$; is the actuation signal, and $w_k, v_k \ \in \Re^q$ are state and output disturbances. For $l = 1, 2, ..., r$, A_{mg}^{l}, B_{mg}^{l}, C_{mg}^{l} large system matrices of rule-l with appropriate dimensions. The controlled output is $z_k \ \in \Re^q$, which is the signal to be estimated.

The measured output y_k is transmitted through a logarithmic quantizer that yields y_k. The network constraints namely packet dropout can be represented by two Bernoulli probability processes α_k and β_k for controller/actuator and sensor/controller respectively. Also, the set of quantized levels be defined as

$$
\begin{aligned}
\mathcal{V} &= \{\pm v_j, \ v_j = \sigma^j v_0, \ j = 0, \pm 1, \ \pm 2, ...\} \cup \{0\}, \\
& 0 < \sigma < 1, \ v_0 \ > \ 0
\end{aligned}
$$

In which σ, $\mathbf{q}(.)$ denote the density and the function of the logarithmic quantizer. The

later can be prescribed as [208]:

$$\mathbf{q}(\eta) = \begin{cases} v_j, & if\ v_{mj} < \eta \leq v_{Mj}, \\ 0, & if\ \eta = 0, \\ -\mathbf{q}(-\eta), & if\ \eta < 0 \end{cases} \tag{3.6}$$

where $\omega = (1-\sigma)/(1+\sigma),\ v_{mj} = v_j/(1+\omega),\ v_{Mj} = v_j/(1-\omega)$. The quantizer impacts is bounded for σ such that:

$$\mathbf{q}(\eta)\ -\ \eta\ =\ \mathbf{\Delta}\eta,\ \ ||\mathbf{\Delta}||\ \leq\ \omega \tag{3.7}$$

The control system is developed to sustain the appropriate systems performance (3.5) in the presence of communication constraints.

$$y_k = \begin{cases} (1+\mathbf{\Delta})(C^l_{mg}x_k + v_k), & \beta^l_k = 0 \\ (1+\mathbf{\Delta})(C^l_{mg}x_{k-\tau^m} + v_{k-\tau^m}), & \beta^l_k = 1 \end{cases} \tag{3.8}$$

where τ^m is measurement time delay. The unreliable aspects of the links is formed by Bernoulli process as:

$$Prob(\beta_k) = \begin{cases} m_k; & \text{if } \beta_k = 1; \\ 1 - m_k = \bar{m}_k; & \text{if } \beta_k = 0. \end{cases}$$

and

$$Prob(\alpha_k) = \begin{cases} p_k; & \text{if } \alpha_k = 1; \\ 1 - p_k = \bar{p}_k; & \text{if } \alpha_k = 0. \end{cases}$$

We could also develop in following form:

$$\begin{aligned}
\bar{x}_{k+1} &= \begin{bmatrix} x_k \\ \xi_k \end{bmatrix} \\
&= \begin{bmatrix} A^l_{mg} & (1-\alpha^l_k)B^l_{mg} \\ 0 & \alpha^l_k I_k \end{bmatrix} \bar{x}_k \\
&+ \begin{bmatrix} \alpha^l_k B^l_{mg} \\ (1-\alpha^l_{k-1})I_k \end{bmatrix} \bar{u}_k + \begin{bmatrix} I_k \\ 0 \end{bmatrix} \bar{w}_k \qquad (3.9) \\
\bar{y}_k &= (1+\mathbf{\Delta}) \begin{bmatrix} \beta^l_k C^l_{mg} & 0 \end{bmatrix} \bar{x}_k + (1+\mathbf{\Delta}) \begin{bmatrix} I_{vk} \\ 0 \end{bmatrix} \bar{v}_k \qquad (3.10)
\end{aligned}$$

In this sense, the new state is further illustrated as:

$$\begin{aligned}
\bar{x}_{k+1} &= A^l_k \bar{x}_k + B^l_k \bar{u}_k + B_{wk} \bar{w}_k \\
\bar{y}_k &= (1+\mathbf{\Delta})(C^l_k \bar{x}_k + D_{vk} \bar{v}_k) \qquad (3.11)
\end{aligned}$$

where

$$\begin{aligned}
A^l_k &= \begin{bmatrix} A^l_{mg} & (1-\alpha^l_k)B^l_{mg} \\ 0 & \alpha^l_k I_k \end{bmatrix}, \; B^l_k = \begin{bmatrix} \alpha^l_k B^l_{mg} \\ (1-\alpha^l_{k-1})I_k \end{bmatrix}, \\
C^l_k &= \begin{bmatrix} \beta^l_k C^l_{mg} & 0 \end{bmatrix}; \; B_{wk} = \begin{bmatrix} I_k \\ 0 \end{bmatrix}; \; D_{vk} = \begin{bmatrix} I_{vk} \\ 0 \end{bmatrix}
\end{aligned}$$

The output of the fuzzy system is deduced as:

$$\begin{aligned} \bar{x}_{k+1} &= \sum_{l=1}^{r} H_k^l \left\{ A_k^l \bar{x}_k + B_k^l \bar{u}_k + B_{wk} \bar{w}_k \right\} \\ \bar{y}_k &= \sum_{l=1}^{r} H_k^l \left\{ (1 + \mathbf{\Delta})(C_k^l \bar{x}_k + D_{vk} \bar{v}_k) \right\} \end{aligned} \tag{3.12}$$

With $\bar{A}_k^l = \sum_{l=1}^{r} H_k^l A_k^l$, $\bar{B}_k^l = \sum_{l=1}^{r} H_k^l B_k^l$, $\bar{C}_k^l = \sum_{l=1}^{r} H_k^l C_k^l$, $\bar{B}_{wk} = \sum_{l=1}^{r} H_k B_{wk}$, $\bar{D}_{vk} = \sum_{l=1}^{r} H_k D_{vk}$, we deduce:

$$\begin{aligned} \bar{x}_{k+1} &= \bar{A}_k \bar{x}_k + \bar{B}_k \bar{u}_k + \bar{B}_{wk} \bar{w}_k \\ \bar{y}_k &= (1 + \mathbf{\Delta})(\bar{C}_k^l \bar{x}_k + \bar{D}_{vk} \bar{v}_k) \end{aligned} \tag{3.13}$$

In case of one or few parameters are lost, a hold input strategy can be utilized to compensate for the lost signals. Furthermore, an estimator strategy is implemented to estimate unknown states in the presence of disturbance.

$$\hat{\bar{x}}_{k+1} = A_k \bar{x}_k + B_k \bar{u}_k + L_o^l (\bar{y}_k - \hat{\bar{y}}_k) \tag{3.14}$$

Where L_o^l denotes the estimator gain. $\hat{(...)}$ are the estimated parameters The fuzzy logic observations:

$For \quad k = 1, 2, ..., n$

$IF \;\; \theta_{k1} \;\; is \;\; M_{k1}^l \;\; and \;\; ...and \, \theta_{kp} \;\; is \;\; M_{kp}^l \;\; THEN$

$$\begin{aligned}\hat{\bar{x}}_{k+1} &= \sum_{l=1}^{r} H_k^l \left\{ A_k \bar{x}_k + B_k \bar{u}_k + L_o^l (\bar{y}_k - \hat{\bar{y}}_k) \right\} \\ &= \bar{A}_k \bar{x}_k + \bar{B}_k \bar{u}_k + L^l (\bar{y}_k - \hat{\bar{y}}_k) \end{aligned} \tag{3.15}$$

where $L^l = \sum_{l=1}^{r} H_k^l L_o^l$.

$$\hat{\bar{y}}_k = \begin{cases} (1 + \boldsymbol{\Delta}) C_k \hat{\bar{x}}_k, \;\; \beta_k = 0 \\ (1 + \boldsymbol{\Delta}) C_k \hat{\bar{x}}_{k-\tau^m}, \;\; \beta_k = 1 \end{cases} \tag{3.16}$$

The fuzzification estimated outputs:

$$\begin{aligned}\hat{\bar{y}}_k &= \sum_{l=1}^{r} H_k^l \left\{ (1 + \boldsymbol{\Delta}) C_k \bar{x}_k \right\} \\ &= (1 + \boldsymbol{\Delta}) \bar{C}_k \bar{x}_k \end{aligned} \tag{3.17}$$

$\hat{\bar{x}}_k \in \Re^n$, $\hat{\bar{y}}_k \in \Re^p$, and $L \in \Re^{n \times p}$ denote the estimator state, output , and gain receptively.

3.4 Control Design

A reliable compensator scheme has been extremely utilized to sustain a constant operation of the system in the presence of the control signal lost. The tracking control input is given by

$$\bar{u}_k = -K_o^l \hat{\bar{x}}_k + r$$

The applied tracking controller can be stated as

$$u_{pk} = \begin{cases} -K_o^l \hat{\bar{x}}_k + r; & \text{if } \alpha_k = 0; \\ u_{pk-\tau^c} \equiv u_{pk-1}; & \text{if } \alpha_k = 1. \end{cases}$$

where τ^c is the time delay occur for the control signal.

$$For \quad k = 1, 2, ..., n$$

$$IF \;\; \theta_{k1} \;\; is \;\; M_{k1}^l \;\; and \;\; ...and \, \theta_{kp} \;\; is \;\; M_{kp}^l \;\; THEN$$

$$\bar{u}_k \;\; = \;\; \sum_{l=1}^{r} H_k^l \left\{ -K_o^l \hat{\bar{x}}_k + r \right\}$$

$K^l = \sum_{l=1}^{r} H_k^l K_o^l$. Hence, the stability and filter synthesis issues of the error estimator have been studied by means of packet dropouts $\beta = \alpha = 1$. The error $e_{k+1} = \bar{x}_{k+1} - \hat{\bar{x}}_{k+1}$ can be introduced as

$$\begin{aligned} e_{k+1} \;\; = \;\; & \bar{A}_k e_k - (1 + \mathbf{\Delta}) L \bar{C} e_{k-\tau^m} + \bar{B}_{wk} \bar{w}_k \\ & -(1 + \mathbf{\Delta}) L \bar{v}_k \end{aligned} \tag{3.18}$$

The intention is to develop intelligent observer to sustain the stability and the performance of the system (3.5) subjects to networks constraints, so that the error (3.18) is exponentially stable.

3.5 Main Results

This part provides the stability analysis for constrained process.The error dynamic is mainly implemented and studied. Furthermore, related capital and sufficient stability situations have been evolved in terms of appropriate Lyapunov functions.

$$\begin{aligned} V(e_k) &= \sum_{i=1}^{3} V_i(e_k), V_1(e_k) = \sum_{j=1}^{2} e_k^T P e_k \\ V_2(e_k) &= \sum_{j=1}^{2} \sum_{i=k-\tau_k^m}^{3} e_k^T Q_j e_k, \\ V_3(e_k) &= \sum_{j=1}^{2} \sum_{l=-\tau_m^+ +2}^{-\tau_m^- +1} \sum_{i=k+l-1}^{k-1} e_k^T Q_j e_k, \end{aligned} \tag{3.19}$$

where $Q_j = Q_j^T \geq 0$ $P_j > 0$s. If there exist items $\mu > 0$ and $\eta > 0$ cause $\mu \|e\|^2 \leq V(e_k) \leq \eta \|e_k\|^2$. The former consequence is definitely settled using the coming theorem:

Theorem 3.1 *Supposing that the gains matrices K^l and L^l are well-known. The error system 3.18 under HI strategy is exponentially stable if there exist matrices $0 < P_j = P_j^T$, and $0 < Q_j = Q_j^T, j = 1, 2, .., 4$ and matrices R, S, and M so that LMIs holds.*

$$
\begin{aligned}
\Lambda_j &= \begin{bmatrix} \Lambda_{1j} & \Lambda_{2j} & G^T \\ \bullet & \Lambda_{3j} & 0 \\ \bullet & \bullet & -I \end{bmatrix} < 0 \\
\Lambda_{1j} &= \begin{bmatrix} \Psi_j + \Phi_{j1} & -R + S^T & \Sigma_1 \\ \bullet & -S - S^T - \sigma_j Q_j & 0 \\ \bullet & \bullet & \Sigma_2 \end{bmatrix} \\
\Lambda_{2j} &= \begin{bmatrix} \Phi_{j2} & \Phi_{j7} \\ -S - M^T & 0 \\ \Phi_{j5} & \Phi_{j8} \end{bmatrix} \\
\Lambda_{3j} &= \begin{bmatrix} -M + M^T + \Phi_{j4} & \Phi_{j9} \\ \bullet & \Phi_{j10} \end{bmatrix}
\end{aligned} \tag{3.20}
$$

where

$$
\begin{aligned}
\Sigma_1 &= -R + M^T + \Phi_{j6}; \quad \Sigma_2 = -M - M^T - \Phi_{3j} \\
\Psi_j &= -P + R + R^T + \hat{\sigma}_j(1 + \tau_m^+ - \tau_m^+)Q_j, \\
\Phi_{j1} &= (\bar{A}_k - (1+\boldsymbol{\Delta})L\bar{C}_k)^T P * (\bar{A}_k - (1+\boldsymbol{\Delta})L\bar{C}_k) \\
\Phi_{j2} &= (\bar{A}_k - (1+\boldsymbol{\Delta})L\bar{C}_k)^T P\bar{B}_w, \\
\Phi_{j3} &= (1+\boldsymbol{\Delta})\bar{C}_k^T L^T P(1+\boldsymbol{\Delta})L\bar{C}_k; \;\; \Phi_{j4} = \bar{B}_w^T P\bar{B}_w, \\
\Phi_{j5} &= \bar{B}_w^T P(1+\boldsymbol{\Delta})L\bar{C}_k, \\
\Phi_{j6} &= (\bar{A}_k - (1+\boldsymbol{\Delta})L\bar{C}_k)^T P(1+\boldsymbol{\Delta})L\bar{C}_k, \\
\Phi_{j7} &= (\bar{A}_k - (1+\boldsymbol{\Delta})L\bar{C}_k)^T P(1+\boldsymbol{\Delta})L, \\
\Phi_{j8} &= (1+\boldsymbol{\Delta})L^T P(1+\boldsymbol{\Delta})L\bar{C}_k, \\
\Phi_{j9} &= \bar{B}_w^T P(1+\boldsymbol{\Delta})L, \;\; \Phi_{j10} = (1+\boldsymbol{\Delta})L^T P(1+\boldsymbol{\Delta})L.
\end{aligned}
$$

Proof.

Defining

$$
e_{k-\tau_k^m} = e_k - \sum_{i=k-\tau_k^m}^{k-1} y_i = e_k - \lambda_k \tag{3.21}
$$

We rewrite the estimator error (3.18) using above equation (3.21) such:

$$
\begin{aligned}
e_{k+1} &= (\bar{A}_k - (1+\boldsymbol{\Delta})L\bar{C})e_k + (1+\boldsymbol{\Delta})L\bar{C}\lambda_k \\
&\quad + \bar{B}_{wk}\bar{w}_k - (1+\boldsymbol{\Delta})L\bar{v}_k
\end{aligned} \tag{3.22}
$$

for some matrices R, S, and M

$$2[e_k^T R + e_{k-\tau_k^m}^T S + \lambda_k^T M][e_k - e_{k-\tau_k^m} - \lambda_k] = 0 \tag{3.23}$$

Evaluating the $\Delta V_1(e_k)$

$$\begin{aligned}
&\mathbb{E}[\Delta V_1(e_k)] = V_1(e_{k+1}) - V_1(e_k) \\
&= \sum_{j=1}^{4} \big[e_k^T [\Phi_{j1} - P] e_k + 2 e_k^T \Phi_{j2} \bar{w}_k + 2 e_k^T \Phi_{j6} \lambda_k \\
&-2 e_k^T \Phi_{j7} \bar{v}_k + \lambda_k^T \Phi_{j3} \lambda_k + 2 \bar{w}_k^T \Phi_{j5} \lambda_k \\
&-2 \bar{v}_k^T \Phi_{j8} \lambda_k + \bar{w}_k^T \Phi_{j4} \bar{w}_k - 2 \bar{w}_k^T \Phi_{j9} \bar{v}_k + \bar{v}_k^T \Phi_{j10} \bar{v}_k \big]
\end{aligned} \tag{3.24}$$

the difference of V_2 is described by

$$\begin{aligned}
&\mathbb{E}[\Delta V_2(e_k)] = \sum_{j=1}^{2} \sigma_j \big[\sum_{i=k+1-\tau_{k+1}^m}^{k} e_i^T Q_j e_i - \sum_{i=k-\tau_k^m}^{k-1} e_i^T Q_j e_i \big] \\
&= e_k^T Q_j e_k - e_{k-\tau_k^m}^T Q_j e_{k-\tau_k^m} + \sum_{i=k+1-\tau_{k+1}^m}^{k-1} e_i^T Q_j e_i - \sum_{i=k-\tau_k^m}^{k-1} e_i^T Q_j e_i \\
&\leq \sum_{j=1}^{2} \sigma_j \big[e_k^T Q_j e_k - e_{k-\tau_k^m}^T Q_j e_{k-\tau_k^m} + \sum_{i=k+1-\tau_m^+}^{k-\tau_m^-} e_i^T Q_j e_i \big]
\end{aligned} \tag{3.25}$$

the difference of V_3 can be expressed by

$$\begin{aligned}
\mathbb{E}[\Delta V_3(e_k)] &= \sum_{j=1}^{2} \sigma_j \big[\sum_{l=2-\tau_m^+}^{1-\tau_m^-} e_k^T Q_j e_k - e_{k+l-1}^T Q_j e_{k+l-1} \big] \\
&= \sum_{j=1}^{2} \sigma_j \big[(\tau_m^+ - \tau_m^-) e_k^T Q_j e_k - \sum_{i=k+1-\tau_m^+}^{k-\tau_m^-} e_i^T Q_j e_i \big]
\end{aligned} \tag{3.26}$$

On combining equation from (3.16)-(3.19), we get

$$\begin{aligned}
&\mathbb{E}[\Delta V(e_k)] = \mathbb{E}[V(e_{k+1})] - V(e_k) \\
\leq\ & \sum_{j=1}^{4} \sigma_j \big[e_k^T[\Psi_j + \Phi_{j1}]e_k + \sum_{j=1}^{2} e_k^T(-2R + 2S^T)e_{k-\tau_k^m} + e_k^T(-2R + 2M^T - 2\Phi_{j6})\lambda_k \\
&+ e_{k-\tau_k^m}^T(-S - S^T - \sigma_j Q_j)\zeta_{k-\tau_k^m} + e_{k-\tau_k^m}^T(-2S - 2M^T)\lambda_k + \lambda_k^T(-M - M^T + \Phi_{j3})\lambda_k \\
&+ \bar{w}_k^T \Phi_{j4} \bar{w}_k + 2\bar{w}_k^T \Phi_{j5} \lambda_k + 2e_k^T \Phi_{j2} \bar{w}_k \big] \\
=\ & \sum_{j=1}^{4} \sigma_j [e_k^T \widetilde{\Lambda}_j e_k] \qquad (3.27)
\end{aligned}$$

where $\zeta_k = [e_k^T\ e_{k-\tau_k^m}^T\ \lambda_k^T\ \bar{w}_k^T]$,

Consider the objective function

$$J_k \ = \ \sum_{0}^{\infty} (z_k^T z_k - \gamma^2 \bar{w}_k^T \bar{w}_k) \leq \sum_{0}^{\infty} (z_k^T z_k - \gamma^2 \bar{w}_k^T \bar{w}_k) \qquad (3.28)$$

For $\bar{w}_k \in \ell[0;\ \infty) \neq 0$, with zero initial condition, we deduce

$J_k = \sum_{\kappa=0}^{k} (z_k^T z_k - \gamma^2 \bar{w}_k^T \bar{w}_k + \Delta V(x)|_1 - \Delta V(e_k)|_1)$

$\leq \sum_{\kappa=0}^{k} (z_k^T z_k - \gamma^2 \bar{w}_k^T \bar{w}_k + \Delta V(x)|_1)$

where $\Delta V(x)|_1$ describes the difference of the Lyapunov functions, we possess

$$z_k^T z_k - \gamma^2 \bar{w}_k^T \bar{w}_k + \Delta V(e_k)|_1 = \sum_{j=1}^{4} \sigma_j [e_k^T \bar{\Lambda}_j e_k] \qquad (3.29)$$

where $\widehat{\Lambda}_j$ adapts with Λ_j in (3.20) by Schur complements. It is shown that $z_k^T z_k - \gamma^2 \bar{w}_k^T \bar{w}_k + \Delta V(e_k)|_1 < 0$

where$\kappa \in [0, k]$, indicates for each $\bar{w}_k \in \ell\ [0,\infty] \neq 0$ that $J < 0$ causes $\|z_k\|_2 < \gamma \|\bar{w}_k\|_2$

Therefore, it can be proved that the error system (3.18) is exponential stable. By this, the proof is finalized. ∎

The coming theorem contributes a developed scheme by determining the gains of the proposed methodology:

Theorem 3.2 *The error system* (3.18) *is exponentially stable if there exist matrices* $0 < X, Y_1, Y_2,\ 0 < \Xi_j,\ j = 1, .., 4$ *, so that the following matrix inequality holds for* $j = 1, .., 4$ *:*

$$\begin{bmatrix} \widehat{\Lambda}_{1j} & \widehat{\Lambda}_{2j} & \widehat{\Omega}_j & \widehat{\Omega}_j & 0 & \widehat{X}\widehat{G}^T \\ \bullet & \widehat{\Lambda}_{3j} & 0 & 0 & 0 & 0 \\ \bullet & \bullet & -\widehat{X} & \widehat{X}\,\widehat{\Gamma}^T & 0 & 0 \\ \bullet & \bullet & \bullet & -\widehat{X} & 0 & 0 \\ \bullet & \bullet & \bullet & \bullet & -\gamma^2 I & \widehat{\Phi}_j^T \\ \bullet & \bullet & \bullet & \bullet & \bullet & -I \end{bmatrix} < 0, \tag{3.30}$$

where

$$\widehat{X} = \begin{bmatrix} X & 0 \\ X & X \end{bmatrix},\ \widehat{\Omega}_j = \begin{bmatrix} \widehat{\Omega}_{1j} & 0 & \widehat{\Omega}_{3j} & 0 \end{bmatrix}^T$$

$$\widehat{\Omega}_{1j} = \begin{bmatrix} X\bar{A}_k^T + Y_1^T\bar{B}_k^T & 0 \\ X\bar{A}_k^T & X\bar{A}_k^T - (1+\Delta)Y_2^T \end{bmatrix},\ \widehat{\Omega}_{3j} = \begin{bmatrix} Y_1^T\bar{B}_k^T & 0 \\ 0 & 0 \end{bmatrix}$$

$$\begin{aligned}\widehat{\Lambda}_{1j} &= -X + \sigma_j(1 + \tau_m^+ - \tau_m^-)\Xi_j + \Pi + \Pi^T, \\ \widehat{\Lambda}_{2j} &= -\Theta_j - \Theta_j^T + \sigma_j \Xi_j, \widehat{\Lambda}_{3j} = -\Pi + \Theta_j^T\end{aligned} \tag{3.31}$$

in which the gains are provided by

$$K = Y_1 X^{-1}; \quad L = Y_2 X^{-1} \bar{C}_k^{\dagger}$$

Proof.

Inequality (3.20) is represented as

$$\Lambda_j = \widetilde{\Lambda} + \Omega_j P_j \Omega_j^T < 0 \tag{3.32}$$

Where

$$\Omega_j = \begin{bmatrix} \bar{A}_k + \bar{B}_k & 0 & -\bar{B}_k & 0 \end{bmatrix}$$

Using Schur complements, matrix Λ_j in (22) can be represented as

$$\begin{bmatrix} \Psi_j & -R + S^T & -R + M^T & 0 & G^T & \Upsilon P_j \\ \bullet & Q_s & -S + M^T & 0 & 0 & 0 \\ \bullet & \bullet & -M - M^T & 0 & 0 & \bar{C}_k L P_j \\ \bullet & \bullet & \bullet & -\gamma^2 I & 0 & \bar{B}_w^T P_j \\ \bullet & \bullet & \bullet & \bullet & -I & \widehat{\Phi}_j^T \\ \bullet & \bullet & \bullet & \bullet & \bullet & -P_j \end{bmatrix} < 0 \tag{3.33}$$

where $\Upsilon = (\bar{A}_k - (1+\mathbf{\Delta})L\bar{C}_k)^T$, $Q_s = -S - S^T - \sigma_j Q_j$. Putting $\widehat{X} = P_j^{-1}$ and employing the congruence transformation

$$T_j = diag[\ \widehat{X}\ , \widehat{X}\ ,\ \widehat{X},\ I\ ,\ \widehat{X},\ I]$$

to matrix inequality in (3.33) and manipulating using (3.30) and

$$\Xi_j = \widehat{X}Q_j\widehat{X},\ \ \Pi_j = \widehat{X}R\widehat{X},\ \ \Gamma_j = \widehat{X}M\widehat{X}\ \ \omega_j = \widehat{X}S\widehat{X}$$

3.6 Simulation Results

Example 1 *A microgrid distribution system given in figure (3.3) is implemented for the analysis of this chapter. The typical microgrid system includes three distributed generation units supplied a local load. The respective state space model after linearizing the system around the operation conditions where the parameter values are stated in Table 3.1 with* $T = 0.1 second$ *as a sampling time.*

3.6.1 Hold input scheme

$$Rule1 : if\ \ \alpha_k\ \ is\ \ S\ \ and\ \ \beta_k\ \ is\ \ S\ \ then$$

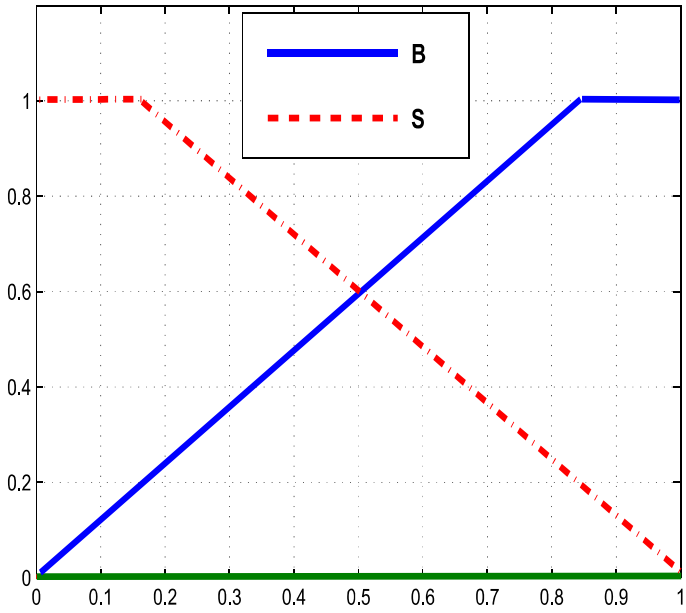

Figure 3.4: Membership functions of four rule models.

$$A_k = \begin{bmatrix} A_{mg} & B_{mg} \\ 0 & 0 \end{bmatrix}, \; B_k = \begin{bmatrix} 0 \\ I_k \end{bmatrix},$$

$$C_k = \begin{bmatrix} C_{mg}(\tau_k^m) & 0 \end{bmatrix}; \; B_{wk} = \begin{bmatrix} I_{wk} \\ 0 \end{bmatrix}; \; D_{vk} = \begin{bmatrix} I_{vk} \\ 0 \end{bmatrix}$$

$$Rule2 : if \;\; \alpha_k \;\; is \;\; B \;\; and \;\; \beta_k \;\; is \;\; S \;\; then$$

$$A_k = \begin{bmatrix} A_{mg} & 0 \\ 0 & I_k \end{bmatrix},\ B_k = \begin{bmatrix} B_{mg} \\ 0 \end{bmatrix},$$

$$C_k = \begin{bmatrix} C_{mg}(\tau_k^m) & 0 \end{bmatrix};\ B_{wk} = \begin{bmatrix} I_{wk} \\ 0 \end{bmatrix};\ D_{vk} = \begin{bmatrix} I_{vk} \\ 0 \end{bmatrix}$$

$$Rule3 : if\ \ \alpha_k\ \ is\ \ S\ \ and\ \ \beta_k\ \ is\ \ B\ \ then$$

$$A_k = \begin{bmatrix} A_{mg} & B_{mg} \\ 0 & 0 \end{bmatrix},\ B_k = \begin{bmatrix} 0 \\ I_k \end{bmatrix},$$

$$C_k = \begin{bmatrix} C_{mg} & 0 \end{bmatrix};\ B_{wk} = \begin{bmatrix} I_{wk} \\ 0 \end{bmatrix};\ D_{vk} = \begin{bmatrix} I_{vk} \\ 0 \end{bmatrix}$$

$$Rule4 : if\ \ \alpha_k\ \ is\ \ B\ \ and\ \ \beta_k\ \ is\ \ B\ \ then$$

$$A_k = \begin{bmatrix} A_{mg} & 0 \\ 0 & I_k \end{bmatrix},\ B_k = \begin{bmatrix} B_{mg} \\ 0 \end{bmatrix},$$

$$C_k = \begin{bmatrix} C_{mg} & 0 \end{bmatrix};\ B_{wk} = \begin{bmatrix} I_{wk} \\ 0 \end{bmatrix};\ D_{vk} = \begin{bmatrix} I_{vk} \\ 0 \end{bmatrix}$$

In this section, we introduce an S that means a small value ($Prob(\alpha_k) = 0$) which is the event when the signal was dropped out or delayed. B means a big value ($Prob(\alpha_k) =$

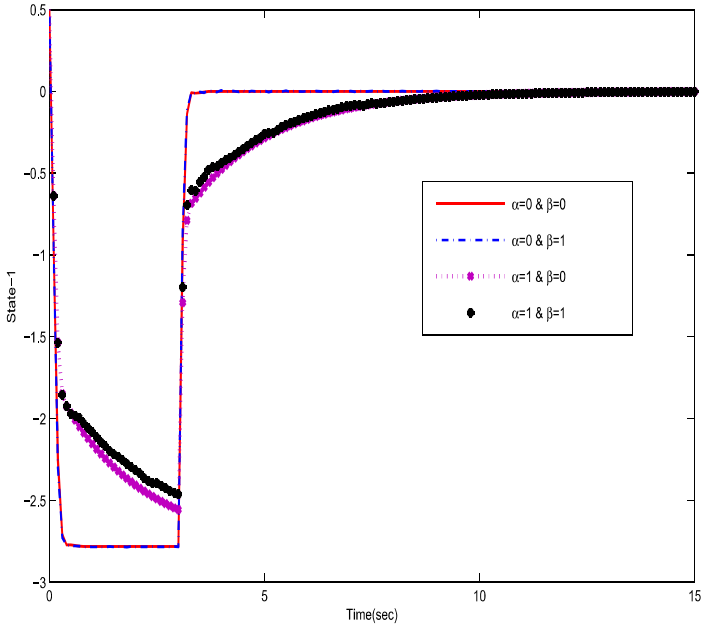

Figure 3.5: Fuzzy state trajectories state 1

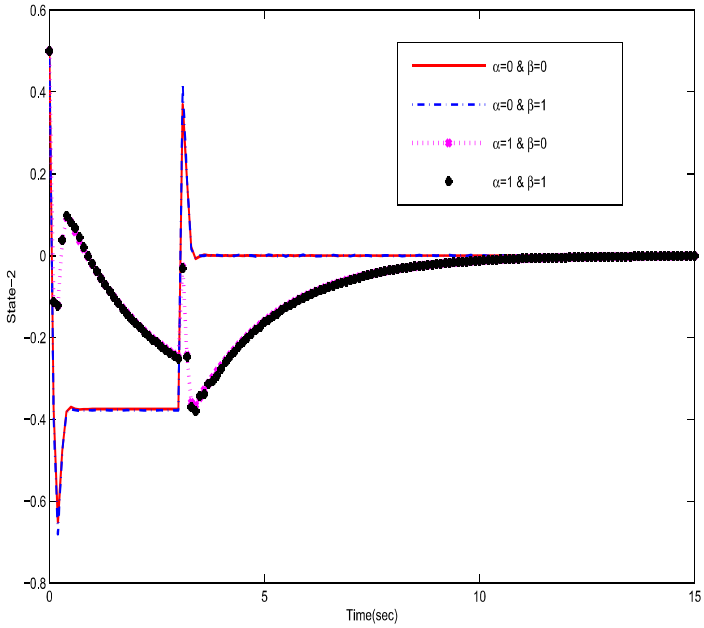

Figure 3.6: Fuzzy state trajectories state 2

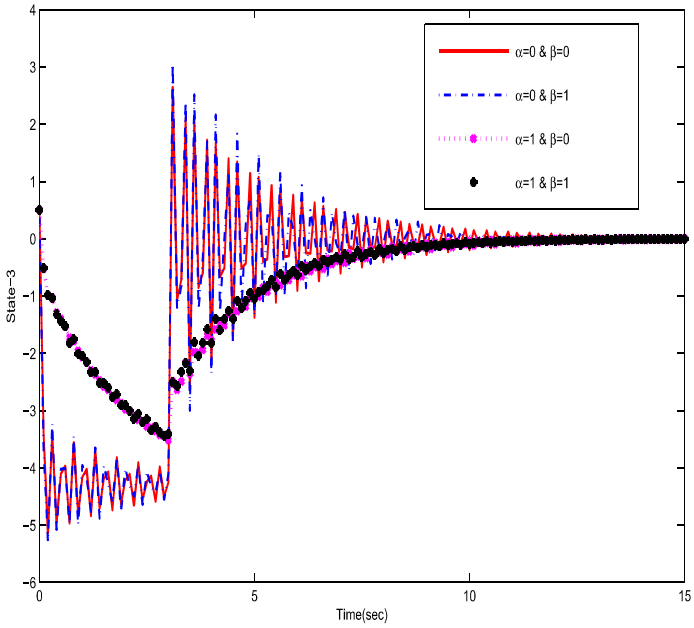

Figure 3.7: Fuzzy state trajectories state 3

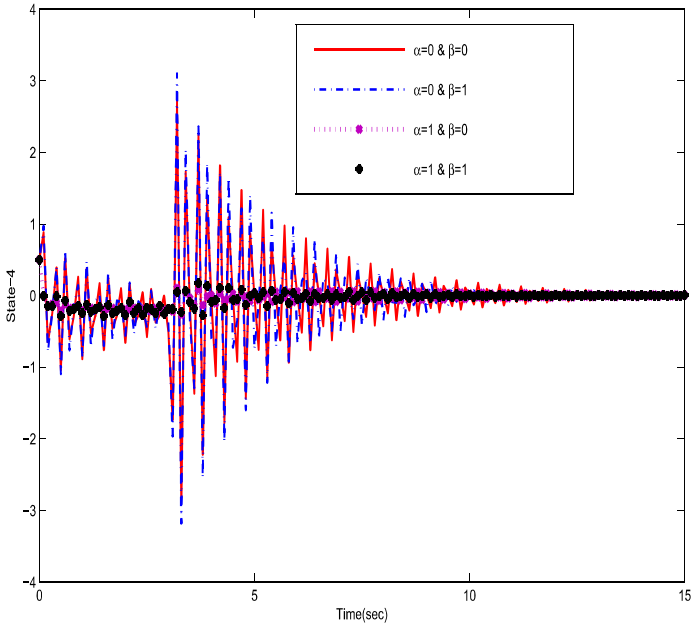

Figure 3.8: Fuzzy state trajectories state 4

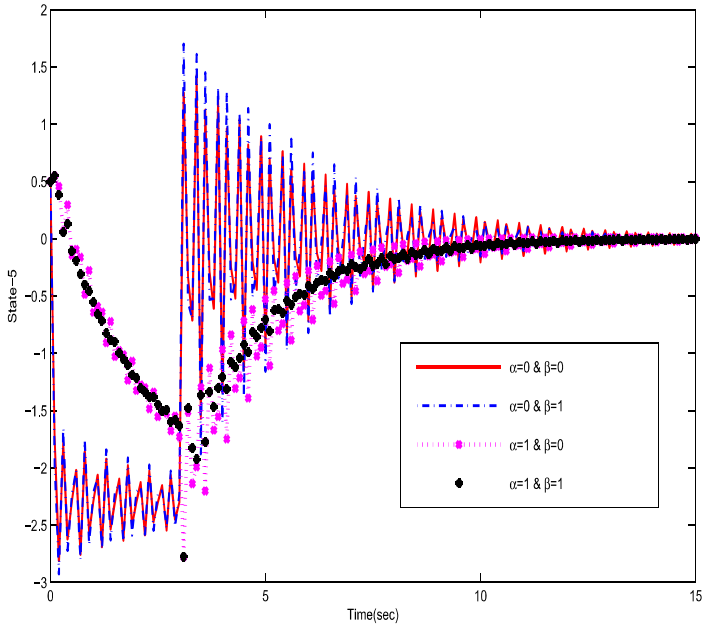

Figure 3.9: Fuzzy state trajectories state 5

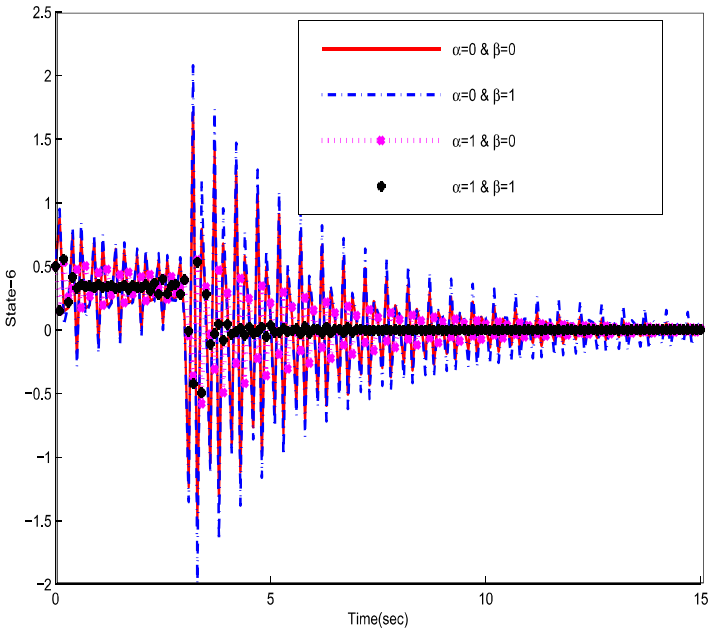

Figure 3.10: Fuzzy state trajectories state 6

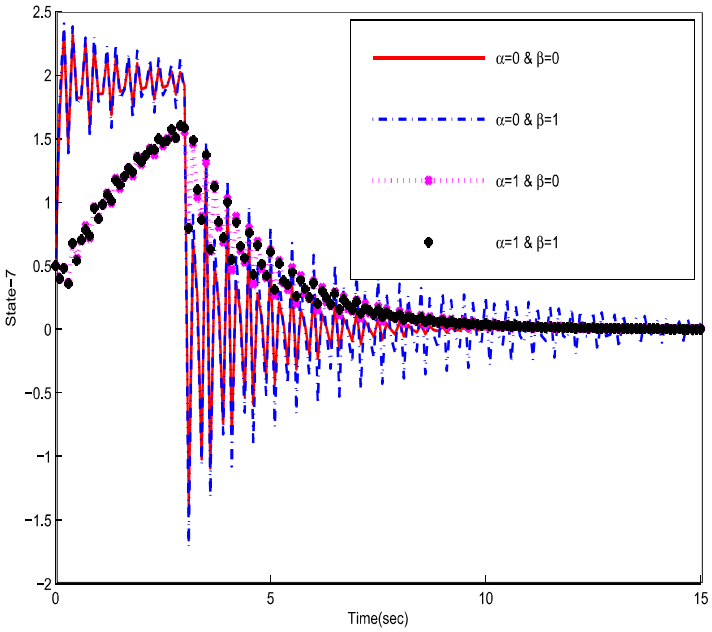

Figure 3.11: Fuzzy state trajectories state 7

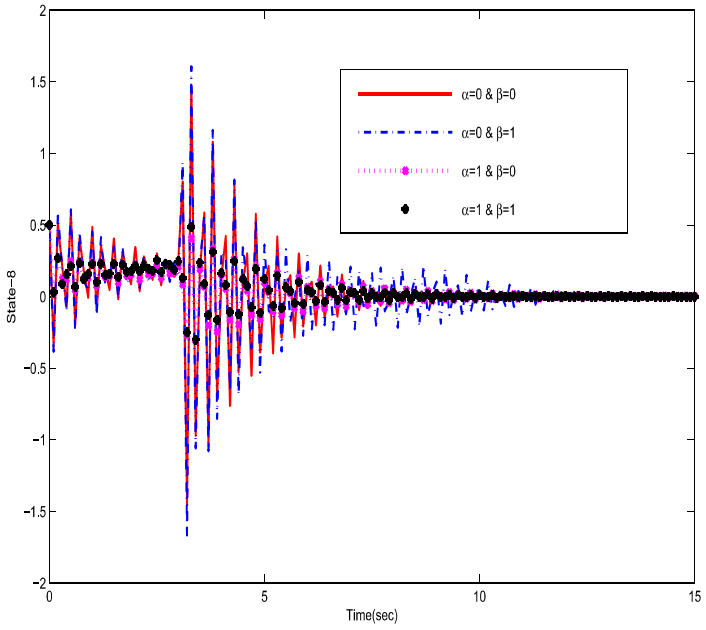

Figure 3.12: Fuzzy state trajectories state 8

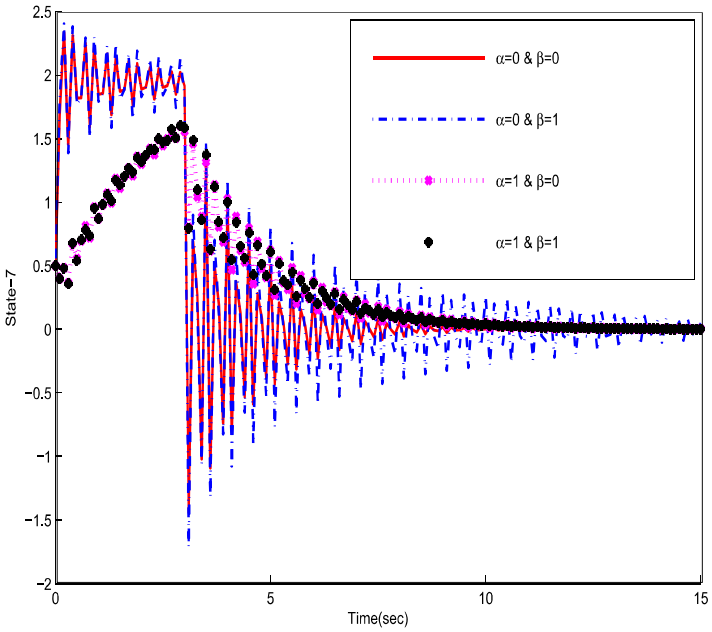

Figure 3.13: Fuzzy state trajectories state 9

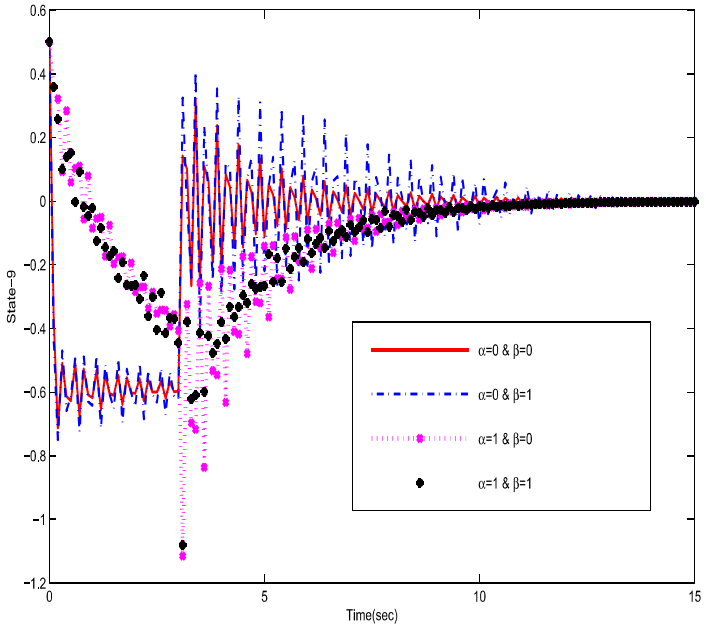

Figure 3.14: Fuzzy state trajectories state 10

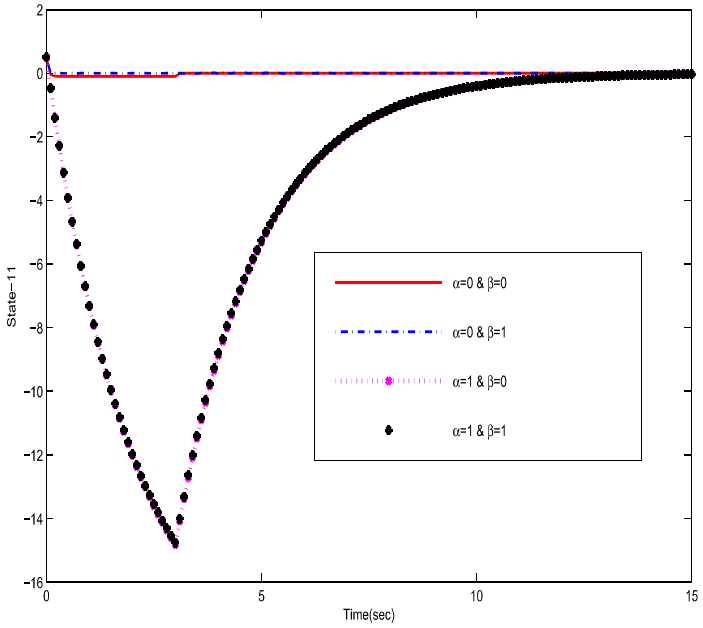

Figure 3.15: Fuzzy state trajectories state 11

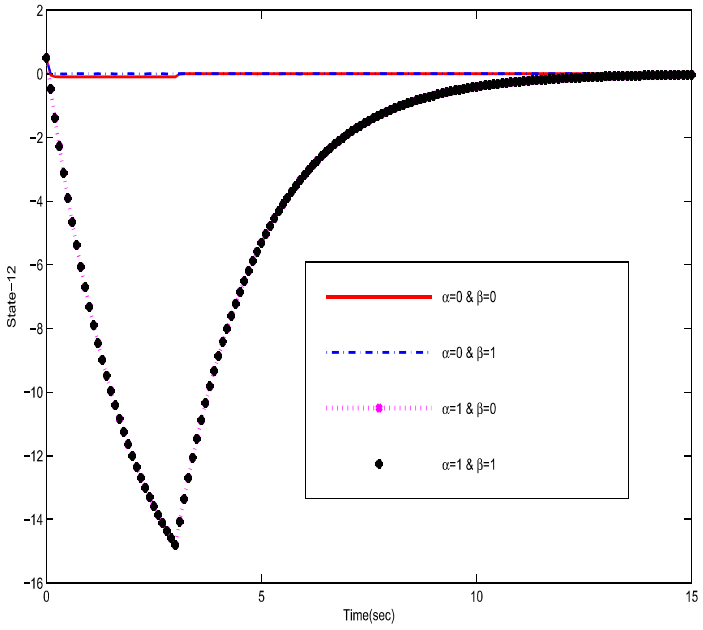

Figure 3.16: Fuzzy state trajectories state 12

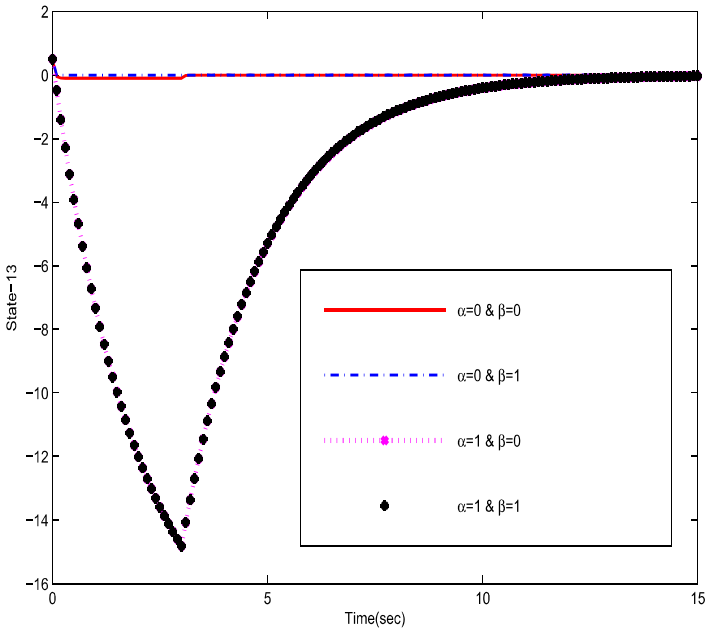

Figure 3.17: Fuzzy state trajectories state 13

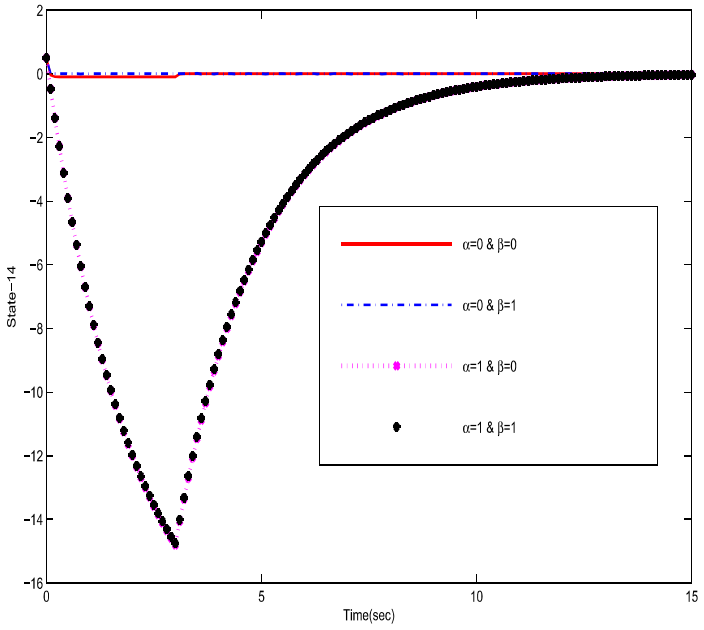

Figure 3.18: Fuzzy state trajectories state 14

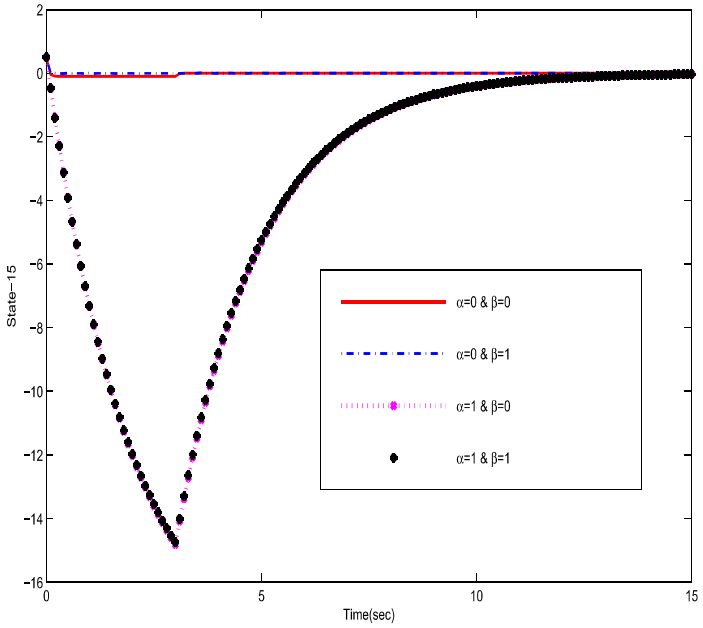

Figure 3.19: Fuzzy state trajectories state 15

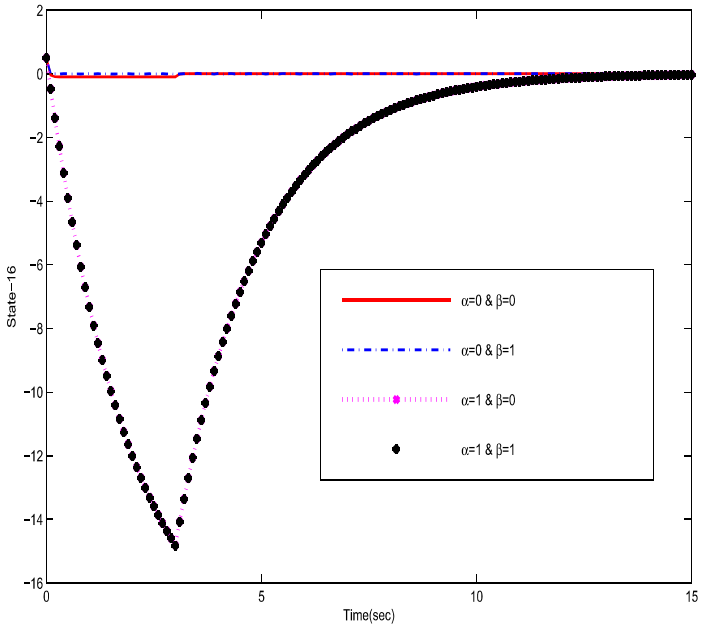

Figure 3.20: Fuzzy state trajectories state 16

1) which is the event when the signal was successfully received. Figs. 3.5–3.20 depict the trajectories of the system states and communication constrains effects. With different values of α_k and β_k and fixed quantization rate, we can see that the states of the augmented model converge asymptotically to a stabilized bound.

As it is clear from the simulation results, the proposed networked control system stabilizes the system in the terms of communication network constraints. Also, based on the obtained figures, the states coverage to desired stabilize case in which it demonstrates the capability of the introduced topology. The d-q components of currents of the distributed generations are controlled with the load currents and voltages of the standalone system in forms of augmented model.

In addition, we tackle the problem of H_∞ estimator subject to packets dropped. We set the initial values of the states to $\bar{x}_0 = [1.3; 1.3; 1.3; 1.3; 1.3; 1.3; 1.3; 1.3; 1.3; 1.3; 1.3; 1.3; 1.3; 1.3; 1.3; 1.3]$, while the initial of the estimated states to $\hat{\bar{x}}_0 = zeros(16, 1)$. With the designed observer-based networked controller, typical simulation results of the networked closed-loop system with time delays and packet losses are depicted in above Figs.

Recall that the load variation within the islanded MG changes the network probability at anytime. In this study, we have tested the proposed controller in the occurrence of load variation. It can be observed from the Figs. 3.5–3.20 that the developed controller regulates the dynamics of the system to the desired level.

All in all, we present the effectiveness and applicability of the proposed fuzzy control design scheme with input packets dropout and quantization effects.

Example 2 *In this example, we test the the effectiveness and robustness of the proposed controller for wind turbine model in the presence of communication constraints, for more*

$$K_{S,S} = \begin{bmatrix} -0.0027 & -0.0061 & -0.0027 & 0.0051 & 0.0031 & 0.0036 & 0.0034 & -0.0086 \\ 0.0042 & -0.0027 & -0.0109 & -0.0001 & -0.0029 & 0.0001 & 0.0037 & 0.0092 \\ 0.0022 & 0.0003 & -0.0006 & -0.0002 & -0.0156 & -0.005 & -0.0009 & 0.0013 \\ 0.0093 & 0.0073 & 0.0005 & 0.0019 & 0.0017 & -0.0006 & -0.0042 & 0.0072 \\ -0.0 & 0.0087 & 0.0025 & 0.0001 & -0.0009 & -0.0004 & -0.0032 & 0.005 \\ -0.0016 & 0.002 & -0.0058 & -0.0037 & 0.0048 & 0.0026 & 0.0005 & 0.0011 \end{bmatrix}$$
$$\begin{bmatrix} -0.0017 & -0.00 & 0.0797 & 0.0022 & 0.0033 & -0.049 & -0.0269 & -0.0012 \\ 0.0093 & 0.005 & -0.0004 & 0.0801 & 0.0219 & 0.0015 & 0.0001 & -0.0283 \\ 0.0011 & -0.00 & -0.0032 & 0.0192 & 0.0706 & -0.0058 & 0.0008 & -0.0097 \\ 0.0056 & 0.0036 & -0.0504 & 0.0022 & 0.001 & 0.0439 & -0.0064 & -0.0004 \\ -0.0002 & 0.0143 & -0.0317 & 0.0022 & -0.0007 & 0.0003 & 0.0265 & 0.0021 \\ -0.0054 & -0.003 & 0.0048 & -0.0301 & -0.0082 & 0.0001 & -0.0013 & 0.0313 \end{bmatrix}$$

Figure 3.21: The controller gain in terms of rule-1

$$L_{S,S} = \begin{bmatrix} 0.0010 & -0.0008 & -0.0045 & 0.0004 & 0.0024 & 0.0023 \\ -0.0022 & 0.0043 & 0.0028 & -0.0057 & -0.0001 & 0.0013 \\ -0.0003 & -0.0006 & -0.0025 & -0.0019 & 0.0020 & 0.0022 \\ -0.0007 & 0.0005 & 0.0043 & -0.0064 & -0.0017 & 0.0039 \\ 0.0017 & 0.0010 & -0.0040 & -0.0024 & 0.0020 & 0.0017 \\ -0.0016 & 0.0011 & 0.0033 & -0.0050 & -0.0002 & 0.0017 \\ 0.0003 & -0.0007 & 0.0027 & -0.0024 & -0.0016 & 0.0021 \\ -0.0012 & 0.0012 & 0.0029 & -0.0045 & 0.0004 & 0.0001 \\ -0.0011 & 0.0001 & 0.0001 & 0.0005 & 0.0002 & -0.0017 \\ -0.0005 & -0.0006 & 0.0012 & -0.0013 & 0.0028 & -0.0016 \\ 0.0011 & -0.0022 & -0.0015 & 0.0003 & -0.0002 & 0.0020 \\ 0.0002 & -0.0046 & 0.0040 & -0.0020 & 0.0014 & -0.0004 \\ -0.0015 & 0.0017 & 0.0012 & -0.0019 & 0.0022 & -0.0007 \\ 0.0001 & -0.0008 & 0.0034 & 0.0014 & -0.0016 & -0.0014 \\ 0.0003 & -0.0036 & 0.0033 & -0.0004 & -0.0001 & 0.0004 \\ -0.0021 & -0.0004 & 0.0027 & 0.0004 & -0.0015 & -0.0020 \end{bmatrix}$$

Figure 3.22: The estimator gain in terms of rule-1

$$K_{S,B} = \begin{bmatrix} -0.0003 & -0.0028 & -0.0100 & -0.0030 & 0.0005 & 0.0050 & 0.0012 & -0.0117 \\ 0.0001 & 0.0001 & -0.0023 & -0.0022 & 0.0046 & 0.0021 & 0.0074 & 0.0016 \\ -0.0001 & -0.0004 & -0.0063 & 0.0021 & -0.0054 & -0.0039 & 0.0039 & 0.0025 \\ -0.0032 & 0.0043 & -0.0032 & -0.0001 & -0.0001 & -0.0046 & -0.0078 & 0.0040 \\ 0.0000 & -0.0000 & -0.0090 & -0.0006 & 0.0003 & 0.0061 & -0.0013 & 0.0023 \\ 0.0012 & -0.0027 & -0.0015 & 0.0029 & -0.0039 & 0.0020 & 0.0011 & 0.0071 \end{bmatrix}$$
$$\begin{bmatrix} -0.0028 & -0.0000 & 0.0792 & 0.0001 & -0.0003 & -0.0529 & -0.0340 & -0.0003 \\ 0.0069 & 0.0012 & 0.0027 & 0.0839 & 0.0215 & 0.0003 & 0.0012 & -0.0289 \\ -0.0108 & -0.0053 & 0.0020 & 0.0220 & 0.0699 & 0.0046 & 0.0023 & -0.0130 \\ 0.0017 & -0.0004 & -0.0507 & 0.0000 & -0.0011 & 0.0482 & -0.0032 & -0.0006 \\ 0.0012 & 0.0037 & -0.0273 & -0.0012 & -0.0022 & 0.0027 & 0.0390 & 0.0028 \\ -0.0019 & -0.0029 & -0.0029 & -0.0289 & -0.0086 & -0.0042 & -0.0015 & 0.0374 \end{bmatrix}$$

Figure 3.23: The controller gain in terms of rule-2

$$L_{S,B} = \begin{bmatrix} 0.0913 & 0.0593 & -0.1449 & -0.1138 & 0.1134 & 0.0812 \\ -0.0836 & 0.1120 & 0.0898 & -0.1326 & -0.1027 & 0.1284 \\ -0.0229 & -0.0121 & -0.2760 & -0.2057 & 0.2789 & 0.2073 \\ 0.0215 & -0.0247 & 0.2153 & -0.3080 & -0.1959 & 0.2829 \\ 0.0587 & 0.0583 & -0.3009 & -0.2240 & 0.0448 & 0.0522 \\ 0.0058 & 0.0123 & 0.2938 & -0.3987 & 0.0187 & 0.0121 \\ -0.0095 & -0.0045 & -0.1071 & -0.0878 & 0.1173 & 0.0849 \\ 0.0106 & -0.0134 & 0.0851 & -0.1215 & -0.0851 & 0.1237 \\ 0.0485 & 0.0519 & -0.0275 & -0.0075 & -0.2275 & -0.1488 \\ 0.0136 & 0.0005 & 0.0752 & -0.0803 & 0.2218 & -0.2796 \\ 0.0025 & -0.0031 & -0.0020 & -0.0008 & 0.0021 & 0.0013 \\ 0.0004 & -0.0011 & -0.0003 & 0.0022 & -0.0006 & -0.0024 \\ -0.0036 & 0.0017 & 0.0007 & -0.0004 & -0.0005 & 0.0020 \\ 0.0019 & 0.0008 & 0.0019 & -0.0027 & 0.0005 & -0.0012 \\ 0.0030 & 0.0006 & -0.0035 & -0.0003 & -0.0014 & -0.0002 \\ 0.0034 & -0.0032 & -0.0000 & 0.0015 & 0.0008 & -0.0003 \end{bmatrix}$$

Figure 3.24: The estimator gain in terms of rule-2

$$K_{B,S} = \begin{bmatrix} 0.0817 & 0.0933 & 0.1003 & 0.1124 & -0.1313 & -0.0648 & 0.0990 & 0.0797 \\ -0.0035 & 0.0008 & -0.0201 & -0.0047 & -0.0003 & -0.0033 & 0.0609 & 0.0250 \\ -0.0012 & -0.0005 & 0.0047 & 0.0007 & -0.0682 & -0.0222 & 0.0038 & 0.0012 \\ 0.0833 & 0.0919 & 0.1073 & 0.0959 & -0.1268 & -0.0832 & 0.0754 & 0.1478 \\ 0.0834 & 0.0901 & 0.1046 & 0.0972 & -0.1251 & -0.0924 & 0.0973 & 0.0863 \\ -0.0015 & 0.0024 & -0.0034 & 0.0029 & 0.0054 & -0.0022 & 0.0578 & 0.0239 \end{bmatrix}$$
$$\begin{bmatrix} 0.1042 & 0.0732 & 0.0473 & -0.0036 & -0.0045 & 0.0310 & 0.0313 & -0.0009 \\ 0.0012 & 0.0023 & 0.0005 & 0.0195 & -0.0002 & -0.0002 & -0.0003 & 0.0012 \\ 0.0036 & 0.0015 & -0.0008 & -0.0004 & 0.0189 & 0.0003 & -0.0003 & 0.0000 \\ 0.1031 & 0.0780 & 0.0293 & -0.0036 & -0.0041 & 0.0506 & 0.0312 & -0.0008 \\ 0.0721 & 0.1624 & 0.0280 & -0.0042 & -0.0043 & 0.0303 & 0.0506 & -0.0012 \\ -0.0867 & -0.0281 & 0.0002 & 0.0015 & 0.0007 & 0.0005 & -0.0010 & 0.0219 \end{bmatrix}$$

Figure 3.25: The controller gain in terms of rule-3

$$L_{B,S} = \begin{bmatrix} -0.0008 & 0.0008 & -0.0026 & -0.0002 & -0.0018 & 0.0038 \\ -0.0014 & 0.0023 & 0.0021 & -0.0034 & -0.0015 & 0.0034 \\ -0.0006 & -0.0036 & 0.0011 & -0.0019 & 0.0038 & 0.0017 \\ 0.0002 & -0.0019 & 0.0005 & 0.0036 & -0.0022 & -0.0008 \\ 0.0026 & -0.0011 & -0.0036 & 0.0004 & -0.0018 & 0.0011 \\ 0.0004 & -0.0009 & 0.0046 & -0.0043 & -0.0009 & 0.0026 \\ -0.0035 & 0.0015 & -0.0015 & -0.0015 & 0.0037 & 0.0012 \\ -0.0003 & 0.0007 & -0.0023 & 0.0018 & 0.0035 & -0.0001 \\ -0.0003 & 0.0004 & 0.0016 & 0.0010 & -0.0020 & -0.0020 \\ -0.0010 & 0.0018 & 0.0019 & 0.0032 & -0.0013 & -0.0042 \\ -0.0004 & -0.0003 & -0.0014 & 0.0011 & 0.0014 & 0.0013 \\ -0.0031 & 0.0018 & -0.0014 & 0.0037 & -0.0000 & 0.0003 \\ 0.0020 & -0.0017 & -0.0030 & 0.0003 & 0.0045 & -0.0027 \\ -0.0016 & -0.0004 & 0.0005 & 0.0002 & 0.0011 & -0.0001 \\ 0.0016 & -0.0008 & 0.0012 & -0.0023 & -0.0012 & 0.0003 \\ 0.0017 & -0.0040 & -0.0003 & 0.0015 & 0.0017 & 0.0002 \end{bmatrix}$$

Figure 3.26: The estimator gain in terms of rule-3

$$K_{B,B} = \begin{bmatrix} 0.0868 & 0.0976 & 0.1034 & 0.1148 & -0.1282 & -0.0659 & 0.1145 & 0.0980 \\ -0.0034 & 0.0010 & -0.0205 & -0.0046 & -0.0009 & -0.0032 & 0.0642 & 0.0249 \\ -0.0008 & -0.0006 & 0.0046 & 0.0005 & -0.0701 & -0.0223 & 0.0035 & 0.0002 \\ 0.0878 & 0.0964 & 0.1101 & 0.0973 & -0.1224 & -0.0841 & 0.0907 & 0.1666 \\ 0.0880 & 0.0950 & 0.1093 & 0.0999 & -0.1201 & -0.0937 & 0.1132 & 0.1038 \\ -0.0005 & 0.0035 & -0.0038 & 0.0023 & 0.0045 & -0.0014 & 0.0598 & 0.0247 \end{bmatrix}$$
$$\begin{bmatrix} 0.1156 & 0.0894 & 0.0503 & -0.0009 & 0.0004 & 0.0286 & 0.0282 & 0.0013 \\ 0.0012 & 0.0028 & 0.0001 & 0.0196 & -0.0003 & -0.0001 & -0.0001 & 0.0008 \\ 0.0051 & 0.0013 & -0.0000 & -0.0003 & 0.0192 & -0.0002 & -0.0001 & 0.0001 \\ 0.1150 & 0.0938 & 0.0313 & -0.0009 & 0.0005 & 0.0481 & 0.0281 & 0.0012 \\ 0.0824 & 0.1824 & 0.0318 & -0.0010 & 0.0004 & 0.0283 & 0.0478 & 0.0012 \\ -0.0894 & -0.0281 & 0.0002 & 0.0011 & 0.0001 & -0.0000 & 0.0000 & 0.0204 \end{bmatrix}$$

Figure 3.27: The controller gain in terms of rule-4

$$L_{B,B} = \begin{bmatrix} 0.1342 & 0.0899 & -0.2169 & -0.1644 & 0.1617 & 0.1102 \\ -0.1225 & 0.1582 & 0.1327 & -0.1926 & -0.1430 & 0.1856 \\ -0.0305 & -0.0204 & -0.4656 & -0.3351 & 0.4707 & 0.3444 \\ 0.0314 & -0.0388 & 0.3458 & -0.4748 & -0.3320 & 0.4623 \\ 0.1025 & 0.1028 & -0.4897 & -0.3285 & 0.0995 & 0.1017 \\ 0.0160 & 0.0161 & 0.4473 & -0.5777 & 0.0181 & 0.0147 \\ -0.0096 & -0.0067 & -0.1616 & -0.1162 & 0.1617 & 0.1182 \\ 0.0107 & -0.0125 & 0.1197 & -0.1648 & -0.1154 & 0.1598 \\ 0.0901 & 0.0936 & -0.0160 & 0.0164 & -0.3559 & -0.2314 \\ 0.0233 & 0.0056 & 0.1016 & -0.1016 & 0.3480 & -0.4404 \\ -0.0009 & 0.0005 & 0.0007 & -0.0021 & -0.0005 & 0.0030 \\ 0.0009 & -0.0006 & 0.0027 & 0.0002 & -0.0039 & -0.0010 \\ 0.0002 & 0.0005 & 0.0058 & 0.0014 & -0.0016 & -0.0007 \\ 0.0003 & 0.0000 & -0.0009 & 0.0013 & -0.0003 & -0.0002 \\ -0.0006 & 0.0007 & -0.0003 & 0.0020 & 0.0008 & -0.0040 \\ 0.0003 & -0.0004 & -0.0007 & -0.0010 & 0.0035 & 0.0010 \end{bmatrix}$$

Figure 3.28: The estimator gain in terms of rule-4

about wind turbine model see [184]. It can see from the Figs.3.29– 3.34that the controller can restore the stability of the model with load fluctuations.

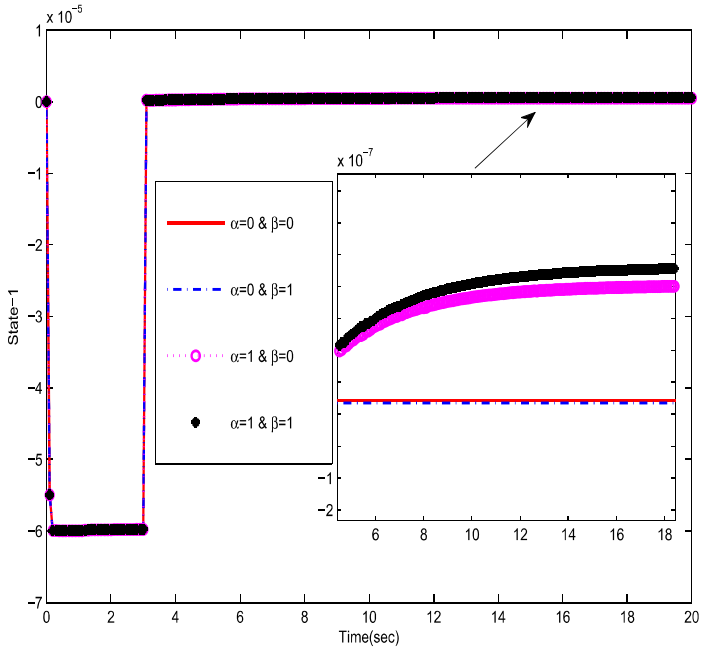

Figure 3.29: Fuzzy state trajectories of wind turbine state 1

3.7 Conclusions

In this chapter, a new quantized H_∞ estimator has been investigated over communication networks for distributed generation systems subject to random packet loss. A typically islanded MG comprises of three DGs supplying a local load. Attention is focused on the develop of networked controller to stabilize the microgrid system and it is suitable to endure any sort of time delays, and packet drops. sufficient conditions for the existence of quantized H_∞ estimator based feedback controller are derived in terms of linear matrix inequalities (LMIs). The effectiveness of the proposed results has been

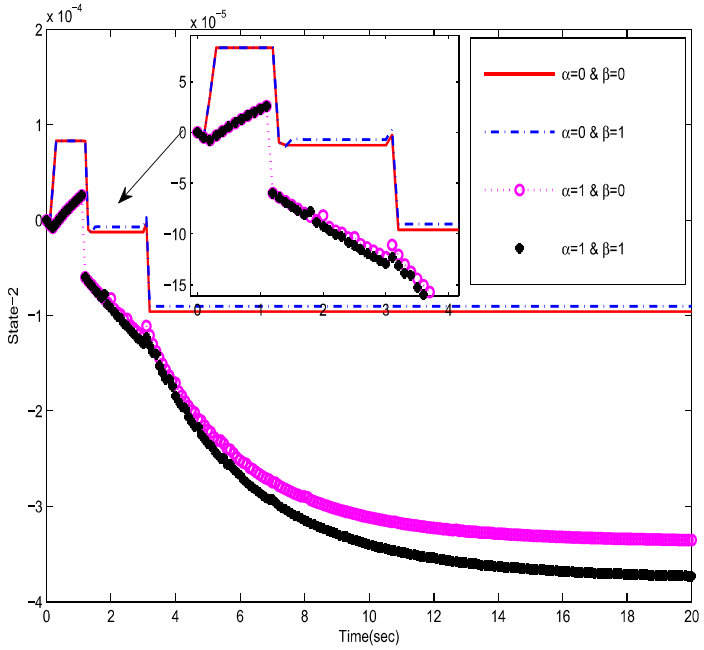

Figure 3.30: Fuzzy state trajectories of wind turbine state 2

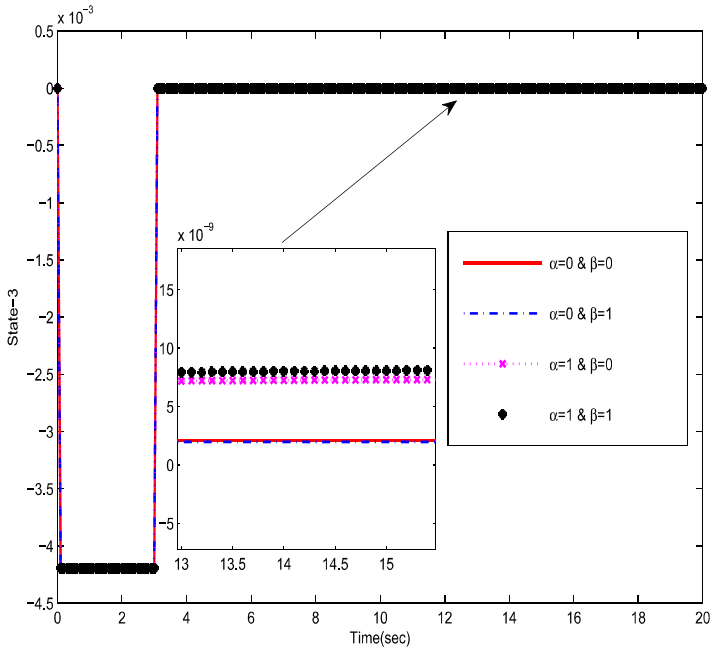

Figure 3.31: Fuzzy state trajectories of wind turbine state 3

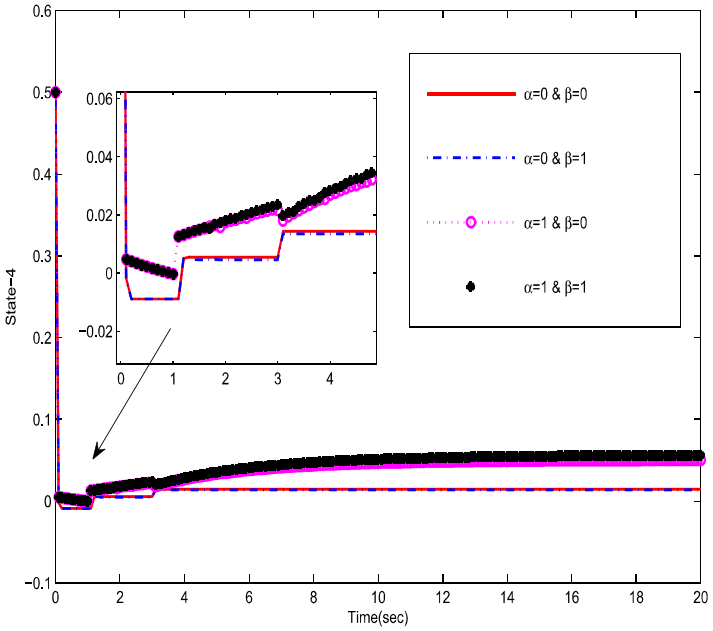

Figure 3.32: Fuzzy state trajectories of wind turbine state 4

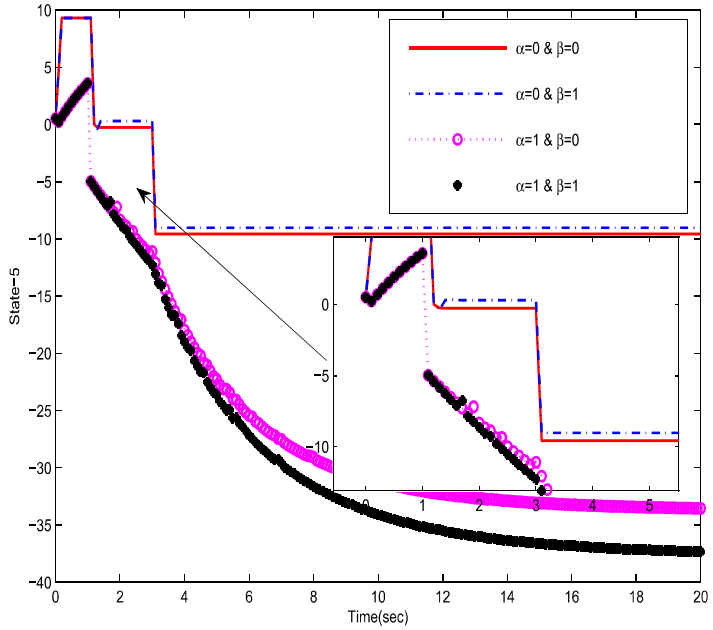

Figure 3.33: Fuzzy state trajectories of wind turbine state 5

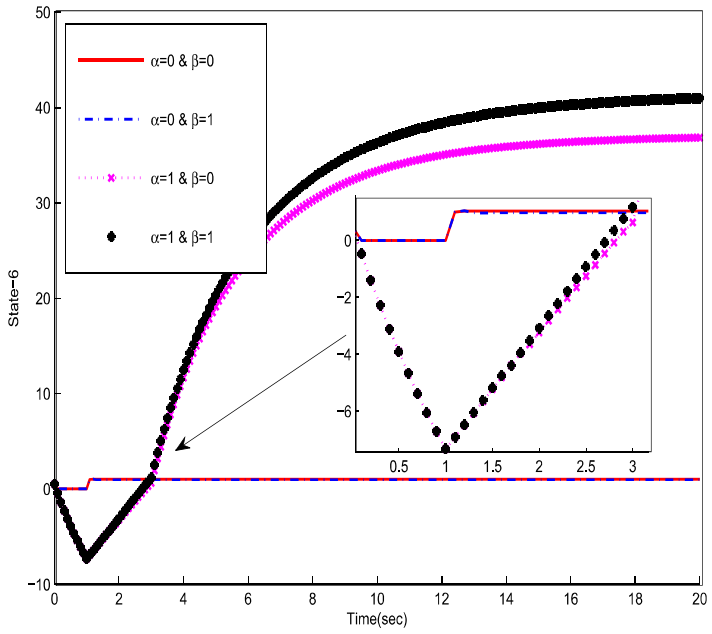

Figure 3.34: Fuzzy state trajectories of wind turbine state 6

$$K_{S,S} = \begin{bmatrix} 0.0010 & 0.0026 & 0.1090 & 0.0119 & -0.0659 & 0.0254 \end{bmatrix}$$
$$L^T_{S,S} = 1.0e^{-02} \begin{bmatrix} -0.0001 & -0.0006 & -0.2650 & 0.2039 & -0.6566 & 0.0000 \end{bmatrix}$$

Figure 3.35: The controller and estimator gains for WT model in terms of rule-1

$$K_{B,S} = \begin{bmatrix} 0.0513 & 0.0435 & 0.1007 & 0.0608 & -0.0000 & 0.315 \end{bmatrix}$$
$$L^T_{B,S} = 1.0e^{-02} \begin{bmatrix} 0.0008 & -0.0011 & 0.0202 & 0.0133 & 0.3975 & 0.0007 \end{bmatrix}$$

Figure 3.36: The controller and estimator gains for WT model in terms of rule-2

$$K_{S,B} = \begin{bmatrix} 0.0003 & 0.0001 & 0.1090 & 0.0000 & -0.0014 & 0.0231 \end{bmatrix}$$
$$L^T_{S,B} = 1.0e^{-03} \begin{bmatrix} 0.1732 & 0.1405 & -0.0601 & 0.0587 & -0.0828 & 0.0086 \end{bmatrix}$$

Figure 3.37: The controller and estimator gains for WT model in terms of rule-3

$$K_{B,B} = \begin{bmatrix} 0.0003 & 0.0001 & 0.0000 & 0.0000 & -0.0076 & 0.0228 \end{bmatrix}$$
$$L^T_{B,B} = 1.0e^{-03} \begin{bmatrix} 0.0003 & 0.0008 & 0.0183 & -0.0166 & 0.3945 & 0.0063 \end{bmatrix}$$

Figure 3.38: The controller and estimator gains for WT model in terms of rule-4

shown through two numerical examples. The results demonstrated the effectiveness of the developed approach.

CHAPTER 4

$\mathfrak{L}_1$ ADAPTIVE NETWORKED CONTROLLER

In this chapter, we investigate the implementation of output-feedback $\mathfrak{L}_1$ adaptive controller for a linear parametrization model of distributed generation systems. Recently, DGs have been introduced in power systems applications to solve increasing energy demands and to incorporate renewable energy resources into power supply networks. Further, a linear parametrization method is used to tackle unknown parameters in terms of time varying parameters. The $\mathfrak{L}_1$ Adaptive controller deals with nonlinearity of dynamic systems and unknown constraints, which consists of predictor, adaptive law, and control law. The proposed controller is worthy for ensuring the network stability of DGs in a microgrid environment in the presence of uncertainties and transmission time delays. A typical simulation example is presented to confirm the effectiveness of the proposed design procedure.

4.1 Introduction

Recently, the utilization of various kinds of renewable energy resources, distributed generation units, and storage systems in power supply systems have been grown up rapidly. The distributed generation systems are mainly located near demand side to feed a generation electric power to the local loads. In general, the distributed generation is an emerging infrastructure predictive to role of traditional central power plants in future. The distributed energy resources (DER) involve a wide range of technologies, such as micro turbines, diesel engines, fuel cells, photovoltaic, wind turbines, etc [11]. Microgrids are very effective networks that are formed by clusters of DGs with controllable loads and storage devices. Thus MG is widely incorporated with utility grid to reduce the losses in the transmission lines, and to enhance the capability of the power supply, and as well as the reliability of the system [185]. The distributed generation systems can work in parallel to the utility grid or in an islanded microgrid mode. The storage devices play a key factor to improve the reliability, power balancing and to supply a generation in the transit mode of the microgrid as well as high critical loads. There is a variety of energy storage devices including flywheels, capacitors, and batteries [186].

The flexibility of microgrid allows exporting/importing energy from/to the utility grid to regulate the voltage and the frequency in MG. Also, it has the capability to connect (connected mode)/disconnect (islanded mode) to/from the main grid. Due to low voltage level of the microgrid, it needs to connect to the main grid to feed some of the loads. In the grid-connected, the utility grid determines the standard output power using microgrid central controller. Thus DGs and storage units are reserved as power quality (PQ) control in this case. On the other hand, MG might be disconnected for the utility grid when a shutdown problem happen. As result of that, microgrid

isolates from the the distributed network to supply the local loads [12]. In particular, slight variations occur in the voltage and the frequency from the standardized values because of load sharing. The energy storage system will provide a solution by injecting or absorbing some active power proportionally to the variations. In this mode, the DGs and storage units are used to droop control [187].

The coordinated control of distributed generation units within microgrid can be mainly realized through centralized control, decentralized control, distributed control. The hierarchy of the microgrid is mostly operating in forms of centralized control technique. Microgrid central controller assigns reference signals to distributed generators to make action relied on the received measurement signals from local plants through a communication network. In this sense, considerable wide-band channels are required to transmit rapidly to and from a centralized station unit. This structure is broadly utilized for distributed generations that meet a common target like industrial microgrid. In large scale systems, the reliability and the flexibility of the centralized control scheme can be impacted by communication constraints such as time delays data dropout and limited bandwidth. Unfortunately, the entire control system fails due to breakdown of the centralized controller. In spite of that the centralized control technique has been usually successful in the primary and secondary level of the microgrid [169].

To avoid such situation, decentralized control is a new technique performed by employing local controllers to avoid the single point of failure based on multi agent theory [202]. Within decentralized control, the structure of the complex systems is divided into a set of small scale subsystems with local controller. Hence, each distributed generators and its load are controlled using only local measurements [197]. Thus decentralized technique enhances system reliability and performance, being able to regulate power with

the main grid. However, when the main feeder fails, local primary droop controllers regulate the voltage and frequency in the standard level and sustain the stability of the standalone microgrid [201, 198]. This structure enables a limited data sharing among the local controller to perform local and global targets. An interesting characteristic of the decentralized method, the control of the subsystem is independent of the neighbor parameters. The primary and secondary controllers can be implemented in decentralized control structure. The drawback of the decentralized control is that it ignores the interactions among some local controllers and allows a limited information shared between them [63].

Recently, a distributed control structure is taken place in the forms of the secondary level in microgrid. Within this structure, an improved communication architecture allow the local controller to share parameters to optimize power regulation without owner interference. Distributed control technique enhance the reliability and the robustness against the entire system failure, in which the outage of any subsystem will not cause the entire microgrid down. Recently, a secondary control level is implemented based distributed control structure [169].

Broadly speaking, the hierarchical structure of the microgrid systems consists of primary, secondary, and tertiary control. Once a microgrid is disconnected from the utility grid, the so-called primary droop controller is used to sustain the voltage and frequency stability and to optimize power management [199, 200]. These purposes can be done by executing the current and voltage control loops of the interface devices. On the other front, thus primary controller might cause variations in the voltage and frequency values [187]. In its literature review, wide range of decentralized control strategies are applied to assure the control and stabilization of frequency/voltage inside microgrids

namely a conventional PI/PID [191], an optimal [192], an adaptive [193, 158], a robust [194], a model predictive [195] control strategies. Droop controllers are implemented without communication architecture among the distributed generation controllers. Furthermore, various droop primary control strategies have been proposed by means of centralized control techniques. In non-droop strategy, the communication architecture is adopted for power sharing and voltage regulation among the distributed generation units using synchronized internal oscillators [188]. However, non-droop methods are pure droop controller with respect to load variations and multi-distributed power generations. Additionally, an other non-droop control called master/slave technique that sustains voltage stability within the standard range by sharing load automatically. In master/slave technique, some of the other PQ buses tackle the load variations by inject/absorb suitable amounts of active/reactive power [189].

The key idea of implementing a secondary control is to compensate for voltage and frequency variations in micro power grid result of primary control loop and to synchronize MG with the utility before shifting to the grid-connected mode. In contrary with primary control, the secondary control uses feedback communication systems to transfer values of the MG parameters to each DG unit [66]–[67]. Shafiee [63] developed a distributed secondary control in droop-controlled islanded microgrids. Authors in [63],[64] considered networked control systems (NCS) as distributed control methods for power grids. Strictly speaking, the reliability of the distributed power generation system is improved in existence of network constraints such time delay, and packet drop[64, 169, 170]. In particular, limited bandwidth communication channels are exercised to provide information flow between a microgrid center controller and local controllers of distributed generators. The influence of this sort of time delay on the microgrid

performance is considered in terms of multiple DGs. The proposed control strategy can stabilize the microgrid systems and compensate the impact the local time delay on the autonomous microgrid [196].

The introduction of networked control systems (NCSs) as a distributed control applications for DGs have been reported in [63, 64, 169]. It is worth noting that NCSs enhance the overall performance and stability for micro power grid at local loops by removing voltage and frequency variations, and inaccuracy in power sharing mechanism. Furthermore, the system's reliability is improved in existence of network constraints [64, 169]. The issues of unreliable communication channels in presence of communication constraints namely, time delay, packet dropout, and quantization effects have been tackled using User Datagram protocol (UDP) and transfer control protocol (TCP) networks [175, 176].

Nowadays, an adaptive control theory and application have received more effort in nonlinear and linearized system to tackle time-varying uncertainties. In particular, the adaptive control method comprise a parameter predictor to produce parameter estimates, and proper control law to ensure system stability [203]. Further insight into the operation of distributed generation systems in microgrid, there are different sort of nonlinearity such the nonlinear dynamics of each DG is formed by directquadrature (d–q) reference frame, nonlinearity because unbalance loads, nonlinearity because of nature of electronic elements. Moreover, some reports have been done to tackle uncertainty issue in distributed generation systems inside microgrid such speed uncertainty, load uncertainty[204]. In fact, uncertainties and time delays impact the parameters in distributed generation systems and regards the performance of the power system. As a result of that, the standard control methodologies may provide undesired perfor-

mance due to operating condition change in uncertain islanded MG. Adaptive control techniques can adapt system parameters to handle and to estimate uncertainties. Furthermore, a decentralized adaptive technique is immensely implemented to avoid singla point of failure that may be occurred centralized microgrid controller such as in (chapter 3).

In this chapter, a developed $\mathfrak{L}_1$ adaptive control strategy is applied to handle uncertainties and nonlinearity issues for multi-input-multi-output (MIMO) distributed generation systems, see Fig. 4.1. An $\mathfrak{L}_1$ adaptive control is a robust strategy because of its a strong capability, fast adaptation, and ensured transient performance. In particular, $\mathfrak{L}_1$ adaptive control comprises of state predictor, adaptive law, and control law. The state predictor eliminates the steady state error by a proper estimate of the system dynamic, and an adaptation strategy is applied to estimate uncertain parameters in which together leads to better design of the controller [206]–[210].

The remainder of this chapter is as follows: Section II describes the considered microgrid system modeling, section III accomplishes an $\mathfrak{L}_1$ adaptive control strategy for islanded microgrid. Section IV represents an analysis of the main result of this chapter and the sufficient stability condition. Section V carries out simulations for the considered numerical example. Finally, section VI concludes the chapter and gives a brief outlook.

4.2 Microgrid System Modeling

MG can operate interconnected to the main distribution grid, or in an islanded mode or or transition operation mode. Usually, MG operates in grid-connected mode but if any

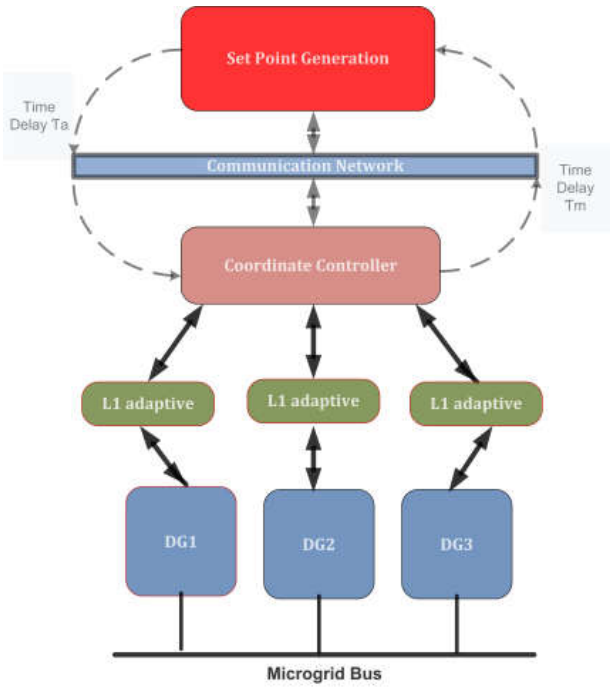

Figure 4.1: A typical microgrid system under $\mathfrak{L}_1$ adaptive control.

fault or disturbance occurs it shifted to islanded operation mode [2]. In this section, we consider a mathematical model of islanded microgrid, which integrates n distributed generation units and a local load as shown in Fig. 4.2. Under the balance condition, a state space model of islanded (autonomous) MG is investigated in the section. Applying Kirchhoffs voltage KVL and current KCL laws on the microgrid system, each DG system is represented by a DC voltage source, a three phase voltage source converter and a series

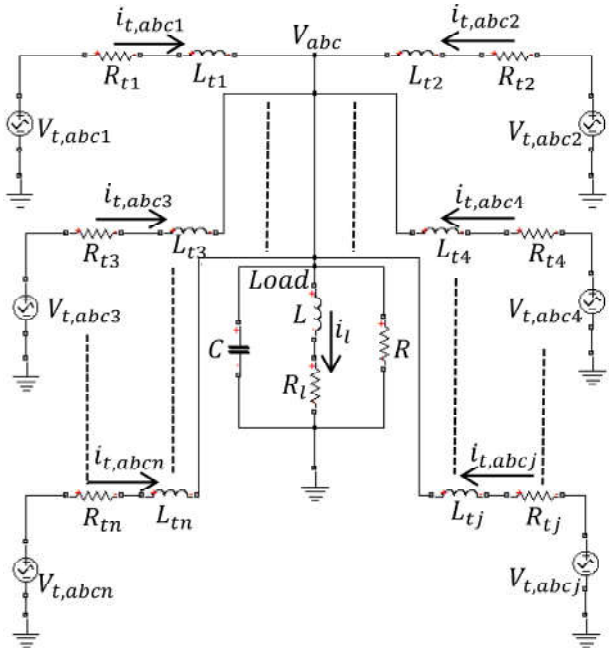

Figure 4.2: Single line diagram of the islanded system consisting of multiple DGs

RL filter.

$$
\begin{aligned}
\nu_{abc} &= L\frac{di_{L,abc}}{dt} + R_l i_{L,abc} \\
\nu_{t,abc_1} &= L_{t_1}\frac{di_{t,abc_1}}{dt} + R_{t_1} i_{t,abc_1} + \nu_{abc} \\
\nu_{t,abc_2} &= L_{t_2}\frac{di_{t,abc_2}}{dt} + R_{t_2} i_{t,abc_2} + \nu_{abc} \\
&\vdots \\
&\vdots \\
\nu_{t,abc_n} &= L_{t_n}\frac{di_{t,abc_n}}{dt} + R_{t_n} i_{t,abc_n} + \nu_{abc} \\
i_{t,abc_1} &+ i_{t,abc_2} + \cdots + i_{t,abc_n} \\
&= \frac{\nu_{abc}}{R} + i_{L,abc} + C\frac{d\nu_{abc}}{dt}
\end{aligned}
\tag{4.1}
$$

where ν_{abc}, $\nu_{t,abc1}$, $\nu_{t,abc2}$, $i_{L,abc}$, $i_{t,abc1}$, $i_{t,abc2}$ are 3×1 vectors containing the three-phase variables. Under the balanced conditions, the zero-sequence of a three-phase variable

x_{abc} in (4.1) is zero.

Thus, the model in (4.1) can be transformed to the $\alpha\beta$-frame using $x_{\alpha\beta} = x_a e^{j0} + x_b e^{j2\pi/3} + x_c e^{j4\pi/3}$ where $x_{\alpha\beta} = x_\alpha + j x_\beta$. Therefore, the state space equations of the system in the $\alpha\beta$-frame are:

$$\begin{aligned}
\frac{d\nu_{\alpha\beta}}{dt} &= -\frac{1}{RC}\nu_{\alpha\beta} + \frac{1}{C}i_{t,\alpha\beta 1} - \frac{1}{C}i_{L,\alpha\beta} \\
&+ \frac{1}{C}i_{t,\alpha\beta 2} + \cdots + \frac{1}{C}i_{t,\alpha\beta_n} \\
\frac{di_{t,\alpha\beta 1}}{dt} &= -\frac{1}{L_{t1}}\nu_{\alpha\beta} - \frac{R_{t1}}{L_{t1}}i_{t,\alpha\beta 1} + \frac{1}{L_{t1}}\nu_{t,\alpha\beta 1} \\
\frac{di_{L,\alpha\beta}}{dt} &= \frac{1}{L}\nu_{\alpha\beta} - \frac{R_l}{L}i_{L,\alpha\beta} \\
\frac{di_{t,\alpha\beta 2}}{dt} &= -\frac{1}{L_{t2}}\nu_{\alpha\beta} - \frac{R_{t2}}{L_{t2}}i_{t,\alpha\beta 2} + \frac{1}{L_{t2}}\nu_{t,\alpha\beta 2} \\
&\vdots \\
&\vdots \\
\frac{di_{t,\alpha\beta_n}}{dt} &= -\frac{1}{L_{t_n}}\nu_{\alpha\beta} - \frac{R_{t_n}}{L_{t_n}}i_{t,\alpha\beta_n} + \frac{1}{L_{t_n}}\nu_{t,\alpha\beta_n}
\end{aligned} \tag{4.2}$$

To simplify the control design procedure the dynamical equations (4.2) should be transformed to the dq-frame as:

$$x_{\alpha\beta} = X_{dq} e^{j\theta} = (X_d + j X_q) e^{j\theta} \tag{4.3}$$

where $\theta(t) = \int_0^t w(\xi)d\xi + \theta_0$ is the phase-angle of any three-phase signal in the system.

The dq-frame state space equation can be written as [190]:

$$\begin{aligned}
\frac{dV_{dq}}{dt} + jw_0 V_{dq} &= -\frac{1}{RC}V_{dq} + \frac{1}{C}I_{t,dq1} - \frac{1}{C}I_{L,dq} \\
&+ \frac{1}{C}I_{t,dq2} + \cdots + \frac{1}{C}I_{t,dqn} \\
\frac{dI_{t,dq_1}}{dt} + jw_0 I_{t,dq1} &= -\frac{1}{L_{t_1}}V_{dq} - \frac{R_{t_1}}{L_{t_1}}I_{t,dq_1} + \frac{1}{L_{t_1}}V_{t,dq_1} \\
\frac{dI_{L,dq}}{dt} + jw_0 I_{L,dq} &= \frac{1}{L}V_{dq} - \frac{R_l}{L}L, dq \\
\frac{dI_{t,dq_2}}{dt} + jw_0 I_{t,dq_2} &= -\frac{1}{L_{t_2}}V_{dq} - \frac{R_{t_2}}{L_{t_2}}I_{t,dq_2} + \frac{1}{L_{t_2}}V_{t,dq_2} \\
&\vdots \quad \vdots \\
\frac{dI_{t,dq_n}}{dt} + jw_0 I_{t,dq_2} &= -\frac{1}{L_{t_n}}V_{dq} - \frac{R_{t_n}}{L_{t_n}}I_{t,dq_n} + \frac{1}{L_{t_n}}V_{t,dq_n}
\end{aligned}$$

State space presentation of real components is:

$$\dot{x} = Ax + Bu, \;\; y = Cx$$

where x is the state vector, u is the control vector and y is the output vector are:

$$\begin{aligned}
x &= [V_d,\ V_q,\ I_{td1},\ I_{tq1},\ I_{Ld},\ I_{Lq},\ I_{td2},\ I_{tq2}, \cdots,\ \cdots,\ I_{td_n},\ I_{tq_n}]^T \\
u &= \begin{bmatrix} V_{td_1} & V_{tq_1} & V_{td_2} & V_{tq_2} & \cdots & V_{td_n} & V_{tq_n} \end{bmatrix}^T \\
y &= \begin{bmatrix} V_d & V_q & I_{td_2} & I_{tq_2} & \cdots & I_{td_n} & I_{tq_n} \end{bmatrix}^T
\end{aligned}$$

and the matrices A, B and C are obtained by decoupling the real and imaginary parts,

the dynamics of the d and q axes are given above:

$$A = \begin{bmatrix}
-\frac{1}{RC} & -w_0 & \frac{1}{C} & 0 & -\frac{1}{C} & 0 & -\frac{1}{C} & 0 & \cdots & \frac{1}{C} & 0 \\
-w_0 & -\frac{1}{RC} & 0 & \frac{1}{C} & 0 & -\frac{1}{C} & 0 & -\frac{1}{C} & \cdots & 0 & \frac{1}{C} \\
-\frac{1}{L_{t1}} & 0 & -\frac{R_{t1}}{L_{t1}} & w_0 & 0 & 0 & 0 & 0 & \cdots & 0 & 0 \\
0 & -\frac{1}{L_{t1}} & -w_0 & -\frac{R_{t1}}{L_{t1}} & 0 & 0 & 0 & 0 & \cdots & 0 & 0 \\
\frac{1}{L} & 0 & 0 & 0 & -\frac{R_l}{L} & w_0 & 0 & 0 & \cdots & 0 & 0 \\
0 & -\frac{1}{L} & 0 & 0 & -w_0 & -\frac{R_l}{L} & 0 & 0 & \cdots & 0 & 0 \\
\frac{1}{L_{t2}} & 0 & 0 & 0 & 0 & 0 & -\frac{R_{t2}}{L_{t2}} & w_0 & \cdots & 0 & 0 \\
0 & \frac{1}{L_{t2}} & 0 & 0 & 0 & 0 & -w_0 & -\frac{R_{t2}}{L_{t2}} & \cdots & 0 & 0 \\
\vdots & \vdots & \vdots & \vdots & \vdots & \vdots & \vdots & \vdots & \ddots & \vdots & \vdots \\
-\frac{1}{L_{tn}} & 0 & 0 & 0 & 0 & 0 & 0 & 0 & \cdots & -\frac{R_{tn}}{L_{tn}} & w_0 \\
0 & -\frac{1}{L_{tn}} & 0 & 0 & 0 & 0 & 0 & 0 & \cdots & -w_0 & -\frac{R_{tn}}{L_{tn}}
\end{bmatrix}$$

$$B = \begin{bmatrix}
0 & 0 & 0 & 0 & \cdots & 0 & 0 \\
0 & 0 & 0 & 0 & \cdots & 0 & 0 \\
\frac{1}{L_{t1}} & 0 & 0 & 0 & \cdots & 0 & 0 \\
0 & \frac{1}{L_{t1}} & 0 & 0 & \cdots & 0 & 0 \\
0 & 0 & 0 & 0 & \cdots & 0 & 0 \\
0 & 0 & 0 & 0 & \cdots & 0 & 0 \\
0 & 0 & \frac{1}{L_{t2}} & 0 & \cdots & 0 & 0 \\
0 & 0 & 0 & \frac{1}{L_{t2}} & \cdots & 0 & 0 \\
\vdots & \vdots & \vdots & \vdots & \ddots & \vdots & \vdots \\
0 & 0 & 0 & 0 & \cdots & \frac{1}{L_{tn}} & 0 \\
0 & 0 & 0 & 0 & \cdots & 0 & \frac{1}{L_{tn}}
\end{bmatrix}^T, \quad C = \begin{bmatrix}
1 & 0 & 0 & 0 & \cdots & 0 & 0 \\
0 & 1 & 0 & 0 & \cdots & 0 & 0 \\
0 & 0 & 0 & 0 & \cdots & 0 & 0 \\
0 & 0 & 0 & 0 & \cdots & 0 & 0 \\
0 & 0 & 0 & 0 & \cdots & 0 & 0 \\
0 & 0 & 0 & 0 & \cdots & 0 & 0 \\
0 & 0 & 1 & 0 & \cdots & 0 & 0 \\
0 & 0 & 0 & 1 & \cdots & 0 & 0 \\
\vdots & \vdots & \vdots & \vdots & \ddots & \vdots & \vdots \\
0 & 0 & 0 & 0 & \cdots & 1 & 0 \\
0 & 0 & 0 & 0 & \cdots & 0 & 1
\end{bmatrix}^T$$

Table 4.1: Parameters of the DGs connected to MG [177].

Quantity	Value
R_{t1} (series filter resistance in DG 1)	1.5 m Ω
L_{t1} (series filter inductance in DG 1)	300 μH
R_{t2} (series filter resistance in DG 2)	6 m Ω
L_{t2} (series filter inductance in DG 2)	900 μH
R_{t3} (series filter resistance in DG 3)	9 m Ω
L_{t3} (series filter inductance in DG 3)	1200 μH
VSC rated power	S_{base}=2.5 MVA
VSC terminal voltage (line-line)	V_{base}=600V
f_{sw} (PWM carrier frequency)	1980 Hz
R (Load nominal resistance)	76 Ω
L (Load nominal inductance)	111.9 mH
C (Load nominal capacitance)	62.86 μF
$q = \frac{L\omega_0}{R_l}$(Inductor quality factor)	120
f_0 (System frequency)	60 Hz

4.2.1 Case of three distributed generation units

In this chapter, we will focus on a microgrid including three distributed generators, in which $n = 3$. The typically distributed systems of the microgrid incorporates three DGs in abc-frame is deduced by the following equations:

$$\begin{aligned} v_{t,abc_i} &= L_{t_i}\frac{di_{t,abc_i}}{dt} + R_{t_i}i_{t,abc_i} + v_{abc}, \\ v_{abc} &= L\frac{di_{L,abc}}{dt} + R_l i_{L,abc}, \\ & \quad i_{t,abc_1} + i_{t,abc_2} + i_{t,abc_3} \\ &= \frac{1}{R}v_{abc} + i_{L,abc_i} + C_i\frac{dv_{abc}}{dt} \end{aligned} \tag{4.4}$$

where equation (4.4), $v_{abc}, v_{t,abc_i}, i_{L,abc}, i_{t,abc_i}$ are essentially 3×1 vectors which contain the three phase quantities, in which v_{abc} is the three phase voltage and i_{abc} is the three phase current. The symbol $i = 1, 2, 3$ represents the number of distributed generation

units in islanded microgrid. Using transformation ($abc\ to\ \alpha\beta$), the 3-phase variable x_{abc} in (4.4) is converted to a $\alpha\beta$ reference frame [178].

$$x_{\alpha\beta} = x_a e^{j0} + x_b e^{j\frac{2\pi}{3}} + x_c e^{j\frac{4\pi}{3}} \tag{4.5}$$

where $x_{\alpha\beta} \triangleq x_\alpha + j x_\beta$. The dynamics of the system in the $\alpha\beta$-frame is expressed as

$$\begin{aligned}
\frac{dv_{\alpha\beta}}{dt} &= -\frac{1}{RC}v_{\alpha\beta} + \frac{1}{C}i_{t,\alpha\beta_1} + \frac{1}{C}i_{t,\alpha\beta_2} \\
&+ \frac{1}{C}i_{t,\alpha\beta_3} - \frac{1}{C}i_{L,\alpha\beta} \\
\frac{di_{t,\alpha\beta_i}}{dt} &= -\frac{R_{t_i}}{L_{t_i}}i_{t,\alpha\beta_i} - \frac{1}{L_{t_i}}v_{\alpha\beta} + \frac{1}{L_{t_i}}v_{t,\alpha\beta_i} \\
\frac{di_{L,\alpha\beta}}{dt} &= \frac{1}{L}v_{\alpha\beta} - \frac{R_l}{L}i_{L,\alpha\beta}
\end{aligned} \tag{4.6}$$

By transferring (4.6) to a rotating frame which has its basis is:

$$x_{\alpha\beta} = x_{dq}e^{j\theta} = (x_d + j x_q)e^{j\theta} \tag{4.7}$$

where $\theta(t) \triangleq \int_0^t \omega(\zeta)d\zeta + \theta_0$. $\theta(t)$ adapts the phase angle of a reference vector ($x_\alpha^{ref} + j x_\beta^{ref}$) in the $\alpha\beta$ frame. This chapter considers frequency of islanded MG for open loop system with a fixed frequency of the internal oscillator $\omega_0 = 2\ \pi\ f_o$, where $f_o = 60HZ$. The dq-frame equations represent as [178]:

$$\begin{aligned}
\frac{dV_{dq}}{dt} + j\omega_0 V_{dq} &= -\frac{1}{RC}V_{dq} + \frac{1}{C}I_{t,dq_1} - \frac{1}{C}I_{L,dq} \\
&+ \frac{1}{C}I_{t,dq_2} + \frac{1}{C}I_{t,dq_3}, \\
&\frac{dI_{t,dq_i}}{dt} + j\omega_0 I_{t,dq_i} = -\frac{1}{L_{t_i}}V_{dq} - \frac{R_{t_i}}{L_{t_i}}I_{t,dq_i} + \frac{1}{L_{t_i}}V_{t,dq_i}, \\
&\frac{dI_{L,dq}}{dt} + j\omega_0 I_{L.dq} = \frac{1}{L}V_{dq} - \frac{R_l}{L}I_{L,dq},
\end{aligned} \tag{4.8}$$

$$A_{1j} = \begin{bmatrix} -\frac{1}{RC} & 0 & -\frac{1}{C} & 0 \\ 0 & -\frac{R_l}{L} & 0 & 0 \\ -\frac{1}{L_{t1}} & 0 & -\frac{R_{t1}}{L_{t1}} & \omega_0 \\ 0 & 0 & -\omega_0 & -\frac{R_{t1}}{L_{t1}} \end{bmatrix}; \; B_{1j} = \begin{bmatrix} 0 & 0 \\ 0 & 0 \\ \frac{1}{L_{t1}} & 0 \\ 0 & \frac{1}{L_{t1}} \end{bmatrix}; \; C_{1j} = \begin{bmatrix} 1 & 0 \\ 0 & 1 \\ 0 & 0 \\ 0 & 0 \end{bmatrix}^T$$

After formulating the above equations, considering the states of the single distributed generation unit is considered as $x_{11} = [V_d, I_{Lq}, I_{td_1}, I_{tq_1}]$, the control input of one of the DGs might be represented as, $u_{11} = [V_{td_1}, V_{tq_1}]$, while the measurement signal of a single DG might be $y_{11} = [V_d, V_q]$. The state of the full coupled system can be formed as:

$x_{1j} = [V_d, V_q, I_{td_1}, I_{tq_1}, I_{Ld}, I_{Lq}, I_{td_2}, I_{tq_2}, I_{td_3}, I_{tq_3}]$, the control vector as $u_{1j} = [V_{td_1}, V_{tq_1}, V_{td_2}, V_{tq_2}, V_{td_3}, V_{tq_3}]$ and output vector as $y_{1j} = [V_d, V_q, I_{td_2}, I_{tq_2}, I_{td_3}, I_{tq_3}]$, the dynamics of the microgrid's system around the operating point may be obtain in the state-space model of islanded MG, see [177].

$$\begin{aligned} \dot{x}_{1j}(t) &= A_{1j}x_{1j}(t) + B_{1j}u_{1j}(t) + H_j(x_1)(t) \\ H_j(x_1)(t) &= \sum_{k \neq j}^{N} A_{jk}x_{1k}(t), \;\; j,k = 1,2...N. \\ y_{1j}(t) &= C_{1j}x_{1j}(t) \end{aligned} \tag{4.9}$$

Where $x_{1j}(t) \in \Re^n$ is the state variable, $u_{1j}(t) \in \Re^m$, is the control input, and $y_{1j}(t) \in \Re^p$ is the output signal, $H_j(x_1)(t)$ is interconnection term between the$th-j$ subsystem. The matrices of dynamic system can be qualified as $A_{1j} \in \Re^{n\times n}$ and the control input matrix $B_{1j} \in \Re^{n\times m}$. The output matrix $C_{1j} \in \Re^{m\times n}$. The parameter

values are stated in Table 4.1 [177]. We denote a real vector space with n-dimensional by $\Re^n \in \Re^+$, and $\Re^m \in \Re^+$ with m-dimensional, $\Re^p \in \Re^+$ with p-dimensional.

4.3 Distributed Generation Network Model

In this section, we implement a networked control model of MIMO distributed generation system in presence of communication constraints, see figure (4.1):

$$\begin{aligned} \dot{x}_j(t) &= A_j x_j(t) + \alpha_j B_j u_j(t) + f_j(t, y_j(t)) + \gamma_j^T(t) x_j(t - \tau_{aj}) + H_j(x)(t), \\ y_j(t) &= \beta_j C_j x_j(t) \end{aligned} \tag{4.10}$$

Where $x_j(t) \in \Re^n$ is the state vector, $y_j(t) \in \Re^p$ is the controlled output by the sensors, $u_j(t) \in \Re^m$ is the control input that is applied by the actuator. The model matrices are, the dynamic matrix $A_j \equiv A_{1j} \in \Re^{n \times n}$, the control input matrix $B_j \equiv B_{1j} \in \Re^{n \times m}$, B_j are assumed to be full rank =m, and the output observation matrix $C_j \equiv C_{1j} \in \Re^{p \times n}$, the pairs (A_j, B_j) is controllable [210]. $\alpha_j,\ \beta_j \in [0,\ 1]$ are bounded parameters in which they represent communication constraints. $\gamma_j^T(t)$, is unknown parameter, while the time delay $\tau_{aj},\ \in \Re^+$ is known time delay. The unknown function $f_j(t, y_j(t)) : [0,\ \infty] \times \Re^n \to \Re$ is a time-varying nonlinear perturbation.

$$Pr(\alpha_j) = \begin{cases} p_j; \ \ when \ \ \alpha_j = 1 \\ 1 - p_j; \ \ when \ \ \alpha_j = 0 \end{cases}$$

$$Pr(\beta_j) = \begin{cases} m_j; \;\; when \;\; \beta_j = 1 \\ 1 - m_j; \;\; when \;\; \beta_j = 0 \end{cases}$$

Where Pr indicates to probability of the unknown random variables.

Assumption 1 *1. Assuming there exist compact convex sets* $\mathbb{R}_1$, $\mathbb{R}_2$, *and* $\mathbb{R}_3$ *where* $\alpha_j \in \mathbb{R}_1$, $\gamma_j^T(t) \in \mathbb{R}_2$, $\beta_j \in \mathbb{R}_3$. *and* $\alpha_{max} \triangleq max_{\alpha \in \mathbb{R}_1} \|\alpha\|_1$, $\gamma_{max} \triangleq max_{\gamma \in \mathbb{R}_2} \|\gamma\|_1$, $\beta_{max} \triangleq max_{\beta \in \mathbb{R}_3} \|\beta\|_1$

Assumption 2 *Let the input and measurement disturbance* $f_j(t, y_j(t))$ *and* $H_j(x;t)$ *are bounded such as*

$$\begin{aligned} ||f_j(y_j(t);t) - f_j(\hat{y}_j(t);t)|| &\leq \varrho ||F_j(y - \hat{y})||, \\ ||H_j(x(t);t) - H_j(\hat{x}(t);t)|| &\leq \varrho_1 ||H_j(x(t) - \hat{x}_j(t))|| \end{aligned} \tag{4.11}$$

Where $\varrho_j, \varrho_{1j} > 0$, and $F_j \in \Re^{nxn}$ are a positive constant and constant matrix respectively. We can obtain

$$\begin{aligned} ||f_j(y_j(t);t)|| &\leq \varrho_j ||F_j(y)|| \\ ||H_j(x;t)|| &\leq \varrho_{1j} ||H_j(x)|| \end{aligned} \tag{4.12}$$

Assumption 3 *The communication time delay, which is produced by the low-bandwidth distributed networks, when the information transfers between the microgrid distributed/centralized controller to local controllers can be defined as:*

$$x_j(t - \tau_{aj}) = \begin{cases} x_j(t) : \tau_{aj} = 0 \\ x_j(t - \tau_{aj}) : \tau_{aj} = 1 \end{cases}$$

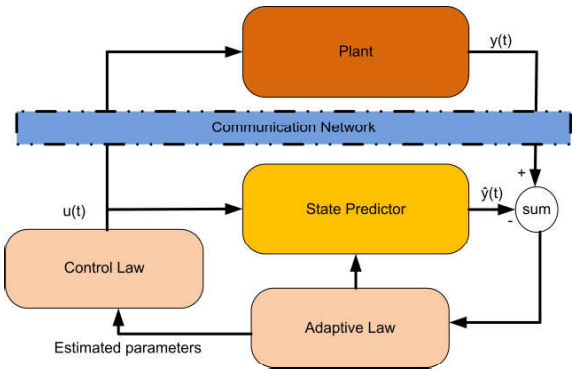

Figure 4.3: L_1 adaptive controller with uncertainties.

4.1 $\mathfrak{L}_1$ Adaptive Controller

The objective of this chapter is to design an $\mathfrak{L}_1$ adaptive output feedback controller for the microgrid model to realize reference model behavior, in which it comprises of state predictor, adaptation law, and control law with stable low-pass filter as stated in Fig. 4.3. The adaptation law fits an adaptive estimate of unknown parameters, in which they use in the design the state estimator. This adaptation law plays a key role to retain the estimated values of unknown parameters bounded. In reality, the system dynamics may be affected by a high frequency or low frequency disturbances. low pass filter is needed to eliminate the high frequency components. The control law provides an adaptation rate and robust performance, that guarantees asymptotic performances. The state predictor which can help to improve the performance of the closedloop control system, by estimates the state for the control system in presence of the communication constraints.

For the considered distributed generation dynamic systems in (4.10), the controller can be investigated as

$$u_j(t) \quad = \quad u_{1j}(t) + u_{aj}(t) + u_{Hj}(t) \tag{4.13}$$

Where $u_{1j}(t) = -K_j x_j(t)$ is the baseline controller, and $u_{aj}(t)$ is adaptive control, while $u_{Hj}(t)$ is the coordinate control response. We apply a linear quadratic regulation LQR strategy to design an optimal gain matrix $K_j \in \Re^{m\times n}$, such that the closed loop system of distributed generation units $A_{cj} = A_j - B_j K_j$ is Hurwitz. By means of LQR design, weighted matrices $Q_{1j} \geq 0$ and $R_{1j} > 0$ of states and inputs respectively are selected to minimize the objective function $J_{aj} \geq 0$. Increase the values of these weighted matrices cause a more penalty to the inputs and the states.

$$J_{aj} = \frac{1}{2}\sum_{tk=0}^{\infty} x_j^T(t) Q_{1j} x_j(t) + u_j^T(t) R_{1j} u_j(t) \tag{4.14}$$

In general, to compute the solution of the resulting Algebraic Riccati equation, we assume that there exists a symmetric matrix $P_{1j} = P_{1j}^T > 0$ and $Q_{1j} \in \Re^{m\times n}0$ such that:

$$A_{cj}^T P_{1j} + P_{1j} A_{cj} = -Q_{1j} \tag{4.15}$$

Remark 1 *The coordinated controller is designed in which it has a significant experience to organize numerous controllers for achieving objective effectively. Based on relative and local information from the other regulators, the local regulators follows the control signals from leader to sustain the common objective. Thus coordinated controller figures out the conflicts, enhances the performance, and minimizes the control cost.*

Based on (4.10) and (4.13), the state predictor is expressed by

$$\begin{aligned}\dot{\hat{x}}_j(t) &= A_{cj}\hat{x}_j(t) + \hat{\alpha}_j B_j u_{aj}(t) + \hat{f}_j(t, y_j(t)) + \hat{\gamma}_j^T(t)\hat{x}_j(t-\tau_{aj}) + \hat{H}_j(x)(t) \\ \hat{y}_j(t) &= \hat{\beta}_j C_j \hat{x}_j(t) \end{aligned} \tag{4.16}$$

Where $\hat{x}_j(t) \in \Re^n$ is the estimated state vector, $\hat{y}_j(t) \in \Re^p$ is the estimated output, also $\hat{\alpha}_j$, $\hat{\gamma}_j$, $\hat{f}_j(t)$, $\hat{v}_j(t)$ and $\hat{\beta}_j$ are the estimation parameters of the predictor.

4.0.1 Adaptation law

The adaptive law of the estimated parameters is obtain as following:

$$\begin{aligned}\dot{\hat{\alpha}}_j(t) &= \Gamma_j Proj(\hat{\alpha}_j(t), -e_j^T(t)P_{1j}B_j u_{aj}(t)), \\ \dot{\hat{\gamma}}_j(t) &= \Gamma_j Proj(\hat{\gamma}_j(t), -e_j^T(t)P_{1j}B_j x_j(t-\tau_{aj})), \\ \dot{\hat{f}}_j(t) &= \Gamma_j Proj(\hat{f}_j(t), -e_j^T(t)P_{1j}B_j), \\ \dot{\hat{\beta}}_j(t) &= \Gamma_j Proj(\hat{\beta}_j(t), -e_j^T(t)P_{1j}B_j x_j(t)) \end{aligned} \tag{4.17}$$

Let $e_j(t) = y_j(t) - \hat{y}_j(t)$ is the tracking error. Where the adaptive rate Γ_j is a positive constant, and the projection operator based adaptive law denotes by $Proj(,)$, which is implemented to block parameter deviations in applying an adaptive strategy [205, 206].

4.0.2 Control law

Taking the Laplace transform of (4.16), the predictive signal can be expressed as:

$$\begin{aligned} s\hat{x}_j(s) &= A_{cj}\hat{x}_j(s) + \hat{\alpha}_j B_j u_{aj}(s) + \hat{f}_j(s, y_j(s)) + \hat{\gamma}_j^T(s) x_j(s) e^{-\tau_{aj} s} + \hat{H}_j(s, x(s)) \\ (sI - A_{cj})\hat{x}_j(s) &= \hat{\alpha}_j B_j u_{aj}(s) + \hat{f}_j(s, y_j(s)) + \hat{\gamma}_j^T(s) x_j(s) e^{-\tau_{aj} s} + \hat{H}_j(s, x(s)) \end{aligned} \tag{4.18}$$

$$\hat{x}_j(s) = (sI_j - A_{cj})^{-1} \left\{ \hat{\alpha}_j B_j u_{aj}(s) + \hat{f}_j(s, y_j(s)) + \hat{\gamma}_j^T(s) x_j(s) e^{-\tau_{ja} s} + \hat{H}_j(s, x(s)) \right\} \tag{4.19}$$

and the output is represented:

$$\hat{Y}_j(s) = \hat{\beta}_j C_j (sI_j - A_{cj})^{-1} \left\{ \hat{\alpha}_j B_j u_{aj}(s) + \hat{f}_j(s, y_j(s)) + \hat{\gamma}_j^T(s) x_j(s) e^{-\tau_{aj} s}) + \hat{H}_j(s, x(s) \right\} \tag{4.20}$$

$$(\hat{\beta}_j C_j (sI_j - A_{cj})^{-1})^{-1} \hat{Y}_j(s) = (\hat{\alpha}_j B_j u_{aj}(s) + \hat{f}_j(s, y_j(s)) + \hat{\gamma}_j^T(s) x_j(s) e^{-\tau_{aj} s}) + \hat{H}_j(s, x(s))$$

$$\begin{aligned} B_j^{-1}(\hat{\beta}_j C_j (sI_j - A_{cj})^{-1})^{-1} \hat{Y}_j(s) &= (\hat{\alpha}_j u_{aj}(s) + B_j^{-1} \hat{f}_j(s, y_j(s)) + B_j^{-1} \hat{\gamma}_j^T(s) x_j(s) e^{-\tau_{aj} s}) \\ &+ B_j^{-1} \hat{H}_j(s, x(s)) \end{aligned} \tag{4.21}$$

Let us consider new state vector $\Upsilon(t)$ as following:

$$\begin{aligned}\Upsilon_j(s) &= G_j(s)\left\{B_j^{-1}(\hat{\beta}_j C_j(sI_j - A_{cj})^{-1})^{-1}\hat{Y}_j(s) - K_{gj}r_{aj}(s)\right\} \\ &= G_j(s)\Psi_j(s) \end{aligned} \tag{4.22}$$

Where $r_{aj}(s)$ transfer function of the reference signal, and $G_j(s)$ in an integral term has a transfer function $\frac{1}{s}$. Next, the control law is implemented in feedback form:

$$u_{aj}(s) = -K_{aj}\Upsilon_j(s) \tag{4.23}$$

Where $\Psi_j(t) = \hat{\alpha}_j u_{aj}(t) + B_j^{-1}\hat{f}_j(t, y_j(t)) + B_j^{-1}\hat{\gamma}_j^T(t)x_j(t - \tau_{aj}) + B_j^{-1}\hat{H}_j(s, x(s)) - K_{gj}r_{aj}(t)$, and $K_{gj} = -B_j^{-1}(\hat{\beta}_j C_j(sI_j - A_{cj})^{-1})^{-1}$, $K_{aj} > 0$ is output feedback gain. In particular, the G(s) a strictly proper transfer function leading to a strictly proper stable low pass filter $C_j(s)$ with transfer function is given as :

$$C_j(s) \triangleq \frac{\hat{\alpha}K_{aj}G_j(s)}{1 + \hat{\alpha}_j K_{aj}G_j(s)}$$

Where $j = 1, .., m$ for multi-input systems and the feedback gain matrix is $K_{aj} > 0$.

With the objective of designing L_1 adaptive controller such that the measurement output signal $y_j(t)$ follows a reference signal $r_{aj}(t)$ such that [207]:

$$y_j(s) \approx C_{aj}(s)r_{aj}(s)$$

Where $C_{aj}(s) = \frac{m_a}{s+m_a}$, is a minimum-phase stable transfer function, m_a is positive real

number, and $r_{aj}(s)$ is the reference of the minimum model.

4.0.3 Performance analysis

Stability Analysis of the Reference Model:

Consider a reference model of distributed generation system such as:

$$\begin{aligned} \dot{x}_{rj}(t) &= A_j x_{rj}(t) + \alpha_j B_j u_{rj}(t) + f_j(t, y_{rj}(t)) + \gamma_j^T(t) x_{rj}(t - \tau_{aj}) + H_j(x_r)(t), \\ y_{rj}(t) &= \beta_j C_j x_{rj}(t) \end{aligned} \tag{4.24}$$

Where $x_{rj}(t) \in \Re^n$ is the state vector of the reference model, $y_{rj}(t) \in \Re^p$ is the measured output of the reference model, $u_{rj}(t) \in \Re^m$ is the control input of the reference model. The Laplace function of low pass filter:

$$C_{rj}(s) \triangleq \frac{\hat{\alpha} K_{aj} G_{rj}(s)}{1 + \hat{\alpha}_j K_{aj} G_{rj}(s)}$$

The $\mathfrak{L}_1$ adaptive framework comprises of (4.13), (4.16) and (4.17), subject to the $\mathfrak{L}_1$ norm condition.

$$\left\| G_H(s) \right\|_{L_1} (\alpha_{max} + \beta_{max} + \gamma_{max}) < 1$$

Where $H_j(s) \triangleq (sI_H - A_j)^{-1} B_j$, and $G_{Hj}(s) \triangleq H_j(s)(C_j(s) - 1)$, The transfer form of control input of reference model is defined as:

$$u_{rj}(s) = C_{rj}(s) \Upsilon_{rj}(s) \tag{4.25}$$

with

$$\Psi_{rj}(t) = \hat{\alpha}_j u_{rj}(t) + B_j^{-1}\hat{f}_j(t, y_j(t)) + B_j^{-1}\hat{\gamma}_j^T(t)x_{rj}(t-\tau_{aj}) + B_j^{-1}\hat{H}_j(s, x_r(s)) - K_{gj}r_{aj}(t)$$

The following result holds

Lemma 4.1 *If the $\mathfrak{L}_1$ norm condition holds, then the reference model in (4.24) and its control law are BIBO stable with respect to reference signal.*

Proof. Let consider a closed-loop reference model as:

$$x_{rj}(t) \quad = \quad G_{Hj}(s)\Upsilon_{rj}(s) \tag{4.26}$$

Using the $\mathfrak{L}_1$ norm properties, we deduce:

$$\|x_{rj}\|_{L_\infty} \quad \leq \quad \|G_{Hj}\|_{L_1} \|\Upsilon_{rj}\|_{L_\infty} \tag{4.27}$$

With the following:

$$\begin{aligned} \|\Upsilon_{rj}\|_{L_\infty} &\leq \alpha_{max} \|x_{rj}\|_{L_\infty} + \gamma_{max} \|x_{rj}(\tau - \tau_{aj})\|_{L_\infty} + \beta max \|x_{rj}\|_{L_\infty} + \|f_{rj}(t, y_j(t))\|_{L_\infty} \\ &\leq (\alpha_{max} + \gamma_{max} + \beta_{max}) \|x_{rj}\|_{L_\infty} + \|f_{rj}(t, y_j(t))\|_{L_\infty} \end{aligned} \tag{4.28}$$

Substituting into above equation, we get:

$$\|x_{rj}\|_{L_\infty} \quad \leq \quad \|G_{Hj}\|_{L_1} (\alpha_{max} + \gamma_{max} + \beta_{max}) \|x_{rj}\|_{L_\infty} + \|G_{Hj}\|_{L_1} \|f_{rj}(t, y_j(t))\|_{L_\infty} \tag{4.29}$$

If the $\mathfrak{L}_1$ norm condition $\|x_{rj}\|_{L_\infty}$ is uniformly bounded:

$$\|x_{rj}\|_{L_\infty} \leq \frac{\|G_{Hj}\|_{L_1} \|f_{rj}(t, y_j(t))\|_{L_\infty}}{1 - \|G_{Hj}\|_{L_1} (\alpha_{max} + \gamma_{max} + \beta_{max})} \tag{4.30}$$

From the above, we can deduce that, the closed-loop reference model is BIBO stable.

∎

Prediction Error Analysis:

$$\begin{aligned} \dot{\tilde{x}}_j(t) &= A_j \tilde{x}_j(t) + \tilde{\alpha}_j B_j \tilde{u}_j(t) + \tilde{f}_j(t, \tilde{y}_j(t)) + \tilde{\gamma}_j^T(t) \tilde{x}_j(t - \tau_{aj}) + \tilde{H}_j(\tilde{x})(t), \\ \tilde{y}_j(t) &= \tilde{\beta}_j C_j \tilde{x}_j(t) \end{aligned} \tag{4.31}$$

where $\tilde{\ldots}_j$ represents the error between actual and estimated parameter, where the states error is defined as $\tilde{x}_j(t) = \hat{x}_j(t) - x_j(t)$, in the same sequence, we have $\tilde{\alpha}_j$, $\tilde{\beta}_j$, $\tilde{\gamma}_j$, $\tilde{f}_j$, $\tilde{y}_j$, and $\tilde{H}_j$. Assume that, $\tilde{\Psi}_{1j}(t) \triangleq \tilde{\Psi}_{rj}(t) + K_{gj} r_{aj}(t)$, then the transfer function of the prediction error is given as:

$$\tilde{x}_j(s) = (sI_j - A_j)^{-1} B_j \tilde{\Psi}_{1j}(t) \tag{4.32}$$

The following result holds

Lemma 4.2 *Regarding the system 4.10 and control law 4.13, we have*

$$\|\tilde{x}_j(t)\|_{\mathfrak{L}_\infty} \leq \sqrt{\frac{\Pi_j}{\lambda_{min}(P_{1j}) \Gamma_j}} \tag{4.33}$$

where $\Pi_j \triangleq 4\sum_{m=0}^{2} \max_{\chi_j \in \Xi_j} \|\Pi_j\|_2^2 + 4\Delta_j^2 + (\alpha_{1j} - \alpha_{2j})^2 + 4\frac{\lambda_{max}(P_j)}{\lambda_{min}(Q_j)}(d_{\Pi_j} \max_{\chi_j \in \Xi_j} \|\Pi_j\| + d_{\Pi_j}\Delta_j)$.

where $\lambda_{min}(S)$, $\lambda_{max}(S)$ denote, respectively, the smallest and largest eigenvalues of matrix S.

Proof.

Stability Analysis:

To prove the input and state are bounded, we introduce a candidate Lyapunov function as:

$$V_j(t) = \tilde{e}_j^T(t)P_{1j}\tilde{e}_j(t) + \frac{1}{\Gamma_j} tr\left(\tilde{\alpha}_j^T\tilde{\alpha}_j + \tilde{\beta}_j^T\tilde{\beta}_j + \tilde{\gamma}_j\tilde{\gamma}_j^T + \tilde{f}_j^T\tilde{f}_j\right) \tag{4.34}$$

By taking the derivative of the Lyapunov function:

$$
\begin{aligned}
\dot{V}_j(t) &= \dot{\tilde{e}}_j^T(t)P_{1j}\tilde{e}_j(t) + \tilde{e}_j^T(t)P_{1j}\dot{\tilde{e}}_j(t) + \frac{2}{\Gamma_j}tr\left(\tilde{\alpha}_j^T\dot{\tilde{\alpha}}_j + \tilde{\beta}_j^T\dot{\tilde{\beta}}_j + \tilde{\gamma}_j\dot{\tilde{\gamma}}_j^T + \tilde{f}_j^T\dot{\tilde{f}}_j\right) \\
&= \tilde{\beta}_j^2\tilde{x}_j^T(t)C_j^T(A_j^TP_{1j} + P_{1j}A_j)C_j\tilde{x}_j(t) + 2\tilde{\alpha}_j\tilde{\beta}_j\tilde{x}_j^T(t)C_j^TP_{1j}B_ju_{aj} \\
&+ 2\tilde{\beta}_j\tilde{x}_j^T(t)C_j^TP_{1j}\tilde{f}_j(t,\tilde{y}_j(t)) + 2\tilde{\beta}_j\tilde{x}_j^T(t)C_j^TP_{1j}\tilde{f}_j(t,\tilde{y}_j(t)) \\
&+ 2\tilde{\beta}_j\tilde{x}_j^T(t)C_j^TP_{1j}\tilde{x}_j(t-\tau_{aj}) + 2\tilde{\alpha}_j\tilde{\beta}_j\tilde{x}_j^T(t)C_j^TP_{1j}B_ju_{aj} \\
&+ 2\tilde{\beta}_j\tilde{x}_j^T(t)C_j^TP_{1j}\tilde{H}_j(\tilde{x})(t) + \frac{2}{\Gamma_j}tr\left(\tilde{\alpha}_j^T\dot{\tilde{\alpha}}_j + \tilde{\beta}_j^T\dot{\tilde{\beta}}_j + \tilde{\gamma}_j\dot{\tilde{\gamma}}_j^T + \tilde{f}_j^T\dot{\tilde{f}}_j\right) \\
&= -\tilde{\beta}_j^2\tilde{x}_j^T(t)C_j^TQ_{1j}C_j\tilde{x}_j(t) + 2\tilde{\alpha}_j\tilde{\beta}_j\tilde{x}_j^T(t)C_j^TP_{1j}B_ju_{aj} + 2\tilde{\beta}_j\tilde{x}_j^T(t)C_j^TP_{1j}\tilde{f}_j(t,\tilde{y}_j(t)) \\
&+ 2\tilde{\beta}_j\tilde{x}_j^T(t)C_j^TP_{1j}\tilde{x}_j(t-\tau_{aj}) + 2\tilde{x}_j^T(t)P_{1j}\tilde{H}_j(\tilde{x})(t) \\
&+ 2tr(\tilde{\alpha}_j^TProj(\hat{\alpha}_j(t), -e_j^T(t)P_{1j}B_ju_{aj}(t)) + \tilde{\beta}_j^TProj(\hat{\beta}_j(t), -e_j^T(t)P_{1j}B_j\tilde{x}_j(t)) \\
&+ \tilde{\gamma}_jProj(\hat{\gamma}_j(t), -e_j^T(t)P_{1j}B_jx_j(t-\tau_{aj})) + \tilde{f}_j^TProj(\hat{f}_j(t), -e_j^T(t)P_{1j}B_j)), \\
&\leq -\tilde{\beta}_j^2\tilde{x}_j^T(t)C_j^TQ_{1j}C_j\tilde{x}_j(t) + 2\tilde{x}_j^T(t)P_{1j}\tilde{H}_j(\tilde{x})(t) \\
&\leq -\tilde{\beta}_j^2\tilde{x}_j^T(t)C_j^TQ_{1j}C_j\tilde{x}_j(t) + 2\left\|\tilde{x}_j^T(t)\right\|\|P_{1j}\|\left\|\tilde{H}_j(\tilde{x})(t)\right\| \\
&\leq -\lambda_{min}(C_j^TQ_{1j}C_j)\left\|\tilde{\beta}_j\right\|^2\left\|\tilde{x}_j^T(t)\right\|^2 + 2\left\|\tilde{x}_j^T(t)\right\|\|P_{1j}\|\left\|\tilde{H}_j(\tilde{x})(t)\right\| \\
&= -\left\|\tilde{x}_j^T(t)\right\|(\lambda_{min}(C_j^TQ_{1j}C_j)\left\|\tilde{\beta}_j\right\|^2\left\|\tilde{x}_j^T(t)\right\| + 2\|P_{1j}\|\tilde{H}_j(\tilde{x})(t)) \qquad (4.35)
\end{aligned}
$$

Therefore, $\dot{V}_j(t) \leq 0$, if the output error and state error are bounded such (4.29) and (4.30) hold, for more analysis see [208] [210]. ∎

4.1 Simulation Studies

In this section, a lab scale distributed generation systems presented in Fig. 4.4 is considered to demonstrate the effectiveness of the proposed control strategy. A control

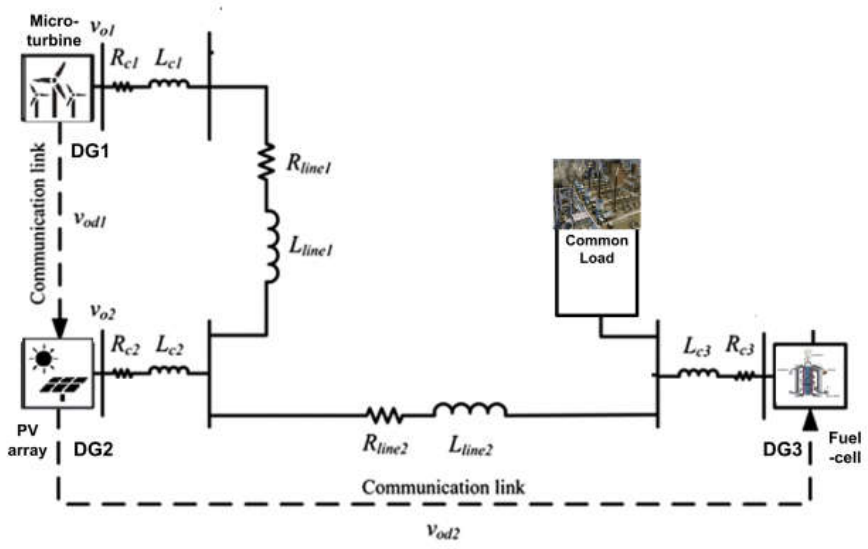

Figure 4.4: Lab. scale distributed generations architecture.

methodology for DGs operating in an islanded microgrid is investigated using $\mathfrak{L}_1$ adaptive controller. The state space model of the islanded microgrid that composes of three distributed generation systems with local loads is given in equations (4.9). The values of state-space parameters are given in Table 4.1. The probability of the communication time delay is varying from $0 \leq \tau_{aj} \leq 1$. We apply the $\mathfrak{L}_1$ adaptive control strategy with specific range of uncertain parameters in their convex compact sets $\alpha_j \in \mathbb{R}_1 = [0, 1]$, $\beta_j \in \mathbb{R}_2 = [0, 1]$, and $\gamma_j \in \mathbb{R}_3 = [45.5, 2]$. To see the influence of time delay on the system performance, in the first case the time delay is considered to be $\tau_{aj} = 0.05$. The relevant simulation results are shown in Figs. 4.5–4.9. In this example, we compare the performance of the proposed controller in the case when the time delay is $\tau_{aj} = 0.5$ *second*, with the case when frequency varying and the performance of LQR in the nominal case. It can be recognized that there are significant increasing in the settling time in Figs. 4.5–4.9. Further, these figures show that the microgrid has a good performance with time delay, in which it proves the robustness of the proposed $\mathfrak{L}_1$ controller. For the

current example, the low pass filter is selected to be:

$$C_j(s) = \frac{7.5s + 2.501}{s^3 + 2.063s^2 + 11.5s + 4.2}$$

The weighted matrices of optimal linear quadratic regulator are chosen as: $Q_{1j} = diag[10,\ 1,\ 1,\ 10]$, $R_{1j} = diag[.1,\ .1]$, the adaptive rate $\Gamma_j = 1000$. They can represent that the proposed $\mathfrak{L}_1$ adaptive with τ_a= 0.5 is very smooth and converges faster compared to LQR and $\mathfrak{L}_1$ adaptive in terms of frequency varying.

The proposed controller sustains the stability and the control the reference framework (dq) components for the DGs inside islanded MG in the presence of different uncertainties comparing LQR. The results of the simulation example elucidate that the proposed $\mathfrak{L}_1$ adaptive control provides considerable enhancement in of the DGs in terms

of system uncertainties.

$$P_{1j} = \begin{bmatrix} P_{1j1} & P_{1j2} \\ \bullet & P_{1j3} \end{bmatrix}$$

$$P_{1j1} = \begin{bmatrix} 2.871 & -2.504 & -8.397 & 18.8 & 8.43 \\ -2.50 & 47.87 & -78.34 & -35.11 & 78.19 \\ -8.39 & -78.34 & 195.85 & -5.17 & -195.65 \\ 18.77 & -35.11 & -5.17 & 176.14 & 5.39 \\ 8.43 & 78.19 & -195.65 & 5.39 & 195.56 \end{bmatrix}$$

$$P_{1j2} = \begin{bmatrix} -18.68 & -8.57 & 18.82 & -8.40 & 18.6 \\ 34.75 & -73.05 & -36.75 & -78.29 & -35.07 \\ 5.59 & 186.93 & -2.38 & 195.79 & -5.19 \\ -175.51 & -7.61 & 176.82 & -5.21 & 176.04 \\ -5.57 & -186.76 & 2.61 & -195.61 & 5.41 \end{bmatrix}$$

$$P_{1j3} = \begin{bmatrix} 175.65 & 7.99 & -176.19 & 5.62 & -175.42 \\ 7.99 & 178.66 & -5.02 & 186.88 & -7.63 \\ -176.19 & -5.02 & 177.59 & -2.42 & 176.72 \\ 5.62 & 18688 & -2.42 & 195.76 & -5.22 \\ -175.42 & -7.63 & 176.71 & -5.22 & 175.97 \end{bmatrix}$$

4.2 Conclusions

This chapter investigates the implementation of $\mathfrak{L}_1$ adaptive control for distributed generation systems in microgrid. An L_1 adaptive controller is a robust controller which

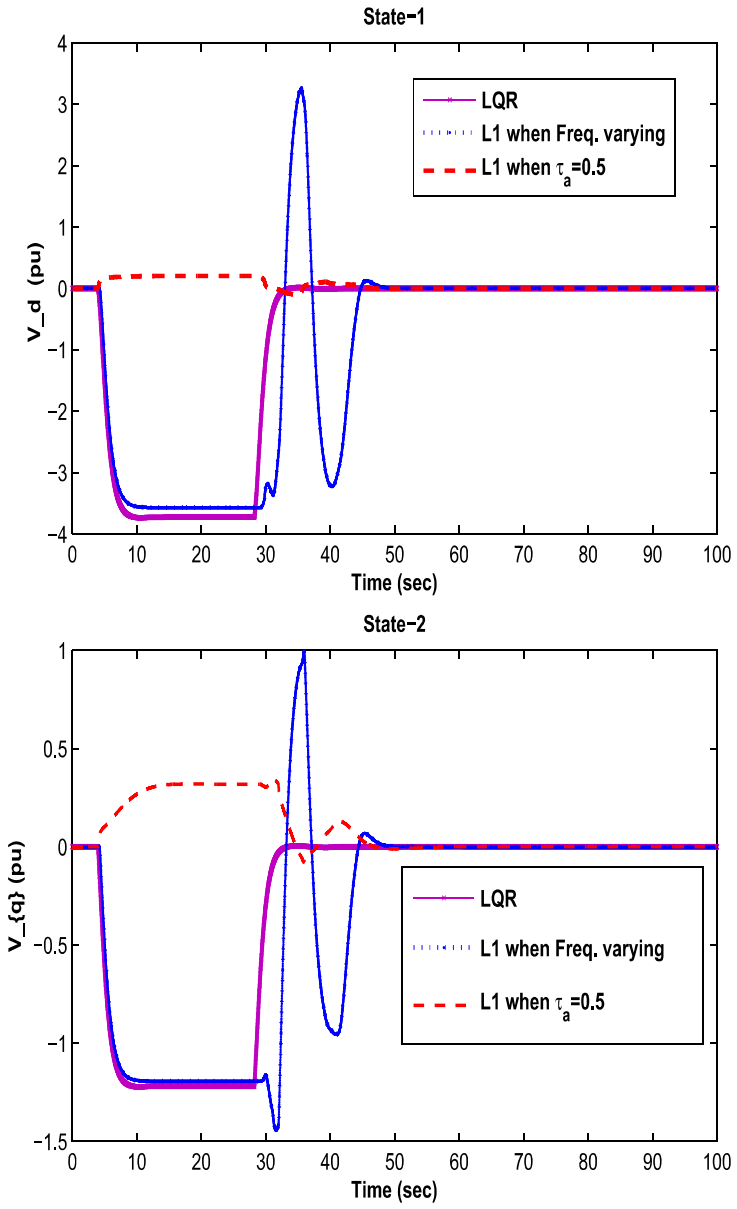

Figure 4.5: d and q component of load voltage.

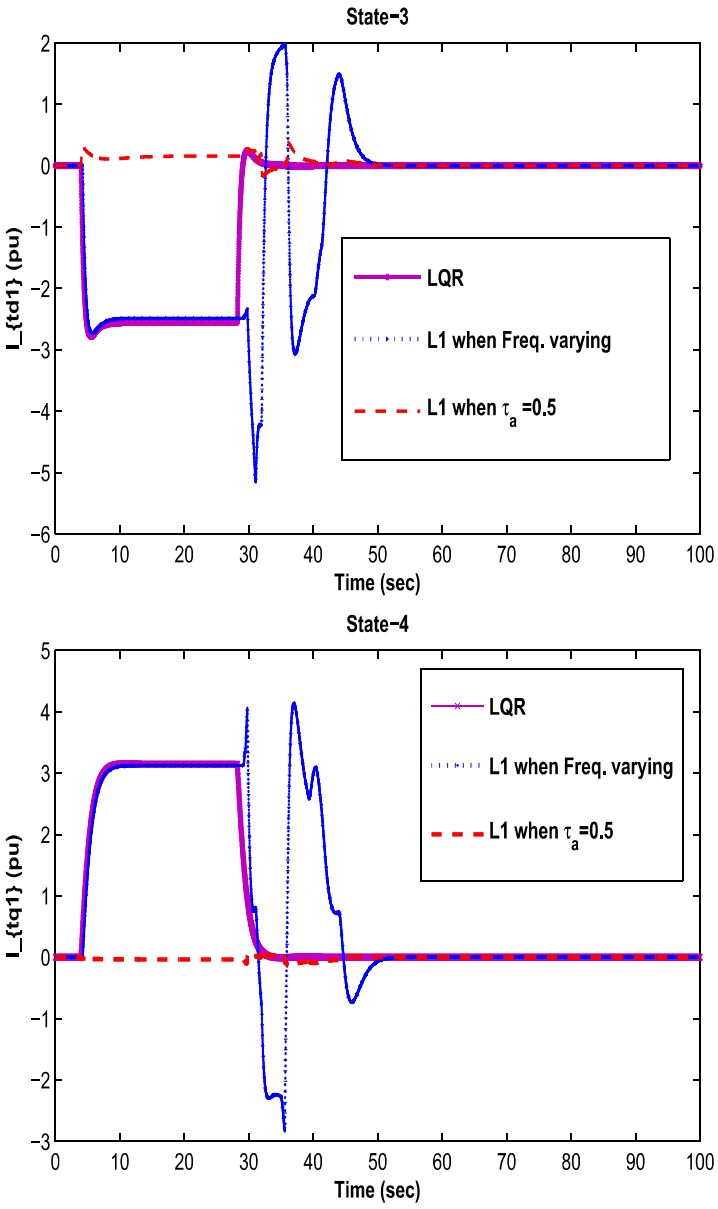

Figure 4.6: d and q component of DG1 current.

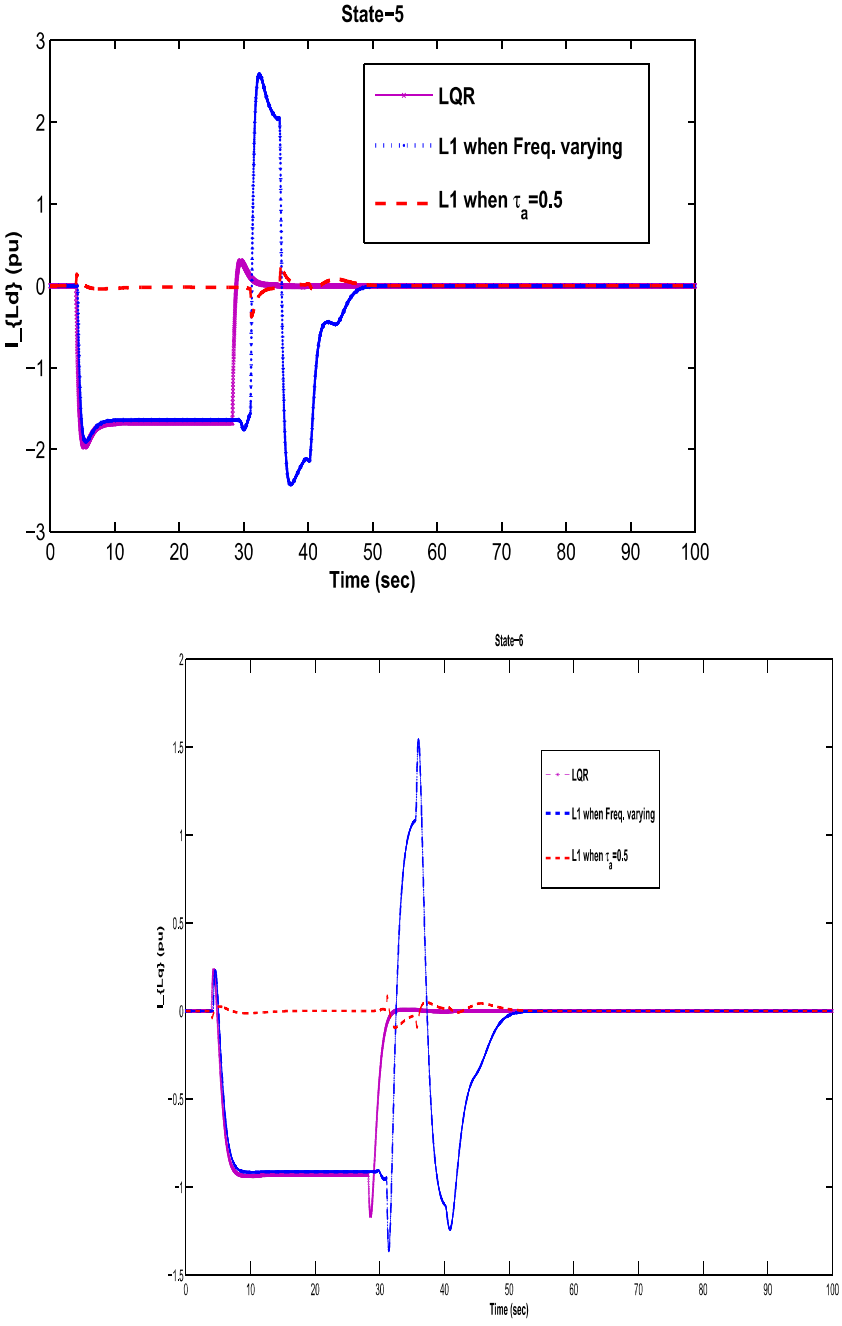

Figure 4.7: d and q component of load current.

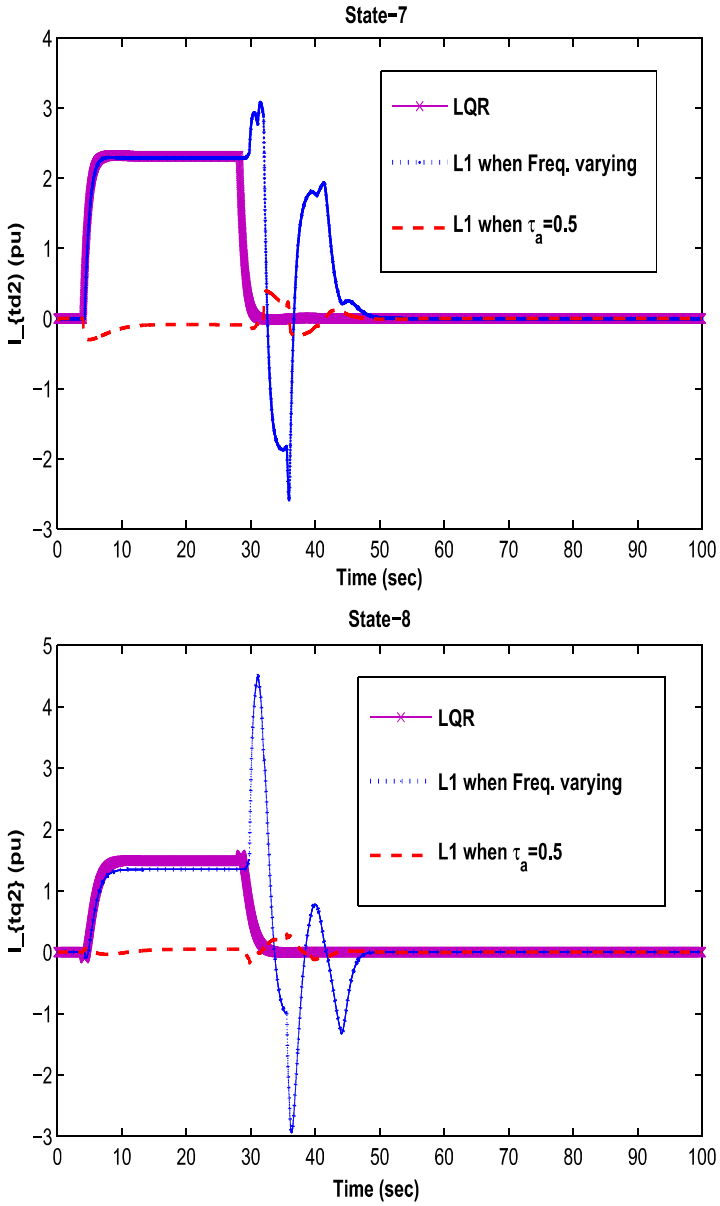

Figure 4.8: d and q component of DG2 current.

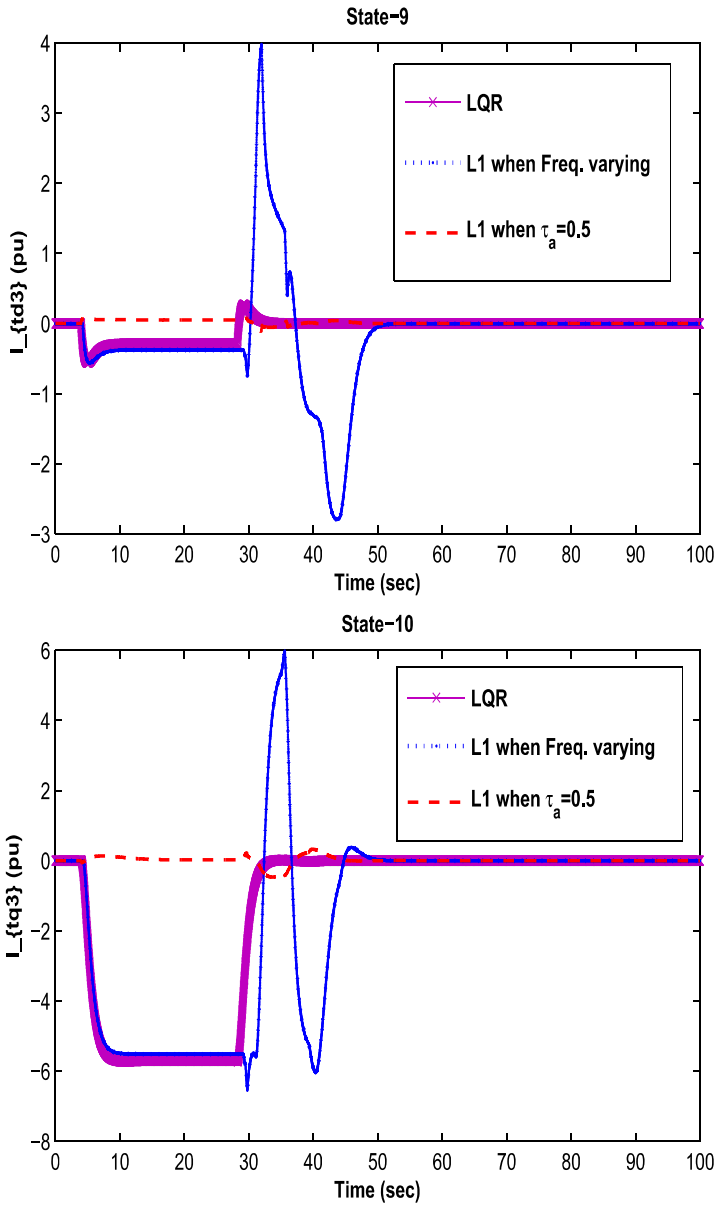

Figure 4.9: d and q component of DG2 current.

controls and ensures the network stability of DGs in presence of uncertainties and transmission time delays. The results demonstrate that the proposed $\mathfrak{L}_1$ adaptive control provides considerable enhancement in steady state error and transient performance of the DGs in terms of system uncertainties.

CHAPTER 5

A MULTI-AGENT CONTROL SCHEME

This chapter introduces a novel distributed control scheme for islanded microgrids in the presence of disturbances. The information flow among the distributed energy sources is limited by a communication graph. The dynamics of the distributed energy sources are interactive. Synchronization ideas from the cooperative control problem are utilized to track the dynamics of the distributed energy sources to a leader's dynamics. The cost function is selected to reflect the interplay between the distributed energy sources. The distributed energy sources are considered as players forming a dynamic game. An online adaptive learning technique based on Kalman filtering is used to estimate the dynamics of the distributed energy sources. Once the separation principle is held, the control input of every agent(node) and the estimator can be designed independently. This adaptive learning technique is used to figure out the dynamic game in realtime, using incomplete knowledge about the dynamics of the distributed energy sources. Means of Actor-critic neural networks (ACNNs) are utilized to establish this adaptive learning

technique. Simulation is performed on a network of Photovoltaic cells.

5.1 Introduction

Microgrids or Distributed Generation sources have been widely used for supplying local demands in remote areas in distributed power networks. Microgrids exhibited marvelous promise as clean and efficient sources of energy compared to fossil fuels [6, 7]. Microgrid is a combination of active load demands and distributed generation units especially wind turbines, fuel cells, and photovoltaic cells. Energy storage units like bank of batteries, flywheels, and super capacitors coexist with the distributed generation sources to sustain the active and reactive power at the nominal levels. The microgrids work in two main modes of operation. In islanded mode, the microgrids supply the power to local areas, and the voltage and frequency are regulated locally. While in the grid-tied mode, the utility grid along with the microgrids supply electric power to the network loads [7].

Multi-agent cooperative control techniques are developed for the robotic systems, unmanned vehicles, sensor grids [211]-[219]. The cooperative control problems for multi-agent systems (MAs) are divided as consensus and synchronization (tracking) control schemes [211]-[219]. In the first scheme, all agents reach the same state. In the second case, the agents follow the leader's dynamics. Selecting the utility or the cost function of the agents is crucial to the development of the control schemes [220]. Applying multi-agent control techniques to distributed generation sources have received a considerable attention in the last decade [221]. The related theoretical work and the application sides of the multi-agent control schemes in the wide area networks are introduced in [222]. Practical implementations of multi-agent strategies of power electric units are

introduced in [6]. A secondary level control scheme is used to control islanded network of microgrids in [6]. Distributed control structures with sparse communication network topologies became an interesting field to develop a variety of control strategies [222].

Dynamic Programming (DP) schemes are applied to figure out the optimal control problems. Approximate / Adaptive DP is a neuro-dynamic programming scheme, it uses adaptive critic design learning techniques that solves the optimal control problem [223, 224]. Approximate Dynamic Programming can be classified into Heuristic DP (HDP), Dual HDP, Action-Dependent HDP and Action Dependent Dual HDP [225]. ADP optimizes the objective cost function to find the optimal policies [226]–[230]. DP is effectively utilized to develop sub-optimal / approximate solution for infinite horizon optimal control issues [223].

Reinforcement Learning (RL) are temporal difference techniques that are used to implement the ADP [212][231]–[232]. RL is used to select the optimal policies in a learning environment [233, 234]. Reinforcement learning is used to find the optimal strategies for games with finite-state systems in [216],[231]. Furthermore, online RL methods are adopted to figure out differential graphical games in realtime [221], [217], [235]. RL has been applied for multi-agent control problems [212, 213, 214].Temporal difference methods are effective ADP tools that evaluate the utility cost functions and the associated control policies [236]. These methods involve two techniques known as value iteration (VI) and policy iteration (PI) [237]–[238]. In value iteration, the optimal policies can be found without the need for initial admissible control policies [239]–[243]. While, in the policy iteration, initial admissible control policies are required [234], [244]. Online temporal difference methods are employed to find the optimal decisions in realtime [231]. Online ACNNs are developed to establish the ADP scheme in real-time.

The critic structure is applied to assess the cost function, while the actor structure assesses the evaluated cost function and selects the control law that will minimize the cost-to-go function [225].

In the dynamic graphical games (DGGs) theoretic frame work, the information flow among nodes is limited by a communication graph [212]. Differential graphical games are sufficiently promoted for multi-agent systems in [239]. The dynamic graphical games combine game theory, cooperative control, and optimal control [239, 240]. A solution of the cost-to-go objective function is evaluated by figuring out the respective Hamiltonian-Jacobi-Bellman (HJB) equations [240]. In [225], policy iteration technique is introduced for MAs. Nash solutions for the standard games are achieved by solving the Hamilton-Jacobi (HJ) equations [237]–[240]. On line adaptive value iteration technique is proposed to figure out DGGs in [212].

Various methodologies have been considered to overcome the disturbance problem in a distributed network of the multi-agent systems. In [245], [246], a model-free ADP scheme based on H_∞ optimal control problem is proposed to reject the undesired disturbances. Kalman filtering (KF) has earned a considerable attention due to its robustness in parameters and states estimations. Kalman filter is a recursive scheme realized evaluating the mean square error covariance of the state, and it is applicable to linear state estimation problems. In [175], a discrete-time Kalman filter with linear quadratic regulator is used to estimate unknown states in a lossy communication network. However, the extended Kalman filter is used to estimate nonlinear systems [250]. A distributed KF has been developed, where the state's estimation is performed using the local information available to a set of local Kalman filters [247]–[249]. In the sequel, a distributed Kalman filter is developed for a network of photovoltaic cells that are distributed on

a communication graph. Furthermore, optimal and cooperative control techniques will be utilized to sustain synchronization among the photovoltaic cells to its leader.

The chapter is arranged as follows. Section 5.2, introduces the dynamic model of photovoltaic cells. Section 5.3 introduces the mathematical setup of the cooperative control problem, by briefly introducing graphs, Synchronization control ideas, and game definition. Section 5.4 introduces the cooperative control problem for the graphical game along with the Kalman filtering structure. Section 5.5 introduces an online adaptive learning technique (Policy Iteration) to control a network of distributed energy unit with Kalman filtering. Convergence analysis for the policy iteration algorithm is given. Section 5.6, introduces critic neural network (CNN) implementation for the solution to the graphical game with Kalman filtering. Section 5.7,introduces a simulation example to test the validity of the proposed control scheme.

5.2 Dynamical Model of Photovoltaic Cell

The integration of the solar energy to the main power grids is rapidly growing. Consequently, the dynamic model of the photovoltaic cell is introduced. The solar panels mainly built up of tiny PV cells. The current generated by photovoltaic cell is varying according to solar irradiation fluctuation. The Solar panel operating point can be governed by controlling the terminal current and voltage of the panel. Thus solar energy has a non linear and stochastic nature. Thus, novel control schemes are required to integrate this type of energy in a safe and reliable manner to the main power grid. The basic model of the PV cell involve a DC current source I_{DC} parallel with a diode and an internal resistance R_1, and a series internal resistance R_2 as shown in Fig. 5.1.

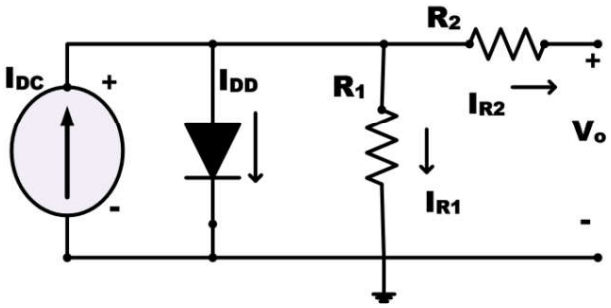

Figure 5.1: Photovoltaic Cell Electrical Model.

$$I_{R_2} = I_{DC_c} - I_{DD_o}[exp\,(\frac{V_o + R_2\, I_{R_2}}{V_T\, a_d}) - 1], \tag{5.1}$$

where I_{R_2}, V_o denote the output current and voltage of the PV cell. I_{DD} represents the diode current, I_{DD_o} is the diode's saturation current, V_T is thermal voltage of the PV panel, k_c is the standard Boltzmann constant, $a_d \in [0\ 1.5]$ is a diode ideal parameter, and I_{DC_c} denotes the current produced by sun light [251], and is given by

$$I_{DC_c} = (I_{DC_p} + K_i \Delta T)\frac{G}{G_p}, \tag{5.2}$$

where $I_{DC_c} = I_{DC_p}$, at nominal conditions, ΔT is the change in temperature (in Kelvin), G and G_p are the cell irradiation and nominal cell irradiation respectively.

$$I_{DD_o} = (I_{sl} + K_i \Delta T)(exp\,(\frac{V_{ol} + K_v \Delta T}{V_T\, a_d}) - 1)^{-1}, \tag{5.3}$$

where K_v and K_i are open loop parameters, V_{ol} denotes open loop voltage, and I_{sl} denotes short loop current.

Photovoltaics systems use boost converter to couple the solar energy to the power

system network load. Fig. 5.2 demonstrates a linear model of PV based boost converter so that the converter output voltage is given by

$$V_{c_o} = \frac{1}{1-D} V_{source}. \tag{5.4}$$

Where $D = 0.5$ denotes the duty ratio of the switch. The converter output current is given by

$$I_{c_o} = \frac{V_{c_o}}{R}. \tag{5.5}$$

This yields the converter output power so that

$$P_{c_o} = V_{c_o}\, I_{c_o}. \tag{5.6}$$

Thus a generalized dynamical model for the PV cell can be described by

$$\begin{aligned} \dot{x}_{1pv} &= \frac{1+K}{L}\, x_{2pv} + \frac{1}{L}\, u_{pv}, \\ \dot{x}_{2pv} &= \frac{1-K}{C}\, x_{1pv} + \frac{1}{R\,L}\, x_{2pv}, \\ y_{pv} &= x_{2pv}, \end{aligned} \tag{5.7}$$

where the dynamics vector of the PV cell is $x = [I_L\ V_c]^T$. The dynamic system of the PV cell is given by

$$\begin{aligned} \dot{x}_{pv} &= A_{pv}\, x_{pv} + B_{pv}\, u_{pv}, \\ y_{pv} &= C_{pv}\, x_{pv} + D_{pv}\, u_{pv}, \end{aligned} \tag{5.8}$$

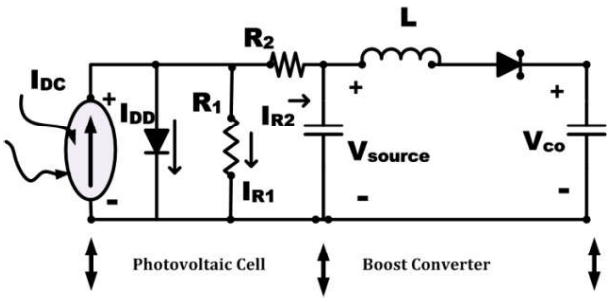

Figure 5.2: PV cell with DC boost converter.

where $A_{pv} = \begin{bmatrix} 0 & \frac{1+K}{L} \\ \frac{1-K}{C} & \frac{1}{RL} \end{bmatrix}, B_{pv} = \begin{bmatrix} \frac{1}{L} \\ 0 \end{bmatrix}, C_{pv} = \begin{bmatrix} 0 \\ 1 \end{bmatrix}$, and $D_{pv} = 0$.

5.3 Dynamic Graphical Games (DGGs)

This section considers the synchronization of MAs on communication networks, where the agents are exchanging information based on communication graph structures [212]. The agents select their optimal control policies to follow the leader's dynamics.

5.3.1 Graph notations

A directed graph $\hat{G}$ prescribes the information flow between the agents in two directions. The connectivity matrix is $E_p = [e_{ij}]$, where e_{ij} represent the weight between any two agents i, j. The connectivity weight e_{ij} has a positive value if there is communication link between the agents and *0* otherwise. $D_p = diag(\sum_{j \in N_i} e_{ij})$ is a diagonal matrix. The Laplacian matrix L_p is calculated so that $L_p = D_p - E_p$ [218].

5.3.2 Problem formulation

The dynamic equation for every agent (node) i in existence of stochastic disturbance is given by:

$$x_{i(k+1)} = A_i x_{i(k)} + B_i u_{i(k)} + B_{di} w_{i(k)}, \tag{5.9}$$

$$y_{i(k)} = C_i x_{i(k)} + v_{i(k)}; \tag{5.10}$$

where $x_{i(k)} \in \Re^n$ denotes the state, $y_{i(k)} \in \Re^p$ denotes the output measurement, and $u_{i(k)} \in \Re^m$ denotes the control signal. $w_{i(k)} \in \Re^q$, denotes disturbance, while $v_{i(k)} \in \Re^p$ denotes observation disturbance, see [175, 176].

The leader dynamics is described by

$$x_{l(k+1)} = A x_{l(k)}, \tag{5.11}$$

where $x_{l(k)} \in \Re^n$ denotes the leader's state.

The local tracking error protocol is described by:

$$\varepsilon_{i(k)} = \sum_{j \in N_i} e_{ij}(x_{j(k)} - x_{i(k)}) + \gamma_i(x_{l(k)} - x_{i(k)}), \tag{5.12}$$

N_i denotes the number of nodes in the neighborhood i and γ_i is the pinning gain.

Thus, the tracking error dynamics for every node i is:

$$\varepsilon_{i(k+1)} = A\varepsilon_{i(k)} - (d_j + \gamma_i)B_i u_{i(k)} + \sum_{j \in N_i} e_{ij} B_j u_{j(k)} + \sum_{j \in N_i} e_{ij} B_{dj} w_{j(k)} - (d_i + \gamma_i) B_{di} w_{i(k)} \tag{5.13}$$

The aim of the optimal control problem is to minimize the local tracking error (5.13). A finite performance index is chosen to reflect the dynamics of the graph. The rendering for individual agent i is evaluated by

$$J_i(\varepsilon_{i(k)}, u_{i(k)}, u_{-i(k)}) = E\left[\frac{1}{2}\sum_{k=0}^{N-1}\left(\varepsilon_{i(k)}^T Q_{ii}\varepsilon_{i(k)} + u_{i(k)}^T R u_{i(k)} + \sum_{j\in N_i} u_{j(k)}^T R_{ij} u_{j(k)}\right)\right], \tag{5.14}$$

where the weighting matrices are $R_{ii} > 0, \quad R_{ij} > 0,\ Q_{ii} \geq 0$.

The individual utility function is:

$$U_i(\varepsilon_{i(k)}, u_{i(k)}, u_{-i(k)}) = \frac{1}{2}\left(\varepsilon_{i(k)}^T Q\varepsilon_{i(k)} + u_{i(k)}^T R_{ij} u_{i(k)} + \sum_{j\in N_i} u_{j(k)}^T R_{ij} u_{j(k)}\right).$$

The objective is to find the optimal performance index $J_i^*, \forall i$. Thus, the optimal control policy is deduced by minimizing the performance index (5.14) such that

$$J_i^*(\varepsilon_{i(k)}, u_{i(k)}, u_{-i(k)}) = min_{u_{i(k)}} E\left[\sum_{k=0}^{N-1} U_i(\varepsilon_{i(k)}, u_{i(k)}, u_{-i(k)}^*)\right], \tag{5.15}$$

$u_{-i(k)}^*$ denote the optimal polices of the neighbors of every agent i.

5.4 Graphical Kalman Filter

In the sequel, a least square estimation strategy using Kalman filter is introduced to reject the disturbances within the graphical games.The expected value of the dynamics

of every agent i is:

$$\hat{x}_{i(k)} = \mathfrak{E}[x_{i(k)}], \tag{5.16}$$

and the state estimation error is expressed by

$$\xi_{i(k)} = x_{i(k)} - \hat{x}_{i(k)}. \tag{5.17}$$

Then, the covariance matrix of the error is expressed as

$$\Psi_{i(k)} = \mathfrak{E}[\xi_{i(k)}\xi_{i(k)}^T] \tag{5.18}$$

The covariance matrices for every node i is

$$\mathfrak{E}[w_{i(k)}^T w_{i(k)}] = \Lambda_{iw1}; \quad \mathfrak{E}[v_{i(k)}^T v_{i(k)}] = \Lambda_{iv},$$

which represents the estimated state for every node i so that

$$\hat{x}_{i(k+1|k)} = A_i\hat{x}_{(k|k)} + B_i u_{i(k)}. \tag{5.19}$$

Using (5.17), the update of the error is given by

$$\begin{aligned} \xi_{i(k+1|k)} &= x_{i(k+1)} - \hat{x}_{i(k+1)} \\ &= A_i\xi_{i(k)} + B_{di}w_{i(k)}. \end{aligned} \tag{5.20}$$

Then the updated covariance of the error is given by

$$\begin{aligned}\Psi_{i(k+1|k)} &= [A_i\xi_{i(k)} + B_{di}w_{i(k)}][A_i\xi_{i(k)} + B_{di}w_{i(k)}]^T, \\ &= A_i\Psi_{i(k)}A_i^T + \Lambda_{iw}. \end{aligned} \tag{5.21}$$

Where $\Lambda_{iw} = B_{di}\Lambda_{iw1}B_{di}^T$.

The Kalman observer is:

$$\hat{x}_{i(k+1|k)} = A_i\hat{x}_{i(k)} + B_iu_{i(k)} + K_{i(k)}(y_{i(k)} - C_i\hat{x}_{i(k)}), \tag{5.22}$$

where $K_{i(k)} \in \Re^{n\times m}$ denotes Kalman gain.

The estimated dynamics for the individual agent i (5.19) is weighted by a matrix Γ_i [175]. Thus (5.22) yields

$$\hat{x}_{i(k+1|k+1)} = \Gamma_{i(k+1)}\hat{x}_{i(k+1|k)} + K_{i(k+1)}C_ix_{i(k+1|k)} + K_{i(k+1)}v_{i(k+1|k)}, \tag{5.23}$$

where the weighted matrix $\Gamma_{i(k+1)}$ is [175]

$$\Gamma_{i(k+1)} = I - K_{i(k+1)}C_i, \tag{5.24}$$

where $\Gamma_{i(k)} \in \Re^{n\times n}$ then,

$$\hat{x}_{i(k+1|k)} = (I - K_{i(k+1)}C_i)\hat{x}_{i(k+1|k)} + K_{i(k+1)}C_i\hat{x}_{i(k+1|k)} - K_{i(k+1)}v_{i(k+1)} \tag{5.25}$$

The update of the covariance is

$$\Psi_{i(k+1|k+1)} = (I - K_{i(k+1)}C_i)\Psi_{i(k+1|k)}(I - K_{i(k+1)}C_i)^T + K_{i(k+1)}\Lambda_{iv}K_{i(k+1)}^T. \tag{5.26}$$

Minimizing the covariance equation (5.26) yields

$$\begin{aligned}\mathcal{L} &= min_{K_{i(k+1)}} trace[\Psi_{i(k+1|k+1)}] \\ &= min_{K_{i(k+1)}} trace[(I - K_{i(k+1)}C_i)\Psi_{i(k+1|k)}(I - K_{i(k+1)}C_i)^T + K_{i(k+1)}\Lambda_{iv}K_{i(k+1)}^T],\end{aligned} \tag{5.27}$$

$$\frac{\partial \mathcal{L}}{\partial K_{i(k+1)}} = -2(I - K_{i(k+1)}C_i)\Psi_{i(k+1|k)}C_i^T + 2K_{i(k+1)}\Lambda_{iv} = 0.$$

The Kalman gain

$$K_{i(k+1)} = \Psi_{i(k+1|k)}C_i^T[C_i\Psi_{i(k+1|k)}C_i^T + \Lambda_{iv}]^{-1}. \tag{5.28}$$

The estimation of the leader dynamics (5.11) can be done in a similar fashion. The estimation of tracking error is given so that

$$\hat{\varepsilon}_{i(k)} = \sum_{j\in N_i} e_{ij}(\hat{x}_{j(k)} - \hat{x}_{i(k)}) + \gamma_i(\hat{x}_{0(k)} - \hat{x}_{i(k)}). \tag{5.29}$$

The update of the error dynamics estimation is given by

$$\hat{\varepsilon}_{i(k+1)} = A\hat{\varepsilon}_{i(k)} - (d_j + \gamma_i)B_i u_{i(k)} + \sum_{j\in N_i} e_{ij}B_j u_{j(k)} + \sum_{j\in N_i} e_{ij}B_{dj}\hat{w}_{j(k)} - (\gamma_i + d_i)B_{di}\hat{w}_{i(k)}, \quad . \tag{5.30}$$

5.4.1 Bellman equations for the DGGs

The objective cost to go function for every agent i is

$$V_i(\hat{\varepsilon}_{i(k)}) = \sum_{k=0}^{\infty} U_i(\hat{\varepsilon}_{i(k)}, \pi_{i(k)}, \pi_{-i(k)}), \tag{5.31}$$

where $\pi_{i(k)}$ and $\pi_{-i(k)}$ are the admissible procedures for every agent and its neighbors. Coupled Bellman equations for DGGs are developed in [212]. Bellman equation for every agent i is:

$$V_i^{\pi}(\hat{\varepsilon}_{i(k)}) = \frac{1}{2}\left(\hat{\varepsilon}_{i(k)}^T Q_{ii}\hat{\varepsilon}_{i(k)} + \pi_{i(k)}^T R_{ii}\pi_{i(k)} + \sum_{j\in N_i} \pi_{i(k)}^T R_{ij}\pi_{i(k)}\right) + V_i^{\pi}(\hat{\varepsilon}_{i(k+1)}), \tag{5.32}$$

where $V_i^{\pi}(0) = 0$.

The optimal policies are obtained by applying Bellman optimality principles so that

$$V_i^o(\hat{\varepsilon}_{i(k)}) = \min_{u_i} V_i(\hat{\varepsilon}_{i(k)}) = \min_{u_i}\left(\sum_{l=k}^{\infty} U_i(\hat{\varepsilon}_{il}, , u_{il}, \pi_{-il})\right). \tag{5.33}$$

Thus, the optimal control policy is

$$u_{i(k)}^o = M_i \nabla V_i(\hat{\varepsilon}_{i(k+1)}), \tag{5.34}$$

where $M_i = R_{ii}^{-1}([..\ (\gamma_i + d_i)..-\ \ e_{ji}..\ ] \otimes B_i^T) \nabla V_i^o(\bar{\hat{\varepsilon}}_{i(k+1)})$ and $\nabla V_i(\hat{\varepsilon}_{i(k)}) = \dfrac{\partial V_i(\hat{\varepsilon}_{i(k)})}{\partial \hat{\varepsilon}_{i(k)}}$.

The coupled Bellman optimality equation for every agent i is

$$V_i^o(\hat{\varepsilon}_{i(k)}) \ = \ \frac{1}{2}\left(\hat{\varepsilon}_{i(k)}^T Q_{ii}\hat{\varepsilon}_{i(k)} + u_{i(k)}^{oT} R_{ii} u_{i(k)}^o + \sum_{j\in N_i} u_{j(k)}^{oT} R_{ij} u_{j(k)}^o\right) + V_i^o(\hat{\varepsilon}_{i(k+1)}) \tag{5.35}$$

5.4.2 Nash equilibrium solution for DGGs

Nash equilibrium (NE) conditions for the graphical games are introduced in [212].

Definition 5.1 *The N-learners DGG with N-tuple of optimal regulation policies* $\{u_1^*, u_2^*, .. ., u_N^*\}$ *is considered to possess a NE if* $\forall i \in N$

$$J_i^o \ \triangleq \ J_i(u_i^o, u_{\bar{i}}^o) \leq J_i(u_i, u_{\bar{i}}^o). \tag{5.36}$$

5.5 Online Adaptive Reinforcement Learning

An online policy iteration is proposed to find solution for the dynamic graphical game with disturbances online in real-time. This scheme doesn't need the information about the whole dynamics of the agents. This algorithm finds the solution of the coupled Bellman optimality equations (5.35). The algorithm is outlined as follows

Algorithm 1 *PI Algorithm*

Step 1: Initialize admissible policies $u_{i(k)}^0$, $\forall i$, *and the values* $\tilde{V}_i^0(\hat{\varepsilon}_{i(k)}), \forall i$.

Step 2: Kalman filter estimation $(\hat{\varepsilon}_{i(k)}, u_{i(k)}, \Psi_{i(k)})$.

Step 2.1: Dynamics estimation $\hat{x}_{i(k+1|k)} = A_i \hat{x}_(k|k) + B_i u_{i(k)}$.

Calculate the error $e_{i(k+1|k)} = A_i \xi_{i(k)} + B_{di} w_{i(k)}$.

Calculate the covariance $\Psi_{i(k+1|k)} = A_i \Psi_{i(k)} A_i + \Lambda_{iw}$.

Step 2.2: Correct the Kalman filter gain $K_{i(k+1)} = \Psi_{i(k+1|k)} C_i^T [C_i \Psi_{i(k+1|k)} C_i^T + S_v]^{-1}$

Perform Kalman filter observer calculations as follows

$\hat{x}_{i(k+1)} = A_i \hat{x}_{i(k)} + B_i u_{i(k)} + K_{i(k)}(y_{i(k)} - C_i \hat{x}_{i(k)})$

$\Psi_{i(k+1|k+1)} = (I - K_{i(k+1)} C_i) \Psi_{i(k+1|k)} (I - K_{i(k+1)} C_i)^T + K_{i(k+1)} S_v K_{i(k+1)}^T$

Step 3: (Value iteration). Solve for $\tilde{V}_i^l(.), \forall i$

$$\tilde{V}_i^l(\hat{\varepsilon}_{i(k)}) = U_i(\hat{\varepsilon}_{i(k)}, u_{i(k)}^l, u_{-i(k)}^l) + \tilde{V}_i^l(\hat{\varepsilon}_{i(k+1)}^{u_{i(k)}^l, u_{-i(k)}^l}), \tag{5.37}$$

l denotes iteration index. Step 4: (Policy iteration)

$$u_{i(k)}^{l+1} = R_{ii}^{-1}([..(\gamma_i + d_i).. - e_{ji}..] \otimes B_i^T) \nabla \tilde{V}_i^0(\hat{\varepsilon}_{i(k+1)})^l, \forall i \tag{5.38}$$

Step 5: On convergence of $\left\| \tilde{V}_i^{l+1} - \tilde{V}_i^l \right\|, \forall i$*, End.*

Policy iteration *Algorithm (1)* doesn't need the complete information of the system dynamics (only control matrices $B_i, \forall i$ are needed). The subsequent theorem introduces the PI convergence proof for *Algorithm 1*, while the entire nodes update their own policies concurrently.

Theorem 5.1 *Assume that all the initial values of the control policies* $u_{i(k)}^0, \forall i$ *are admissible, and the maximum singular value of* $(R_{jj}^{-1} R_{ij})$ *is selected based on the graph. Then*

1. $u_{i(k)}^o, \forall i$ *are stabilizing control policies.*

2. *PI Algorithm 1 produces monotonically decreasing value functions* $\tilde{V}_i^l, \forall i$ *so that* $0 \leq \tilde{V}_{i(k)}^{l+1} \leq \tilde{V}_{i(k)}^l, \forall i$ *and they converge to the outstanding response solutions* $\tilde{V}_{i(k)}^*, \forall i$ *which meet (5.35).*

Proof.

1. The Bellman equation (5.35) yields,

$$\tilde{V}_i^l(\hat{\varepsilon}_{i(k+1)}^{u_{i(k)}^l, u_{i(k)}^l}) - \tilde{V}_i^l(\hat{\varepsilon}_{i(k)}^{u_{i(k)}^l, u_{i(k)}^l}) < 0, \ \forall i, l. \tag{5.39}$$

$\tilde{V}_i^l, \ \forall i, l$ are Lyapunov functions.

Let the controls $u_i^0, \ \forall i, l$ be admissible, then the value functions $\tilde{V}_i^l, \ \forall i, l$ satisfy

$$\tilde{V}_i^l(\hat{\varepsilon}_{i(k)}^{u_{i(k)}^l, u_{-i(k)}^l}) = \sum_{m=k}^{\infty} U_i(\hat{\varepsilon}_{i(m)}, u_{i(m)}^l, u_{-i(m)}^l) = \tilde{V}_i^l(\hat{\varepsilon}_{i(k)}^{u_{i(k)}^{l+1}, u_{-i(k)}^l}) + \Delta\tilde{U}_k(u_{i(m)}^l, u_{i(m)}^{l+1}) \tag{5.40}$$

where

$$\Delta\tilde{U}_k(u_{i(m)}^l, u_{i(m)}^{l+1}) = \sum_{m=k}^{\infty} (\frac{1}{2}(u_{i(m)}^l - u_{i(m)}^{l+1})^T R_{ii}(u_{i(m)}^l - u_{i(m)}^{l+1}) + {u^{l+1}}_{i(m)}^T R_{ii}(u_{i(m)}^l - u_{i(m)}^{l+1})) \tag{5.41}$$

The policies $u_{i(k)}^{l+1}, \ \forall i, l$ are given by (5.38). Therefore, $\Delta\tilde{U}_k(u_{i(m)}^l, u_{i(m)}^{l+1})$ and

(5.40) yield

$$\tilde{V}_i^l(\hat{\varepsilon}_{i(k)}^{u_{i(k)}^l, u_{-i(k)}^l}) > \tilde{V}_i^l(\hat{\varepsilon}_{i(k)}^{u_{i(k)}^{l+1}, u_{-i(k)}^l}). \tag{5.42}$$

Similarly,

$$\tilde{V}_i^l(\hat{\varepsilon}_{i(k)}^{u_{i(k)}^{l+1}, u_{-i(k)}^l}) = \sum_{m=k}^{\infty} U_i(\hat{\varepsilon}_{im}, u_{i(m)}^{l+1}, u_{-i(m)}^l) = \tilde{V}_i^l(\hat{\varepsilon}_{ik}^{u_{i(k)}^{l+1}, u_{-i(k)}^{l+1}}) + \Delta\tilde{U}_k(u_{-i(m)}^l, u_{-i(m)}^{l+1}) \tag{5.43}$$

The condition $\Delta\tilde{U}_k(u_{-i}^l, u_{-i}^{l+1}) > 0$ ensures

$$\tilde{V}_i^l(\hat{\varepsilon}_{i(k)}^{u_{i(k)}^{l+1}, u_{-i(k)}^l}) > \tilde{V}_i^l(\hat{\varepsilon}_{i(k)}^{u_{i(k)}^{l+1}, u_{-i(k)}^{l+1}}). \tag{5.44}$$

Thus $\Delta\tilde{U}_k(u_{-i}^l, u_{-i}^{l+1}) > 0$ is a sufficient condition to stabilize the dynamics given that

$$\sum_{j\in N}(\frac{1}{2}(u_{j(k)}^l - u_{j(k)}^{l+1})^T R_{ij}(u_{j(k)}^l - u_{j(k)}^{l+1}) - {u_{j(k)}^{l+1}}^T R_{ij}(u_{j(k)}^l - u_{j(k)}^{l+1})) > 0 \tag{5.45}$$

Applying the norm properties, (5.45) yields

$$\sum_{j\in N_i}(\frac{1}{2}\underline{\Psi}(R_{ij})\left\|\Delta u_{j(k)}^l\right\| > \sum_{j\in N_i}(\gamma_j + d_j)\bar{\Psi}(R_{jj}^{-1}R_{ij})((\gamma_j + d_j)\left\|\nabla_j \tilde{V}_j^l(\hat{\varepsilon}_{j(k+1)}^{u_{j(k)}^l, u_{-j(k)}^l})\right\| + \sum_{o\in N_j}(e_{jo}\left\|\nabla_o V_j^l(\hat{\varepsilon}_{j(k+1)}^{u_{j(k)}^l, u_{-j(k)}^l})\right\|))\left\|B_{j(k)}\right\|, \tag{5.46}$$

where $\underline{\Psi}(.)$ and $\bar{\Psi}(.)$ are respectively the maximum/minimum singular values. $\Delta u^l_{j(k)} = (u^l_{j(k)} - u^{l+1}_{j(k)})$.

Under this assumption, inequalities (5.42) and (5.44) yield

$$\tilde{V}_i^l(\hat{\varepsilon}_{i(k)}^{u^l_{i(k)},u^l_{-i(k)}}) > \tilde{V}_i^l(\hat{\varepsilon}_{i(k)}^{u^{l+1}_{i(k)},u^l_{-i(k)}}) > \tilde{V}_i^l(\hat{\varepsilon}_{i(k)}^{u^{l+1}_{i(k)},u^{l+1}_{-i(k)}}). \tag{5.47}$$

The careful choice of the weighting matrices guarantees this result in terms of the following condition 5.48. Therefore $u^{l+1}_{i(k)}, \forall i, l$ are stabilizing policies and hence admissible. The inequalities (5.39) and (5.47) yield

$$\tilde{V}_i^l(\hat{\varepsilon}_{i(k+1)}^{u^{l+1}_{i(k)},u^{l+1}_{-i(k)}}) - \tilde{V}_i^l(\hat{\varepsilon}_{i(k)}^{u^{l+1}_{i(k)},u^{l+1}_{-i(k)}}) < 0. \tag{5.48}$$

2. Using (5.37) yields

$$\tilde{V}_i^{l+1}(\hat{\varepsilon}_{i(k+1)}^{u^{l+1}_{i(k)},u^{l+1}_{-i(k)}}) - \tilde{V}_i^{l+1}(\hat{\varepsilon}_{i(k)}^{u^{l+1}_{i(k)},u^{l+1}_{-i(k)}}) + \Delta\tilde{U}_k(\hat{\varepsilon}_{i(k)}, u^{l+1}_{i(k)}, u^{l+1}_{-i(k)}) = 0 \tag{5.49}$$

Inequalities (5.37), (5.48), and equation (5.49) yield

$$\tilde{V}_i^l(\hat{\varepsilon}_{i(k+1)}^{u^{l+1}_{i(k)},u^{l+1}_{-i(k)}}) - \tilde{V}_i^l(\hat{\varepsilon}_{i(k)}^{u^{l+1}_{i(k)},u^{l+1}_{-i(k)}}) \leq \tilde{V}_i^{l+1}(\hat{\varepsilon}_{i(k+1)}^{u^{l+1}_{i(k)},u^{l+1}_{-i(k)}}) - \tilde{V}_i^{l+1}(\hat{\varepsilon}_{i(k)}^{u^{l+1}_{i(k)},u^{l+1}_{-i(k)}}) \tag{5.50}$$

The infinite summation of (5.50) yields

$$\sum_{k=\tilde{K}}^{\infty}(\tilde{V}_i^l(\hat{\varepsilon}_{i(k+1)}^{u^{l+1}_{i(k)},u^{l+1}_{-i(k)}}) - \tilde{V}_i^l(\hat{\varepsilon}_{i(k)}^{u^{l+1}_{i(k)},u^{l+1}_{-i(k)}})) < \sum_{k=\tilde{K}}^{\infty}(\tilde{V}_i^{l+1}(\hat{\varepsilon}_{i(k+1)}^{u^{l+1}_{i(k)},u^{l+1}_{-i(k)}}) - \tilde{V}_i^{l+1}(\hat{\varepsilon}_{i(k)}^{u^{l+1}_{i(k)},u^{l+1}_{-i(k)}})).$$

Then the inequality yields

$$\tilde{V}_i^l(\hat{\varepsilon}_{i\infty}^{u_{i\infty}^{l+1},u_{-i\infty}^{l+1}}) - \tilde{V}_i^l(\hat{\varepsilon}_{i(\tilde{K})}^{u_{i(\tilde{K})}^{l+1},u_{-i(\tilde{K})}^{l+1}}) < \tilde{V}_i^{l+1}(\hat{\varepsilon}_{i\infty}^{u_{i\infty}^{l+1},u_{-i\infty}^{l+1}}) - \tilde{V}_i^{l+1}(\hat{\varepsilon}_{i(\tilde{K})}^{u_{i(\tilde{K})}^{l+1},u_{-i(\tilde{K})}^{l+1}}) \tag{5.51}$$

The results in part (1) imply that $\tilde{V}_i^l(\bar{\varepsilon}_{i\infty}^{u_{i\infty}^{l+1},u_{-i\infty}^{l+1}}) \mapsto 0$ and $\tilde{V}_i^{l+1}(\bar{\varepsilon}_{i\infty}^{u_{i\infty}^{l+1},u_{-i\infty}^{l+1}}) \mapsto 0$ such that

$$\tilde{V}_i^{l+1}(\bar{\varepsilon}_{i(\tilde{K})}^{u_{i(\tilde{K})}^{l+1},u_{-i(\tilde{K})}^{l+1}}) < \tilde{V}_i^l(\bar{\varepsilon}_{i(\tilde{K})}^{u_{i(\tilde{K})}^{l+1},u_{-i(\tilde{K})}^{l+1}}). \tag{5.52}$$

Therefore,

$$0 < .. < \tilde{V}_i^{l+1} < \tilde{V}_i^l < ..\tilde{V}_i^0, \forall i, l. \tag{5.53}$$

The stabilizing control policies (5.38) form a Nash equilibrium tuple. Equation (5.53) is upper bounded by $\left\{0, \tilde{V}_i^0(\hat{\varepsilon}_{i0}^{u_{i0}^0,u_{-i0}^0})\right\}$. Thus the value function $\tilde{V}_i^l$ converges to the best response value $\tilde{V}_i^*$ so that

$$0 < .. < \tilde{V}_i^* < \tilde{V}_i^{l+1} < \tilde{V}_i^l < ..\tilde{V}_i^0, \forall i, l. \tag{5.54}$$

∎

5.6 Critic Neural Network Implementation for The Adaptive Learning Algorithm

An online critic NN technique is proposed to implement the solution of the adaptive learning *Algorithm 1* in real-time. An estimation of the objective function $V_i(\hat{\varepsilon}_{i(k)})$ in the form of the critic network structure $\hat{V}_i(.|\tilde{W}_{ic})$, is

$$\hat{V}_i(.|\tilde{W}_{ic}) \quad = \quad \frac{1}{2} L_{i(k)}^T \tilde{W}_{ic}^T L_{i(k)}, \tag{5.55}$$

where $\tilde{W}_{ic} \quad \in \Re^{nN_{i,j} \times nN_{i,j}}, \forall i$, are the weights of the estimated objective function $\hat{V}_i(.|\tilde{W}_{ic})$, $L_{i(k)} = [\hat{\varepsilon}_{i(k)}^T \; ..\hat{\varepsilon}_{-i(k)}^T]^T$, where $\hat{\varepsilon}_{i(k)}$ represents the dynamics of each agent i and $\hat{\varepsilon}_{-i(k)}$ represents the dynamics of their neighbours. The control policy for every node i depended on the approximated value structure $\hat{V}_i(.|\tilde{W}_{ic})$. Thus the improved policy $\hat{u}_{i(k)}$ given by (5.38) can be formed such that

$$\hat{u}_{i(k)} \quad = \quad R_u^{-1}([.. \; (\gamma_i + d_i).. - \quad e_{ji}.. \;] \otimes B_i^T) \tilde{W}_{ic}^T L_{i(k)}, \forall i. \tag{5.56}$$

The value function (5.55) is represented in an alternate form so that

$$\hat{V}_i(.|\bar{W}_{ic}) \quad = \quad \bar{W}_{ic}^T \bar{L}_{i(k)}, \tag{5.57}$$

where $\bar{L}_{ic} \; \in \Re^{nN_{i,j} \times nN_{i,j}+1/2 \times 1}$, indicates a quadratic polynomial vector, $\bar{W}_{ic} = \nu(\bar{W}_{ic})$, $\nu(.)$ a valued matrix performs on the symmetric matrices and reverts a column vector utilizing the stacking strategy to generate a $\bar{W}_{ic}$ in terms of off-diagonal components, which is the qr-th component of $\tilde{W}_{ic}$.

Bellman equation (5.37) can be written with the value function (5.57) so that

$$\bar{W}_{ic}^{T}(\bar{L}_{i(k)} - \bar{L}_{i(k+1)}) = \frac{1}{2}\left(\hat{\varepsilon}_{i(k)}^{T} Q_{ii} \hat{\varepsilon}_{i(k)} + \hat{u}_{i(k)}^{T} R_{ii} \hat{u}_{i(k)} + \sum_{j \in N_i} \hat{u}_{j(k)}^{T} R_{ij} \hat{u}_{j(k)}\right) \quad (5.58)$$

The critic neural network vectors $\bar{W}_{ic}^{T}, \forall i$, are computed in real-time.

The value $\Im_{\hat{\varepsilon}_{i(k)}}^{\hat{V}_i(\hat{\varepsilon}_{i(k)})}$ is assumed to be the desired value of the critic structure $\tilde{V}_{i(k)}(\hat{\varepsilon}_{i(k)}) = \hat{V}_{i(k)}(.|\tilde{W}_{ic}) - \hat{V}_{i(k+1)}(.|\tilde{W}_{ic})$ for every node i, such that

$$\Im_{\hat{\varepsilon}_{i(k)}}^{\hat{V}_i(\hat{\varepsilon}_{i(k)})} = \frac{1}{2}\left(\hat{\varepsilon}_{i(k)}^{T} Q_{ii} \hat{\varepsilon}_{i(k)} + \hat{u}_{i(k)}^{T} R_{ii} \hat{u}_{i(k)} + \sum_{j \in N_i} \hat{u}_{i(k)}^{T} R_{ij} \hat{u}_{i(k)}\right). \quad (5.59)$$

The error of the critic approximated structure is given by

$$\zeta_{\hat{\varepsilon}_{i(k)}}^{\hat{V}_i(\hat{\varepsilon}_{i(k)})} = \Im_{\hat{\varepsilon}_{i(k)}}^{\hat{V}_i(\hat{\varepsilon}_{i(k)})} - \hat{V}_i(\hat{\varepsilon}_{i(k)}). \quad (5.60)$$

The approximation error is given by

$$err_i = \frac{1}{2}(\zeta_{\hat{\varepsilon}_{i(k)}}^{\hat{V}_i(\hat{\varepsilon}_{i(k)})})^{T} \zeta_{\hat{\varepsilon}_{i(k)}}^{\hat{V}_i(\hat{\varepsilon}_{i(k)})} = \frac{1}{2}\left\| \Im\Im_{\hat{\varepsilon}_{i(k)}}^{\hat{V}_i(\hat{\varepsilon}_{i(k)})} - \bar{W}_{ic}^{T} \Im(\bar{L}_{i(k+1)}) \right\|_2^2, \quad (5.61)$$

where $\Im\Im_{\hat{\varepsilon}_{i(k)}}^{\hat{V}_i(\hat{\varepsilon}_{i(k)})} \in \Re^{1 \times (nN_{i,j})(nN_{i,j})/2}$ is a row vector of the desired contents (5.59) for $1 \times (nN_{i,j})(nN_{i,j})/2$ samples, and $\Im(\bar{L}_{i(k+1)})$ is a square matrix of $(nN_{i,j})(nN_{i,j})/2$ samples of $(\bar{L}_{i(k)} - \bar{L}_{i(k+1)})$.

The gradient of the critic network weights is:

$$-\Delta \bar{W}_{ic}^{IT} = \left[\frac{\partial err_i}{\partial \zeta_{\hat{\varepsilon}_{i(k)}}^{\hat{V}_i(\hat{\varepsilon}_{i(k)})}}\right]\left[\frac{\partial \zeta_{\hat{\varepsilon}_{i(k)}}^{\hat{V}_i(\hat{\varepsilon}_{i(k)})}}{\partial \bar{W}_{ic}^{T}}\right]|_{\bar{W}_{ic}^{T} = \bar{W}_{ic}^{IT}} = (\Im\Im_{\hat{\varepsilon}_{i(k)}}^{\hat{V}_i(\hat{\varepsilon}_{i(k)})} - \bar{W}_{ic}^{lT} \Im(\bar{L}_{k,(k+1)})) \times \Im(\bar{L}_{k,(k+1)}) \quad (5.62)$$

Thus the improved critic weights is:

$$\bar{W}_{ic}^{(l+1)T} = \bar{W}_{ic}^{lT} - \tilde{\mu}_{ic}(\Im\Im_{\hat{\varepsilon}_{i(k)}}^{\hat{V}_i(\hat{\varepsilon}_{i(k)})} - \bar{W}_{ic}^{lT}\Im(\bar{L}_{k,(k+1)})) \times \Im(\bar{L}_{k,(k+1)})^T, \quad (5.63)$$

$0 < \tilde{\mu}_{ic} < 1$, denotes critic NN training rate, which is selected to be 0.1.

5.6.1 Online learning of CNWs in realtime

The critic neural network weights (CNWs) are updated based on the following Algorithm.

Algorithm 2 CNWs Online Tuning

Step 1: Set the critic weights $\bar{W}_{ic}^0, \forall i$.

Step 2: Do Loop (l iterations).

Step 2.1: Kickoff with $\hat{\varepsilon}_{i(k)}, \forall i$.

Step 3: Do Loop (s iterations)

Step 3.1: Update the CNWs so that $\bar{W}_{ic}^s = \bar{W}_{ic}^l, \forall i$.

Step 3.2: Compute $\hat{u}_i^s, \forall i$ *utilizing (5.56).*

Step 3.3: Estimate $\hat{\varepsilon}_{i(k+1)}^s, \forall i$.

Step 3.4: Assess $\tilde{V}_i(\bar{\varepsilon}_{i(k)}), \forall i$ *utilizing (5.57).*

End Loop once $s = (nN_{i,j})(nN_{i,j} + 1)/2$.

Step 2.2: Update CNWs. $\bar{W}_{ic}^{(l+1)T} = \bar{W}_{ic}^{lT} - \tilde{\mu}_{ic}(\Im\Im_{\hat{\varepsilon}_{i(k)}}^{\hat{V}_i(\hat{\varepsilon}_{i(k)})} - \bar{W}_{ic}^{IT}\Im(\bar{L}_{k,(k+1)})) \times \Im(\bar{L}_{k,(k+1)})^T, \forall i$.

Step 2.3: On convergence of $\left\| \tilde{V}_i^{l+1} - \tilde{V}_i^l \right\| \leq 10^{-7}, \forall i$ *End Loop.*

5.7 Simulation example

Example 1

The simulation is performed to check the validity of the proposed control scheme. A set of PV cells distributed on a communication graph is considered. Consider four PV cells distributed on a directed graph as shown in Fig. 5.3.

The leader is pinned to only one PV cell. The isolated dynamical models of the PV cells are given by:

$$A_i = \begin{bmatrix} 0 & \frac{1+K}{L} \\ \frac{1-K}{C} & \frac{1}{RL} \end{bmatrix}, \quad B_1 = \begin{bmatrix} 1 \\ 1 \end{bmatrix},$$

$$B_2 = \begin{bmatrix} 0.695 \\ 0.680 \end{bmatrix}, \; B_3 = \begin{bmatrix} -0.25 \\ 0.32 \end{bmatrix}, \; B_4 = \begin{bmatrix} 0.7 \\ -0.1 \end{bmatrix}.$$

The weighting matrices are chosen such that

$$R = 1.00e-03 \text{ and } Q = \begin{bmatrix} 0.01 & 0 \\ 0 & 0.01 \end{bmatrix}.$$

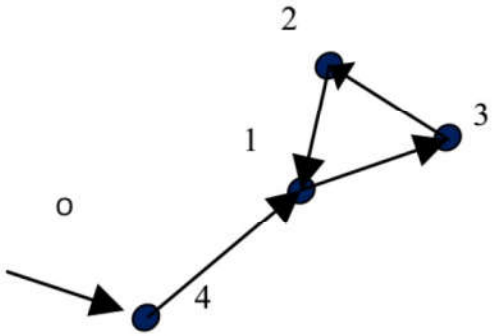

Figure 5.3: The directed graph structure.

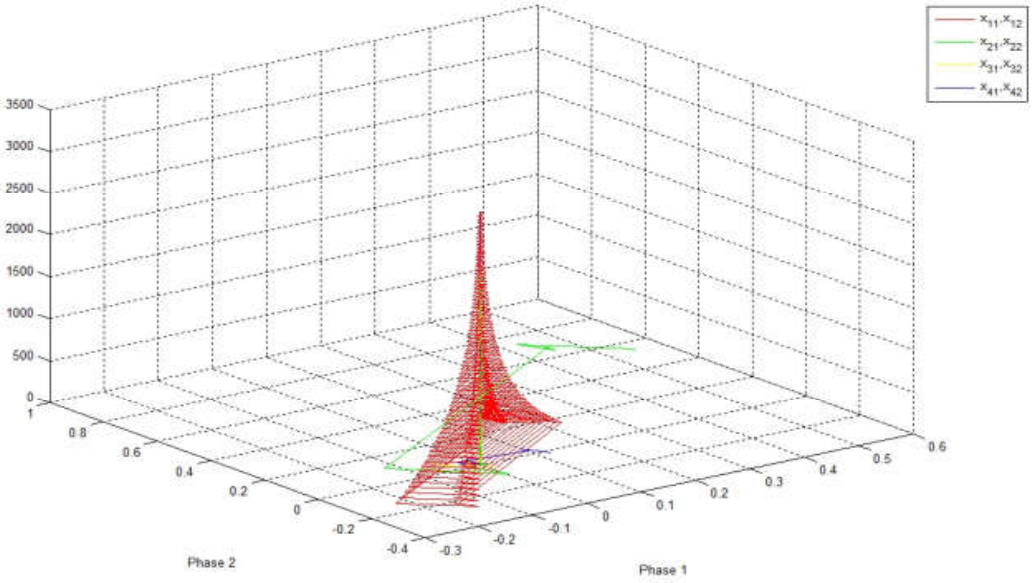

Figure 5.4: Phase plot using Kalman filtering.

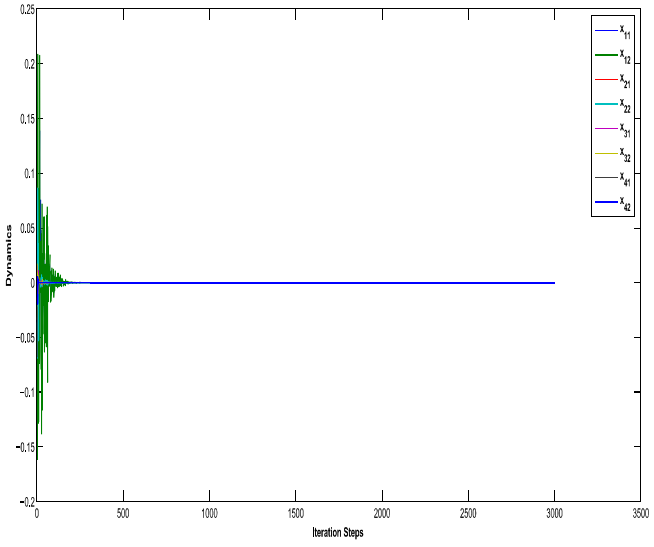

Figure 5.5: The dynamics without Kalman filtering.

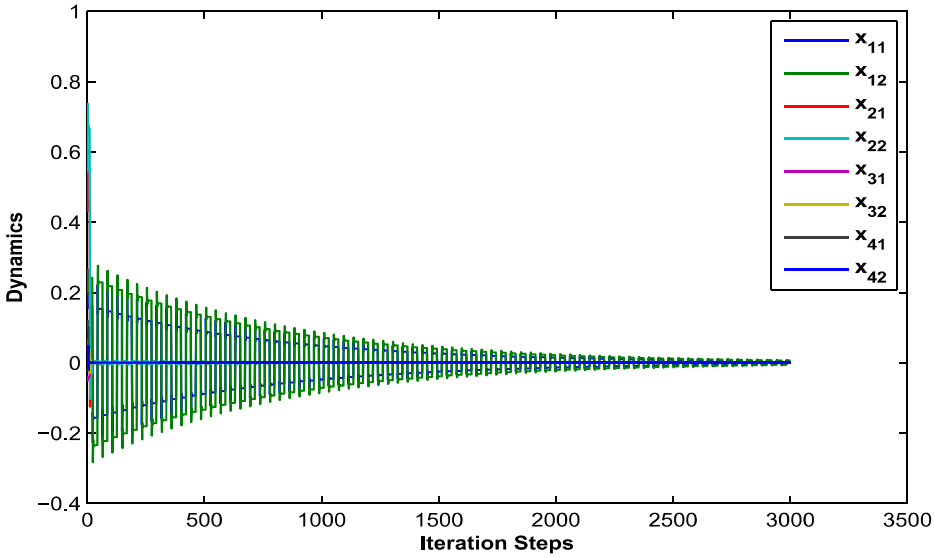

Figure 5.6: The dynamics using Kalman filtering.

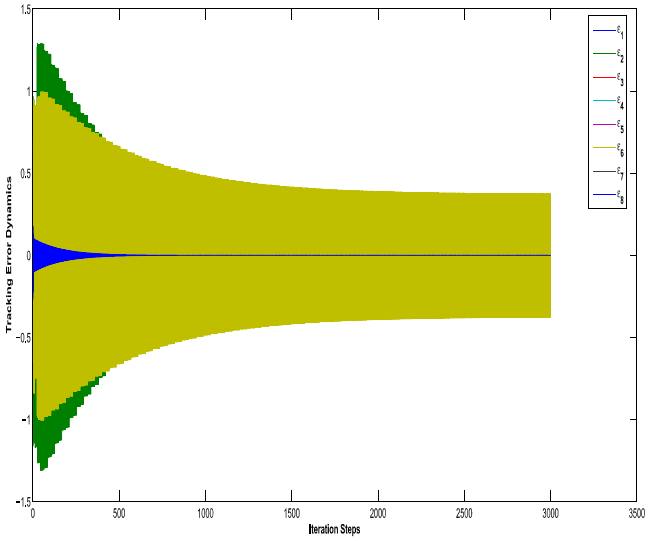

Figure 5.7: Tracking error dynamics without Kalman filtering.

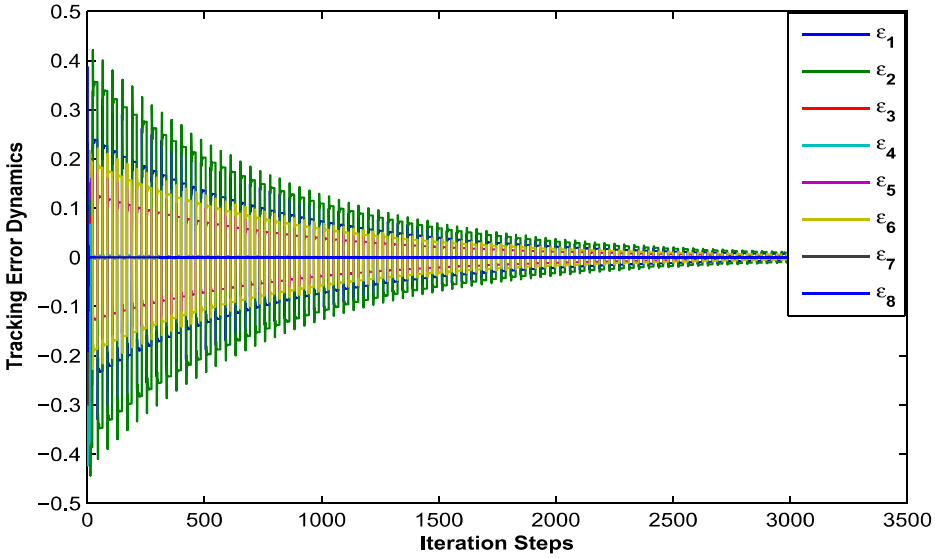

Figure 5.8: Tracking error dynamics using Kalman filtering.

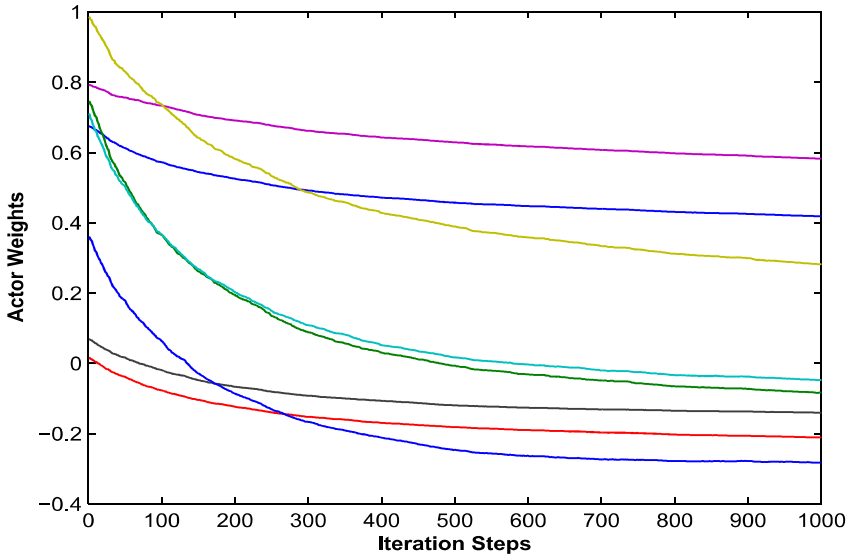

Figure 5.9: Agent 1: Critic weights update in the presence of load variations.

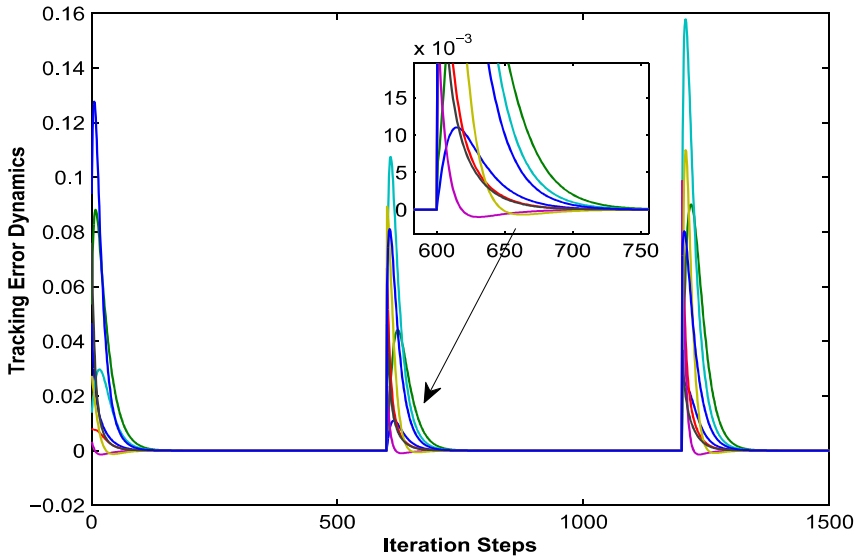

Figure 5.10: Tracking error dynamics using Kalman filtering in the presence of load variations.

Fig.5.11 shows the phase plane plot of the PV cells using Kalman filtering. It shows the importance of Kalman filtering in rejecting the disturbances effect that are imposed on the dynamics of the PV cells. Figs. 5.12 and 5.6 show the dynamics of the PV cells before and after using Kalman filtering. Finally, Figs. 5.7 and 5.8 show the tracking error dynamics with and without Kalman filtering respectively.

Another simulation case is considered to show the robustness of the proposed control scheme. The PV cells are susceptible to multiple Load disturbances. Fig. 5.18 shows the critic weights update of agent (*i=1*). Fig. 5.10, shows that the adaptive based Kalman filtering learning scheme regulate the tracking error dynamics.

Example 2

In this example, we have tested our proposed adaptive controller utilizing four distributed wind turbines systems, for more information see [184].

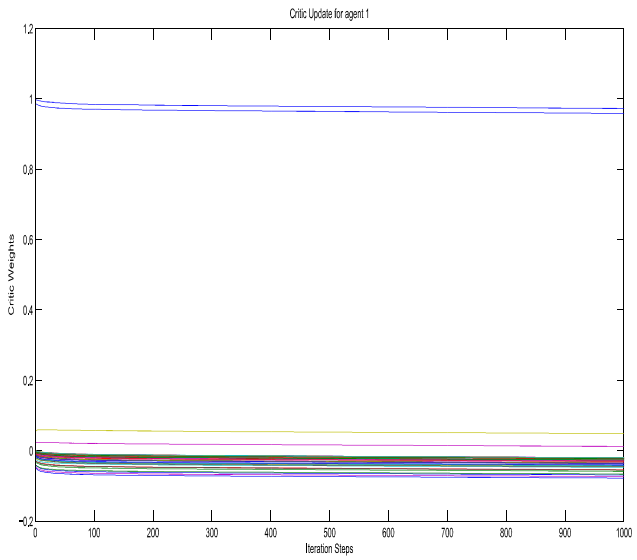

Figure 5.11: Critic weights trajectories.

$$A_i = \begin{bmatrix} 5 & 0 & 0 & 1 & 0 \\ 0 & 0 & 0 & 0 & 1 \\ 419.8 & 0 & -0.55026 & 0 & 0 \\ -507.1 & 0.9707075 & 0.48494 & -0.06538 & 0.00479 \\ 730.26 & -197.76 & -11.681 & -11.681 & -7.3153 \end{bmatrix}, \; B_1 = \begin{bmatrix} 0 \\ 0 \\ 1.3971 \\ -932.5646 \end{bmatrix},$$

$$B_2 = \begin{bmatrix} 0 \\ 0.7 \\ 1 \\ 0.8 \\ 0.3 \end{bmatrix}, \; B_3 = \begin{bmatrix} 0.2 \\ 0.9 \\ 0.4 \\ 0 \\ 1 \end{bmatrix}, \; B_4 = \begin{bmatrix} 0.7 \\ 0.1 \\ 0.4 \\ 0 \\ -1 \end{bmatrix}.$$

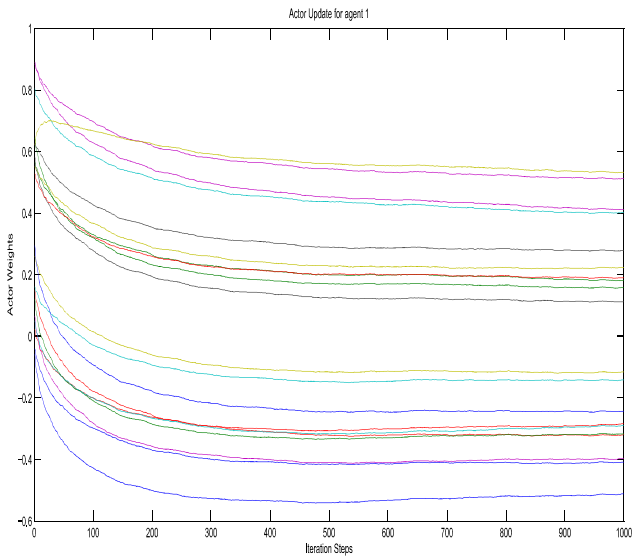

Figure 5.12: Actor weights trajectories.

Figs. 5.11, 5.12 demonstrate critic weights and actor weights trajectories respectively. It shows the importance of Kalman filtering for rejecting the disturbance effects that are imposed on the dynamics of the wind turbines. Figs. 5.13 – 5.16 show the dynamics of the wind turbines states and tracking errors without load variations. Fig.5.17 shows the phase plane plot of the wind turbines using Kalman filtering.

5.8 Conclusion

In this chapter, a novel online adaptive learning control scheme is developed for multi-agent power systems or islanded network of microgrids. This structure is based on a game theoretic approach. The microgrid units are exchanging information based on a communication network. This technique solves the coupled Bellman equations of the graphical game in the presence of disturbances. This is done by using local neighborhood information and partial knowledge about the units dynamics. Networks of photovoltaic

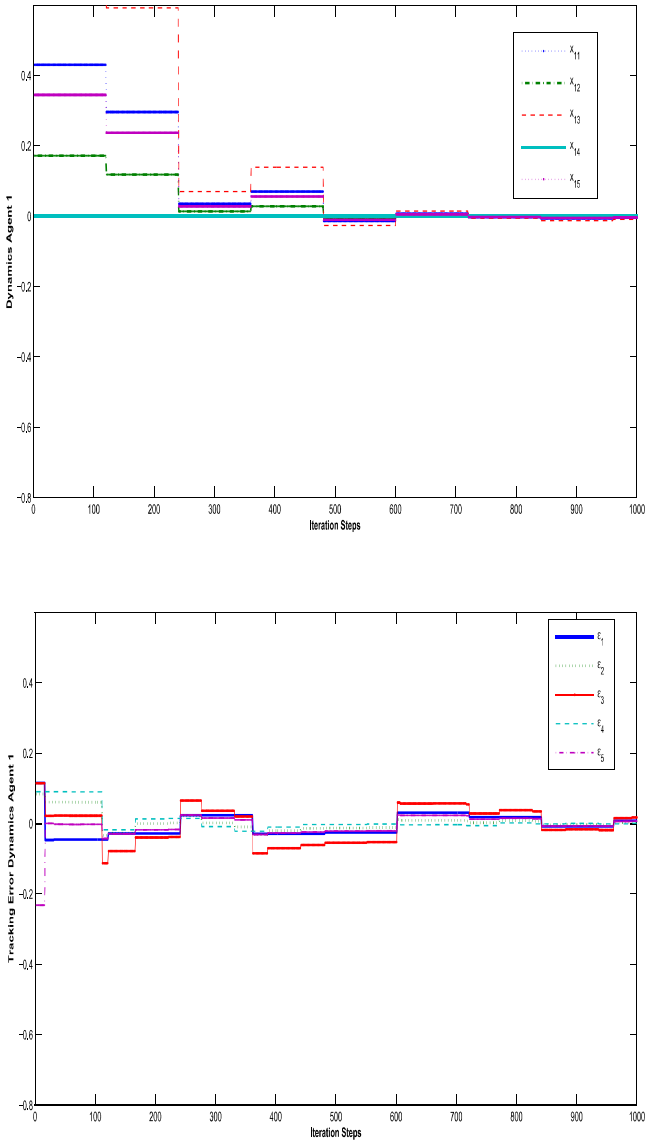

Figure 5.13: The states trajectories and error dynamics of agent-1.

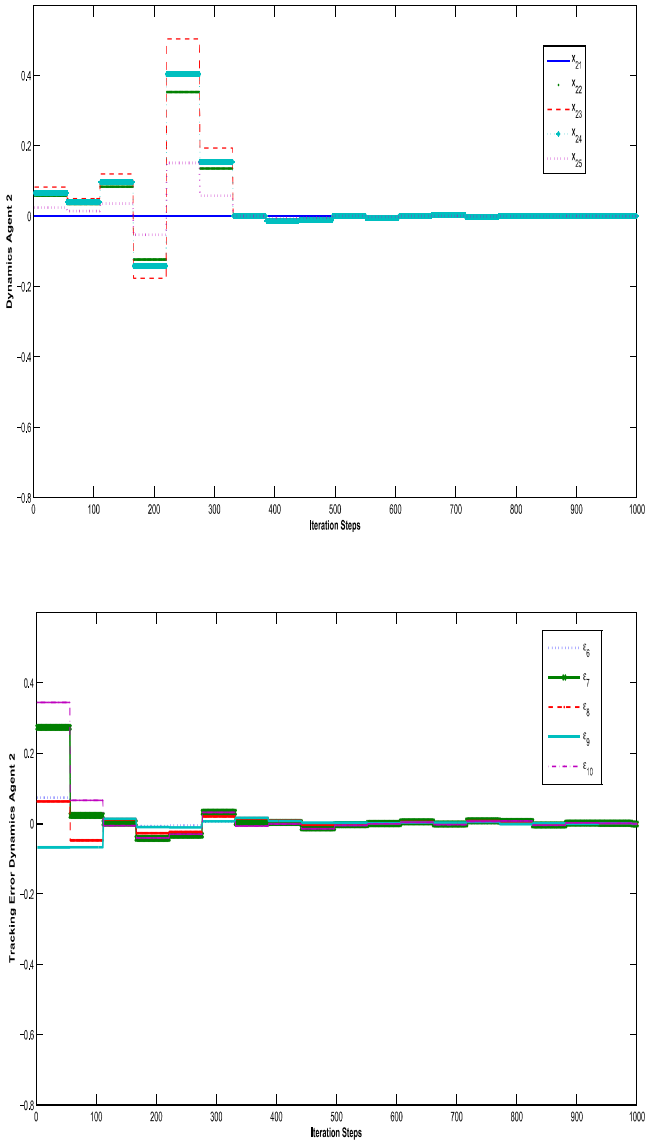

Figure 5.14: The states trajectories and error dynamics of agent-2.

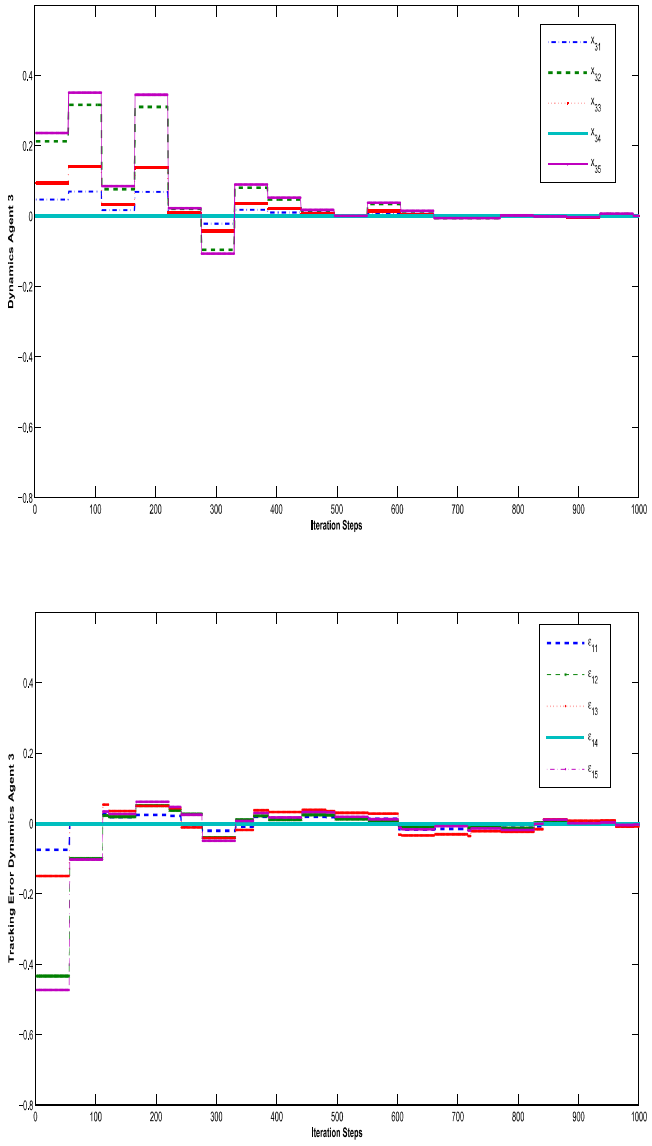

Figure 5.15: The states trajectories and error dynamics of agent-3.

cells and wind turbine are considered. The dynamics of the open loop systems are estimated using Kalman filtering. The developed structure showed robustness against the power systems load disturbances. Furthermore, novel online implementation of the adaptive learning solution is achieved in real-time utilizing critic neural networks.

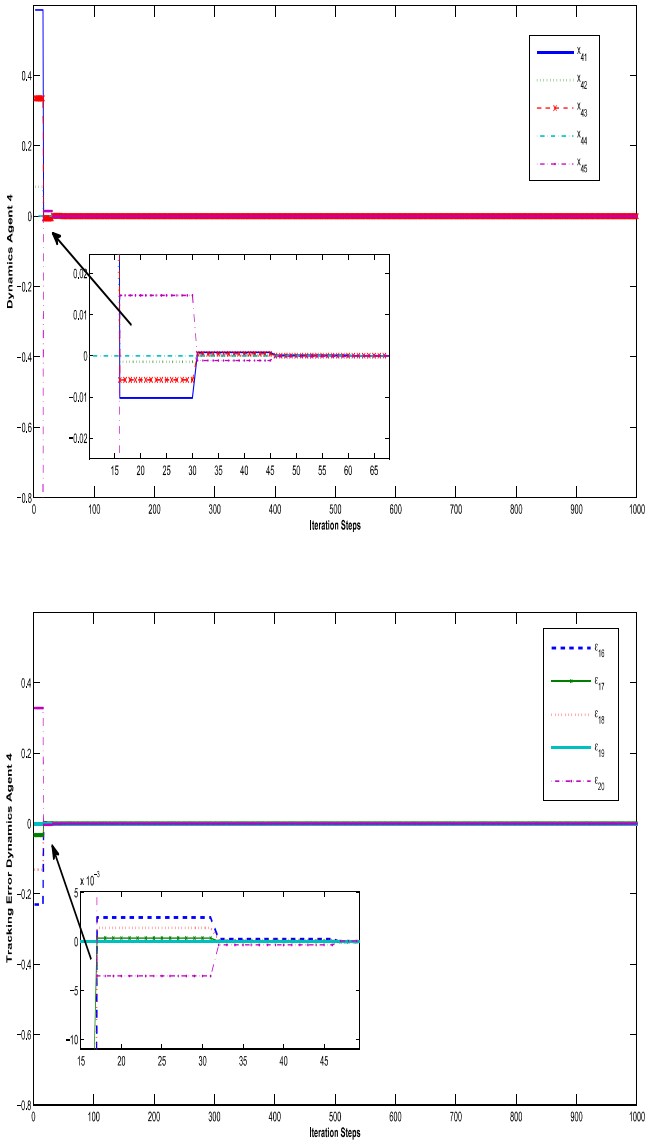

Figure 5.16: The Tracking error dynamics and error dynamics of agent-4.

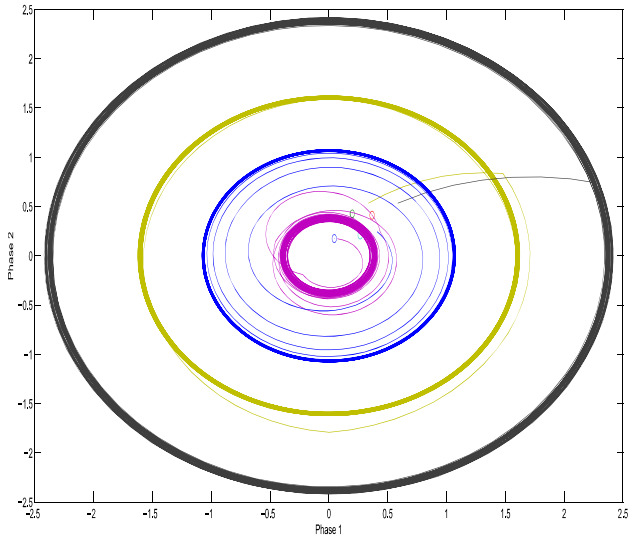

Figure 5.17: Phase plot of the agents.

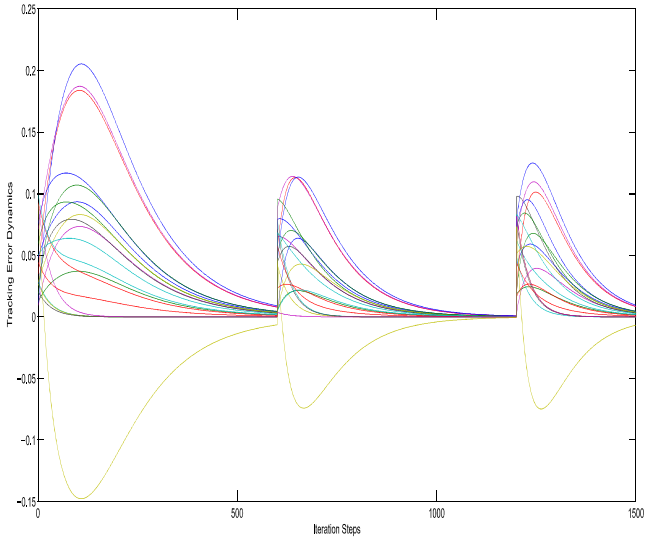

Figure 5.18: Tracking error dynamics in the presence of load variations.

CHAPTER 6

CONCLUSIONS AND FUTURE DIRECTIONS

In this dissertation, numerous designs of intelligent adaptive control and estimation with limited information exchanging over a networked control systems have been investigated to compensate communication constraints and load changes in islanded microgrid control networks. Overall, we also investigate some numerical computations and simulations, which demonstrate the theoretical results. The main contribution of this dissertation are as follows:

6.1 Main Contributions

- In the first part of the thesis, that is Chapters 1 and 2, we considered various control and intelligent algorithms with different operating conditions to handle load variation, communication constraints and fault event in microgrid control systems.

- In Chapter 3, we considered a quantized H_∞ estimator has been investigated over communication networks for distributed generation systems subject to random packet loss. A typically islanded MG comprises of three DGs supplying a local load. Attention is focused on the developing of networked controller to stabilize the microgrid system and to endure the influence of time delays, and packets dropout. Sufficient conditions for the existence of quantized H_∞ estimator based feedback controller are derived in terms of linear matrix inequalities (LMIs). The effectiveness of the proposed results has been shown through two numerical examples. The results demonstrated the effectiveness of the developed approach.

- Chapter 4, we investigated the implementation of $\mathfrak{L}_1$ adaptive control for distributed generation systems in microgrid. An $\mathfrak{L}_1$ adaptive controller is a robust controller which controls and ensures the network stability of DGs in the presence of model uncertainties and transmission time delays. The results demonstrate that the proposed $\mathfrak{L}_1$ adaptive control provides considerable enhancement in steady state error and transient performance of the DGs in terms of system uncertainties.

- Chapter 5, a novel online adaptive learning control scheme is developed for multi-agent DGs in islanded microgrids. This structure is based on a game theoretic approach. The microgrid units exchanged information based on a communication network. This technique solves the coupled Bellman equations of the graphical game in the presence of disturbances. This is done using local neighborhood information and partial knowledge about the units dynamics. A network of pho-

tovoltaic cells is considered. The dynamics of the open loop photovoltaic system is estimated using Kalman filtering. The developed structure showed robustness against the power systems load disturbances. Furthermore, a novel online implementation of the adaptive learning solution is achieved in real-time utilizing critic neural networks.

6.2 Future Directions

There are various interesting open problems on islanded microgrid control and networked control systems as outgrowths of the problems treated in this dissertation. We identify some of future directions:

- In the current work, we considered communication constraints to be uncorrelated in forms of an i.i.d. Bernoulli process. This can be extended to the correlated one with the stochastic model using Markov chain [27, 53].

- In chapter 3, we tackled the problem of communication constraints utilizing H_∞ estimator for standalone microgrid network. This may be extended to minmax control scheme or L_2–L_∞ robust control.

- In chapter 4, we implemented an $\mathfrak{L}_1$ adaptive controller for decentralized microgrid controller in terms of output feedback. In this work, we selected the low pass filter based on trial and error. To extend to work, someone can use an optimization algorithm to turn the low pass filter parameter. Also, we utilized a linear quadratic regulator to design the stabilized nominal model. Further extension can be considered by using a sliding mode controller, or reinforcement learning or an H_∞ controller instead. In addition, an $\mathfrak{L}_1$ adaptive can be integrated with model

predictive control scheme in the presence of communication constraints, in which the $\mathfrak{L}_1$ adaptive predictor can be utilized to estimate the unknown parameters in the problem model predictive control.

- In chapter 5, we introduce a novel distributed control scheme for islanded micro-grids in the presence of Gaussian disturbances. Furthermore, we applied Kalman filtering to estimate the states of the open loop system. Here, we can suggest to utilize a fast least square filtering or an extended Kalman filtering instead of Kalman filtering to handle non-Gaussian disturbance. Additionally, someone may consider a problem of disturbed multi-agent nonlinear systems utilizing output feedback control.

- The large area control systems can be extended to smart-grid control system. Smart grid is a hot and interesting topic, and it is definitely predicted to be the future solution of the electric generation and load sharing.

REFERENCES

[1] F. Blaabjerg, R. Teodorescu, M. Liserre, A. V. Timbus," Overview of control and grid synchronization for distributed power generation systems,"*Industrial Electronics, IEEE Trans.* vol.53, no.5, pp.1398–1409, 2006.

[2] M. S. Mahmoud, S. H. Azher, and M. A. Abido,"Modeling and control of microgrid: An overview." *Journal of the Franklin Institute,* vol. 351, no. 5, pp.2822–2859, 2014.

[3] M.J.H. Moghaddam, M. Bigdeli, and M.R. Miveh," A Review of the Primary-Control Techniques for the Islanded Microgrids", *Electrotechnical Review*, vol. 82, no. 4, pp.169–175, 2015.

[4] R. H. Lasseter, "Microgrids and distributed generation." *Journal of Energy Engineering,* vol. 133, no. 3, pp. 144–149, 2007.

[5] R. Bayindir, E. Hossain, E. Kabalci, and R. Perez," A comprehensive study on microgrid technology," *International Journal of Renewable Energy Research (IJRER)*, vol. 4, no.4 , pp.1094-1107, 2014.

[6] A. Bidram, A. Davoudi, FL. Lewis, JM. Guerrero," Distributed cooperative secondary control of microgrids using feedback linearization," *Power Systems, IEEE Trans.* vol. 28. no. 3. pp. 3462-70, 2013.

[7] A. M. Bouzid, J. M. Guerrero, A. Cheriti, M.Bouhamida, P.Sicard, and M. Benghanem," A survey on control of electric power distributed generation systems for microgrid applications,"*Renewable and Sustainable Energy Reviews,* vol. 44, pp. 751–766, 2015.

[8] R. Lasseter," Control of distributed resources," *Bulk Power Systems Dynamics and Control IV, Restructuring,* pp. 323–329, August 23, 1998.

[9] J. J. Justo, F. Mwasilu, J. Lee, J. and J.W. Jung," AC-microgrids versus DC-microgrids with distributed energy resources: A review," *Renewable and Sustainable Energy Reviews,* vol. 24, pp.387-405, 2013.

[10] T. Ackermann, G. Andersson, and L. Sder," Distributed generation: a definition," *Electric power systems research,* vol. 57, no. 3, pp.195–204, 2001.

[11] F. Katiraei, "Dynamic analysis and control of distributed energy resources in a micro-grid,"*University of Toronto,* 2005.

[12] M. Yazdanian, and A. Mehrizi-Sani, "Distributed control techniques in microgrids," *IEEE Trans. Smart Grid,* vol. 5(6), pp.2901–2909. 2014.

[13] X. Liu, W. Peng, and C. L. Poh, "A hybrid AC/DC microgrid and its coordination control,"*Smart Grid, IEEE Trans.*, vol 2.2, pp. 278–286, 2011.

[14] J. M. Guerrero, et al,"Advanced control architectures for intelligent microGrids, part I: decentralized and hierarchical control, "*IEEE Trans. Industrial Electronics,* vol. 60, no. 4, pp. 1254–1262, 2013.

[15] J. M. Guerrero, et al,"Advanced control architectures for intelligent microgridsPart II: Power quality, energy storage, and AC/DC microgrids."*Industrial Electronics, IEEE Trans.* vol. 60, no. 4, pp. 1263–1270, 2013.

[16] A. Bidram, " Distributed cooperative control of AC microgrids," *Doctor of Philosophy, The University of Texas at Arlington,* Aug. 2014.

[17] Q. Shafiee, T. Dragicevic, J. C. Vasquez, J.M. Guerrero,"Modeling, stability analysis and active stabilization of multiple DC-microgrid clusters,"*Energy Conference (ENERGYCON), 2014 IEEE International,* pp. 1284–1290, May 2014.

[18] M. C. Chandorkar, "Distributed uninterruptible power supply systems," *Ph.D. dissertation, Univ. Wisconsin-Madison, Madison, WI,* 1995.

[19] G. Venkataramanan and M. Illindala, "Small signal dynamics of inverter interfaced distributed generation in a chain-microgrid,"' *in Proc. IEEE PES Gen. Meeting,* pp. 1–6, 2007.

[20] H. R. Chamorro, and N. L. Daz, "Hierarchical power flow control in low voltage microgrids."*North American Power Symposium (NAPS), 2013. IEEE,* 2013.

[21] Q. Shafiee, et al,"Hierarchical control for multiple DC-microgrids clusters." *Multi-Conference on Systems, Signals and Devices (SSD), 2014 11th International. IEEE,* 2014.

[22] J. Shah, F. W. Bruce, and M. Ned, "Decentralized power flow control for a smart micro-grid," *Power and Energy Society General Meeting, 2011 IEEE.* 2011.

[23] J. Cardell, R. Tabors, "Operation and control in a competitive market: distributed generation in a restructured industry, in: The Energy Journal Special Issue: Dis-

tributed Resources: Toward a New Paradigm of the Electricity Business," *The International Association for Energy Economics, Clevland, Ohio, USA,* pp. 111 -135, 1998.

[24] D. Sharma, R. Bartels," Distributed electricity generation in competitive energy markets: a case study in Australia, in: The Energy Journal Special issue: Distributed Resources: Toward a New Paradigm of the Electricity Business, *The International Association for Energy Economics,* Clevland, Ohio, USA, pp. 17 -40, 1998.

[25] X. Fang, et al,"Smart grid– The new and improved power grid: A survey," *Communications Surveys and Tutorials, IEEE,* vol. 14, no. 4, pp. 944–980, 2012.

[26] A. S. Massoud,"Smart grid: Overview, issues and opportunities. advances and challenges in sensing, modeling, simulation, optimization and control," *European Journal of Control,* vol. 17, no.5, pp. 547–567, 2011.

[27] M. Amin, "Security challenges for the electricity infrastructure," *IEEE Computer Society* , vol. 35, no. 4, pp.8–10, 2002.

[28] Y. Yan, et al,"A survey on smart grid communication infrastructures: Motivations, requirements and challenges," *Communications Surveys and Tutorials, IEEE,* vol. 1, no. 1, pp. 5–20, 2013.

[29] W. Wang, Y. Xu, M. Khanna, "A survey on the communication architectures in smart grid", *Computer Networks,* vol. 55, pp. 3604–3629, 2011.

[30] J. A.Cardenas, et al,"A literature survey on Smart Grid distribution: an analytical approach," *Journal of Cleaner Productions,* vol. 65, pp. 202–216, 2014.

[31] K. S. Reddy, et al, "A review of Integration, Control, Communication and Metering (ICCM) of renewable energy based smart grid," *Renewable and Sustainable Energy Reviews* , vol. 38, pp. 180–192, 2014.

[32] J. Gao, Y. Xiao, J. Liu, W. Liang, and C. Chen,"A survey of communication/ networking in smart grids," *Future Generation Computer Systems,* vol. 28, no. 2, pp. 391–404, 2012.

[33] A. T. Sabbah, A. El-Mougy, and M. Ibnkahla, "A survey of networking challenges and routing protocols in smart grids," *Industrial Informatics, IEEE Trans.* vol. 10, no. 1, pp. 210–221, 2014.

[34] N. Saputro, K. Akkaya, and S. Uludag, "A survey of routing protocols for smart grid communications," *J. Computer Networks,* vol. 56, pp. 2742–2771, 2012.

[35] M. Hashmi, S. Hnninen, and K. Mki, "Developing Smart Grid Concepts, Architectures and Technological Demonstrations Worldwide-A Literature Survey," *International Review of Electrical Engineering,* vol. 8, no. 1, 2013.

[36] H. Yang, X. Lin, "A survey of the Smart Grid technologies: background, motivation and practical applications,"*Electrical Review* , 2011.

[37] V. C. Gungor, et al,"A survey on smart grid potential applications and communication requirements," *Industrial Informatics, IEEE Trans.* vol. 9.1 pp. 28–42, 2013.

[38] S. Pierluigi, "Demand response and smart grids—A survey," *Renewable and Sustainable Energy Reviews,* vol. 30, pp. 461–478, 2014.

[39] Y. Melike, et al,"Power line communication technologies for smart grid applications: A review of advances and challenges," *Computer Networks*, 2014.

[40] B. A. Akyol, et al,"A survey of wireless communications for the electric power system," *Prepared for the US Department of Energy,* 2010.

[41] H. E. Brown and S. Suryanarayanan,"A survey seeking a definition of a smart distribution system,"*North American Power Symposium09,* 1–7, 2009.

[42] S. Chen, S. Song, L. Li, and J. Shen,"Survey on smart grid technology (in Chinese)," *Power System Technology,* vol. 33, no. 8, pp. 1–7, April 2009.

[43] Y. Xiao, "Communication and Networking in Smart Grids," *CRC Press,* 2012.

[44] V. C. Gungor and F. C. Lambert, "A survey on communication networks for electric system automation," *Computer Networks,* vol. 50, no. 7, pp. 877–897, 2006.

[45] R. Hassan and G. Radman, "Survey on smart grid," *IEEE South east Con 2010,* pp. 210–213, 2010.

[46] S. Rohjansand, M. Uslar, R. Bleiker, J. Gonzalez, M. Specht, T. Suding, and T. Weidelt, "Survey of smart grid standardization studies and recommendations,"*IEEE Smart Grid Comm10,* pp. 583–587, 2010.

[47] E. D. Knapp and R. Samani, "Applied cyber security and the smart grid: implementing security controls into the modern power infrastructure," *Waltham, MA: Syngress,* 2013.

[48] R. N. Anderson, et al,"Adaptive stochastic control for the smart grid," *Proceedings of the IEEE* , vol. 50, n. 7, pp. 1098–1115, 2011.

[49] F. G. Gonzalez,"An intelligent controller for the smart grid," *Procedia Computer Science 16* , pp. 776–785, 2013.

[50] A. Chakrabortty, M. D. Ili,"Control and optimization methods for electric smart grids," *Power Electronics and Power Systems,Springer,* vol. 3, 2012.

[51] Y. Liang, et al,"Stochastic Control for Smart Grid Users with Flexible Demand," pp. 1–13, 2013.

[52] H. Gharavi and R. Ghafurian "smart grid: the electric energy system of the future",*Proceedings of the IEEE,* vol. 99, no. 6, pp. 917–921, 2011.

[53] V. C. Gungor, et al,"Smart grid technologies: communication technologies and standards," *Industrial informatics, IEEE trans.* vol. 7.4, pp. 529–539, 2011.

[54] J. Huang, W. Honggang, and Q. Yi,"Smart grid communications in challenging environments," *Smart Grid Communications (SmartGridComm), 2012 IEEE Third International Conference on. IEEE,* 2012.

[55] F. Salvadori, et al,"Smart Grid Infrastructure Using a Hybrid Network Architecture," pp. 1–10, 2013.

[56] E. Ancillotti, B. Raffaele and C. Marco "The role of communication systems in smart grids: Architectures, technical solutions and research challenges," *Computer Communications* vol. 36.17, pp. 1665–1697, 2013.

[57] . K. C. Sou, S. Henrik, and H. J. Karl, "On the exact solution to a smart grid cyber-security analysis problem," *Smart Grid, IEEE Trans.* vol. 4.2, pp. 856–865, 2013.

[58] A. A. Aquino-Lugo and T. J. Overbye,"Agent technologies for control application in the power grid,"*43th Hawaii International Conference on System Sciences,* pp. 1–10, 2010.

[59] T. M. Chen,"Survey of cyber security issues in smart grids,"*Cyber Security, Situation Management, and Impact Assessment II; and Visual Analytics for Homeland Defense and Security II (part of SPIE DSS 2010),* pp. 77090D–1–77090D-11, 2010.

[60] K. Clement, E. Haesen, and J. Driesen,"Coordinated charging of multiple plug-in hybrid electric vehicles in residential distribution grids,"*IEEE PSCE09,* pp. 1–7, 2009.

[61] F. M. Cleveland,"Cyber security issues for advanced metering infrastructure (AMI),"*IEEE Power and Energy Society General Meeting: Conversion and Delivery of Electrical Energy in the 21st Century,* pp. 1–5, 2008.

[62] K. Clement-Nyns, E. Haesen, and J. Driesen,"The impact of charging plug-in hybrid electric vehicles on a residential distribution grid,"*IEEE Trans. Power Systems,* vol. 25, no. 1, pp. 371–380, 2010.

[63] Q. Shafiee, J. M. Guerrero, and J. C. Vasquez, "Distributed secondary control for islanded microgrids—A novel approach," *Power Electronics, IEEE Trans.*, vol. 29.2, pp. 1018–1031, 2014.

[64] A. Kahrobaeian, and Y. A. R. I. Mohamed, "Networked-based hybrid distributed power sharing and control for islanded microgrid systems," *IEEE transaction on power electronics,* vol. 30, no. 2, pp. 603–618, 2015.

[65] S. Sivaranjani, and D. Thukaram,"A networked control systems perspective for wide-area monitoring control of smart power grids," *Innovative Smart Grid Technologies-Asia (ISGT Asia), 2013 IEEE. IEEE,* 2013.

[66] M. Savaghebi, A. Jalilian, J. C. Vasquez, and J. M. Guerrero, "Secondary control scheme for voltage unbalance compensation in an islanded droop-controlled microgrid," *IEEE Trans. Smart Grid,* vol. 3, no. 99, pp. 1–11, 2011.

[67] Y. Zhang and H. Ma, "Theoretical and experimental investigation of networked control for parallel operation of inverters," *IEEE Trans. Ind. Electron.,* vol. 59, no. 4, pp. 1961-1970, 2012.

[68] W. Qiao, "Integrated control of wind farms, facts devices and the power network using neural networks and adaptive critic designs," *Doctoral dissertation, Georgia Institute of Technology*, 2008.

[69] M.H. Khooban, and T. Niknam," A new intelligent online fuzzy tuning approach for multi-area load frequency control: Self Adaptive Modified Bat Algorithm," *International Journal of Electrical Power and Energy Systems,* vol. 71, pp.254–261, 2015.

[70] JG. Ziegler and NB. Nichols,"Optimum settings for automatic controllers," *ASME Trans,* vol. 64, pp. 759–68, 1942.

[71] L. Zhang, M. L. Crow, Z. Yang, and S. Chen, "The steady state characteristics of an SSSC integrated with energy storage," *in Proceedings of the 2001 IEEE Power Engineering Society Winter Meeting, Columbus, OH, USA,* vol. 3, pp. 1311-1316, Jan. 28-Feb. 1, 2001.

[72] W. Qiao, R.G. Harley, and G.K. Venayagamoorthy, " A fault-tolerant PQ decoupled control scheme for static synchronous series compensator," *In Power Engineering Society General Meeting, 2006. IEEE,* pp. 1–8, 2006.

[73] M. Jamil," Repetitive current control of two-level and interleaved three-phase PWM utility connected converters,"*doctor of philosophy. Faculty of Engineering and the Environment, University of Southampton,* 2012.

[74] H. S. Heo, G. H. Choe, H. S. Mok," Robust predictive current control of a grid-connected inverter with harmonics compensation," *in 28th annual IEEE applied power electronics conference and exposition (APEC),* pp. 2212–2217, 2013.

[75] Y. Bo, W. Jiande, L. Xiaodong, H. Xiangning,"An improved DSP-based control strategy with predictive current control and fuzzy voltage control for gridconnected voltage source inverters," *in. 34th annual conference on IEEE industrial electronics IECON*, pp. 2296–300,2008.

[76] B. Yohan, L. Kui-Jun, H. Dong-Seok," Improved predictive current control for grid connected inverter applications with parameter estimation," *in IEEE, industry applications society annual meeting, IAS,* pp. 1–6, 2009.

[77] B. Yohan, L. Kui-Jun, H. Dong-Seok," Improved predictive current control by parameter estimation in grid connected inverter applications,"*in IEEE Sixth inter-*

national power electronics and motion control conference, IPEMC 09, pp. 1535-38, 2009.

[78] MA. Rezaei, S. Farhangi, G. Farivar," An improved predictive current control method for grid-connected inverters," *in First power electronic and drive systems and technologies conference (PEDSTC),* pp. 445–9, 2010.

[79] JM. Espi, J. Castello, X. Garci, R. a-Gil, G. Garcera, et al," An adaptive robust predictive current control for three-phase grid-connected inverters,"*IEEE Trans. Indust. Electron,* vol. 58, pp. 3537-46, 2011.

[80] S. Alepuz, A. Gilabert, E. Arguelles, J. Bordonau, J. Peracaula," A new approach for the connection of a three-level inverter to the power grid for applications in solar energy conversion," *in. IEEE 28th annual conference of the IECON 02 [industrial electronics society],* vol. 4, pp. 3285–90, 2002.

[81] S. Alepuz, J. Bordonau, J. Peracaula,"A novel control approach of three-level VSIs using a LQR-based gain-scheduling technique,"*in IEEE 31st annual power electronics specialists conference, PESC 00.,* vol. 2, pp. 743–8, 2000.

[82] S. Alepuz, J. Salaet, A. Gilabert, J. Bordonau, J. Peracaula,"Control of three-level VSIs with a LQR-based gain-scheduling technique applied to DC-link neutral voltage and power regulation," *in. IEEE 28th annual conference of the industrial electronics society IECON,* vol. 02, pp. 914–9, 2002.

[83] S. Alepuz, J. Salaet, A. Gilabert, J. Bordonau, J. Peracaula, "Optimal regulator with integral action and gain-scheduling for the comprehensive control of three-level

NPC VSI," *in IEEE Thirty-fourth annual, power electronics specialist conference, PESC 03,* vol.3, pp. 1420-5, 2003.

[84] S. Alepuz, S. Busquets-Monge, J. Bordonau, J. Gago, D. Gonzalez, J. Balcells, "*Interfacing renewable energy sources to the utility grid using a three-level inverter," IEEE Trans Indust Electron,* vol. 53, pp. 1504—11, 2006.

[85] P. Peltoniemi, P. Nuutinen, M. Niemela, J. Pyrhonen,"LQG-based voltage control of the single-phase inverter for noisy environment," *in. 13th european conference on power electronics and applications. EPE,* vol. 09, pp. 1-10, 2009.

[86] T. Xu, and P. C. Taylor," Voltage control techniques for electrical distribution networks including distributed generation," *In Proc. of the 17th World Congress The International Federation of Automatic Control, Seoul,* pp. 11967-11971, 2008.

[87] SL. Jung, T. Ying-Yu,"Discrete sliding-mode control of a PWM inverter for sinusoidal output waveform synthesis with optimal sliding curve,"*IEEE Trans. Power Electron,* vol. 11, pp. 567-77, 1996.

[88] MA. Sofla, R. King," Control method for multi-microgrid systems in smart grid environmentStability, optimization and smart demand participation,"*in,IEEE PES innovative smart grid technologies (ISGT)*, pp. 1-5, 2012.

[89] L. Shang, D. Sun, and J. Hu,"Sliding-mode-based direct power control of grid connected voltage-sourced inverters under unbalanced network conditions,"*Power Electron IET,* vol. 4, pp. 570-9, 2011.

[90] H. Xiang, Y. Xu, X. Ruiliang, H. Lang, L. Tao, L. Yang," A fixed switching frequency integral resonant sliding mode controller for three-phase grid-connected

photovoltaic inverter with LCL-filter," *in. IEEE ECCE asia downunder (ECCE Asia),* pp. 793-798, 2013.

[91] H. Jiabing, H. Bin," Direct active and reactive power regulation of grid connected voltage source converters using sliding mode control approach," *in. IEEE international symposium on industrial electronics (ISIE),* pp. 3877-3882, 2010.

[92] X. Su, M. Han, J. M. Guerrero, and H. Sun," Microgrid stability controller based on adaptive robust total SMC," *Energies,* vol. 8, no. 3, pp.1784–1801, 2015.

[93] J. Mrida, L. Aguilar, and J. Dvila, "Analysis and synthesis of sliding mode control for large scale variable speed wind turbine for power optimization," *accepted in Renewable Energy,* 2014.

[94] M. Bouzid, et al,"Second-order sliding mode control for DFIG-based wind turbines fault ride-through capability enhancement," *ISA trans.* vol. 53, no.3, pp. 827-833, 2014.

[95] H. K. Khalil, and J. W. Grizzle," Nonlinear systems," *New Jersey: Prentice hall*, vol. 3, 1996.

[96] T. Hornik, QC. Zhong," H_∞ repetitive current controller for grid-connected inverters," *in . 35th annual conference of IEEE industrial electronics IECON 09,* pp.554-559,2009.

[97] T. Hornik, QC. Zhong," H_∞ current control strategy for the neutral point of a three-phase inverter," *in 50th IEEE conference on, decision and control and european control conference (CDC-ECC),* pp. 2994-2999, 2011.

[98] T. Hornik, QC. Zhong," A current-control strategy for voltage-source inverters in microgrids based on H_∞ and repetitive control,"*IEEE Trans Power Electron,* vol. 26, pp. 943-952, 2011.

[99] T. Hornik, C.Z. Qing," Voltage control of grid-connected inverters based on H_∞ and repetitive control,"*in. Eighth world congress on intelligent control and automation (WCICA),* PP. 270-275, 2010.

[100] T. Hornik, C.Z. Qing," H_∞ repetitive current-voltage control of inverters in micro-grids," *in IECON -Thirty-sixth annual conference on IEEE industrial electronics society,* PP. 3000-3005, 2010.

[101] C. Z. Qing, T. Hornik," Cascaded current - voltage control to improve the power quality for a grid-connected inverter with a local load, *IEEE Trans. Indust Electron,* vol. 60, pp. 1344-1355, 2013.

[102] S. Hara, Y. Yamamoto, T. Omata, M. Nakano, "Repetitive control system: a new type servo system for periodic exogenous signals," *IEEE Trans Automat Control,* vol. 33, pp. 659-668, 1988.

[103] A. M. Bouzid, P. Sicard, A. Cheriti, M. Bouhamida, and M. Benghanem," Structured H_∞ design method of PI controller for grid feeding connected voltage source inverter,"*In Control, Engineering and Information Technology (CEIT), 2015 3rd International Conference on,* pp. 1-6, 2015.

[104] A.M. Bouzid, M.S. Golsorkhi, P. Sicard, and A. Cheriti," H_∞ structured design of a cascaded voltage/current controller for electronically interfaced distributed

energy resources,"*In Ecological Vehicles and Renewable Energies (EVER), 2015 Tenth International Conference on,* pp. 1-6, 2015.

[105] W. Al-Saedi, et al,"Power flow control in grid-connected microgrid operation using particle swarm optimization under variable load conditions," *International Journal of Electrical Power and Energy Systems,* vol. 49, pp. 76-85, 2013.

[106] M. Sedighizadeh, et al,"Optimal placement of distributed generation using combination of PSO and clonal algorithm," *Power and Energy (PECon), 2010 IEEE International Conference on,* 2010.

[107] S. Devi, and M. Geethanjali,"Optimal location and sizing determination of Distributed Generation and DSTATCOM using Particle Swarm Optimization algorithm," *International Journal of Electrical Power and Energy Systems,* vol. 62, pp. 562-570, 2014.

[108] W. Al-Saedi, et al,"Stability analysis of an autonomous microgrid operation based on Particle Swarm Optimization," *Power System Technology (POWERCON), 2012 IEEE International Conference on. IEEE,* 2012.

[109] M.U. Siddiqui, "Multiphysics modeling of photovoltaic panels and arrays with auxiliary thermal collectors, "*MS Thesis, King Fahd University of Petroleum and Minerals,* 2011.

[110] C. Carrero, D. Ramrez, J. Rodrguez, C. a. Platero, "Accurate and fast convergence method for parameter estimation of PV generators based on three main points of the I-V curve,"*Renewable Energy,* vol. 36, pp. 2972–2977, 2011.

[111] J.Hu,"Advanced control in smart microgrids,"*Doctoral dissertation,* 2013.

[112] K. Ishaque, Z. Salam, H. Taheri, A. Shamsudin, "A critical evaluation of EA computational methods for Photovoltaic cell parameter extraction based on two diode model," *Solar Energy,* vol. 58, pp. 1768–1779, 2011.

[113] R. Storn, K. Price," Differential Evolution: A simple Efficient Adaptive Scheme for Global Optimization over Continuous Spaces," *ICSI, USA. Tech. Rep. TR95-TR012,*1995.

[114] R. Storn, K. Price,"Differential evolution, a simple and efficient heuristic strategy for global optimization over continuous spaces," *Journal of Global Optimization,* vol. 11, pp. 341–359, 1997.

[115] S. Das, A. Abraham, A. Konar," Particle swarm optimization and differential evolution algorithms: technical analysis," *Applications and Hybridization Perspectives, available from site:www.softcomputing.net/aciis.pdf.*

[116] W. A. B. Al-Saedi, "Optimal control of power quality in microgrids using particle optimisation," 2013.

[117] A. Y. Saber, and K. V. Ganesh, "Smart micro-grid optimization with controllable loads using particle swarm optimization," *Power and Energy Society General Meeting (PES), 2013 IEEE,* 2013.

[118] D. A. V. Veldhuizen and G. B. Lamont, "Multiobjective evolutionary algorithms: Analyzing the state-of-the-art," *Evol. Comput.,* vol. 8, no. 2, pp. 125–147, 2000.

[119] K. Deb, A. Pratab, S. Agarwal, and T. Meyarivan, "A fast and elitist multiobjective genetic algorithm: NSGA-II," *IEEE Trans. Evol. Comput.,* vol. 6, no. 2, pp. 182–197, Apr 2002.

[120] C. A. C. Coello, G. T. Pulido, and M. S. Lechuga, "Handling multiple objectives with particle swarm optimization," *IEEE Trans. Evol. Comput.,* vol. 8, no. 3, pp. 256-279, Jun 2004.

[121] A. Raghami, M. T. Ameli, and M. Hamzeh," Online droop tuning of a multi-DG microgrid using cuckoo search algorithm," *Electric Power Components and Systems,* vol. 43, no. 14, pp.1583-1595, 2015.

[122] Bevrani, H., Habibi, F., Babahajyani, P., Watanabe, M., and Mitani, Y., "Intelligent frequency control in an AC microgrid: Online PSO-based fuzzy tuning approach," IEEE Trans . Smart G r i d, Vol. 3, pp. 1935-1944, 2012.

[123] R. Godoy, J. Pinto, C. Canesin, E. Coelho, and M. Pinto, "Differential-evolution-based optimization of the dynamic response for parallel operation of inverters with no controller interconnection," *IEEE Trans. I nd. Electron.,* vol. 59, pp. 2859-2866, 2012.

[124] W. Al-Saedi, S. Lachowicz, D. Habibi, and O. Bass, "Power quality enhancement in autonomous microgrid operation using particle swarm optimization," *Int. J. Electr. Power Energy Syst.,* vol. 42, pp. 139-149, 2012.

[125] S. Mishra, G. Mallesham, and A. Jha, "Design of controller and communication for frequency regulation of a smart microgrid,"*IET Renewabl e Power Gener.,* vol. 6, pp. 248-258, 2011.

[126] M. Hassan, and M. Abido, "Optimal design of microgrids in autonomous and grid-connected modes using particle swarm optimization," *IEEE Trans. Power Electron.,* vol. 26, pp. 755-769, 2011.

[127] A.A. Hamad, and E.F. El-Saadany,"Multi-agent supervisory control for optimal economic dispatch in DC microgrids," *Sustainable Cities and Society,* 2016.

[128] N. Augustine, S. Suresh, P. Moghe, and K. Sheikh, ,"Economic dispatch for a microgrid considering renewable energy cost functions," *In Innovative Smart Grid Technologies (ISGT), 2012 IEEE PES,* pp. 1-7, 2012.

[129] C. Chen, S. Duan, T. Cai, B. Liu, and G. Hu," Smart energy management system for optimal microgrid economic operation," *Renewable Power Generation, IET,* vol. 5, no. 3, pp.258-267, 2011.

[130] L. Xiaoping, D. Ming, H. Jianghong, H. Pingping, and P. Yali, " Dynamic economic dispatch for microgrids including battery energy storage," *In Power Electronics for Distributed Generation Systems (PEDG), 2010 2nd IEEE International Symposium on*, pp. 914-917, 2010.

[131] M. Mahmoodi, P. Shamsi, and B. Fahimi,"Economic dispatch of a hybrid microgrid with distributed energy storage," *Smart Grid, IEEE Trans.* vol. 6(6), pp.2607-2614, 2015.

[132] S. Wang, X. Fan, L. Han, and L. Ge,"Improved interval optimization method based on differential evolution for microgrid economic dispatch," *Electric Power Components and Systems,* vol. 43(16), pp.1882-1890, 2015.

[133] G. Venter, and S. S. Jaroslaw ,"Particle swarm optimization," *AIAA journal,* vol. 41.8, pp. 1583-1589, 2003.

[134] D. B. F. Van, and P. E. Andries,"A study of particle swarm optimization particle trajectories," *Information sciences,* vol. 176.8, pp. 937-971, 2006.

[135] M. J. Sanjari, and G. B. Gharehpetian, "Game-theoretic approach to cooperative control of distributed engergy resources in islanded microgrid considering voltage and frequency stability," *Neural Comput. A ppl.,* vol. 25, No. 2, pp. 343-351, 2013.

[136] I. Y. Chung, W. Liu, D. A. Cartes, and S.I. Moon, "Control parameter optimization for multiple distributed generators in a microgrid using particle swarm optimization," *Eur. Trans. Electr. Power,* vol. 21, pp. 1200-1216, 2011.

[137] M. Hassan, and M. Abdio, "Optimal autonomous control of an inverter based microgrid using particle swarm optimization," *IEEE International Symposium on Industrial Electronics, pp. 2247-2252, Bari, Italy,* pp. 4-7, July 2010.

[138] I.Y. Chung, W. Liu, D. A. Cartes, and K. Schoder, "Control parameter optimization for a microgrid system using particle swarm optimization," *IEEE International Conference on Sustainable Energ y Technologies (ICSET),* pp. 837-842, 2008.

[139] S.K. Pandey, S.R. Mohanty, and N. Kishor,"A literature survey on load-frequency control for conventional and distribution generation power systems,"*Renewable and Sustainable Energy Reviews,* vol. 25, pp.318-334, 2013.

[140] CS. Chang, W. Fu, "Area load frequency control using fuzzy gain scheduling of PI controllers," *Electric Power System Research,* vol. 42, pp. 144-52, 1997.

[141] M. Denna, G. Mauri, AM. Zanaboni,"Learning fuzzy rules with Tabu Search-an application to control," *IEEE Transactions on Fuzzy Systems,* vol. 7(2), pp. 295-318, 1999.

[142] SP. Ghoshal, "Multi area frequency and tie line power flow control with fuzzy logic based integral gain scheduling," *Journal of Institute of Engineers,* vol. 84, pp. 135-141, 2003.

[143] CAM. Ertugrul, Load frequency control in two area power system," *Teknoloji,* vol. 7(2), pp. 197-203, 2004.

[144] CAM. Ertugrul, I. Kocaarslan,"Load frequency control in two area power systems using fuzzy logic controller,"*Energy Conversion and Management,* vol. 46, pp. 233-43, 2005.

[145] CF. Juang, CF. Lu," Power system load frequency control by genetic fuzzy gain scheduling controller," *Journal of the Chinese Institute of Engineer,* vol. 28(6), pp. 1013-8, 2005.

[146] S. Pothiya, I. Ngmroo, S. Runggeratigul, P. Tantaswadi," Design of optimal fuzzy logic based PI controller using multiple Tabu Search algorithm for load frequency control," *International Journal of Control, Automation and Systems,* vol. 4(2), pp. 155-64, 2006.

[147] SK. Sinha, RN. Patel, R. Prashad,"Application of GA and PSO tuned fuzzy controller for AGC of three area thermal-thermal-hydro power system,"*International Journal of Computer Theory and Engineering,* vol. 2(2), 2010.

[148] T. Kerdphol, Y. Qudaih, M. Watanabe, and Y. Mitani,"RBF neural network-based online intelligent management of a battery energy storage system for stand-alone microgrids," *Energy, Sustainability and Society,* vol. 6(1), p.1-16, 2016.

[149] S. A. Mirjalili, S. Z. M. Hashim, and H. M. Sardroudi, "Training feedforward neural networks using hybrid particle swarm optimization and gravitational search algorithm," *Applied Mathematics and Computation 218.22,* pp. 11125-11137, 2012.

[150] Y.A.R.I. Mohamed, and E.F., El-Saadany,"Adaptive discrete-time grid-voltage sensorless interfacing scheme for grid-connected DG-inverters based on neural-network identification and deadbeat current regulation," *Power Electronics, IEEE Trans.* vol. 23(1), pp.308-321, 2008.

[151] C.J. Huang," Neural network based microgrid voltage control," *Master Thesis, University of Wisconsin-Milwaukee,* 2013.

[152] F. L. Jaramillo, G. Kenne, and F. L. Lamnabhi,"A novel online training neural network-based algorithm for wind speed estimation and adaptive control of PMSG wind turbine system for maximum power extraction," *Renewable Energy,* vol. 86, pp.38-48, 2016.

[153] S. Janpong,K. L. Areerak, and K. N. Areerak, "A literature survey of neural network applications for shunt active power filters," *J. World Acad. Sci., Eng. Technol,* vol. 60, pp.392-398, 2011.

[154] R. Latha, and J. Kanakaraj,"Adaptive neuro-fuzzy interface system-particle swarm optimization based stability maintenance of power system networks," *American Journal of Applied Sciences,* vol. 10.8 pp. 770–779, 2013.

[155] D. Petkovi, C. arko, and N. Vlastimir,"Adaptive neuro-fuzzy approach for wind turbine power coefficient estimation," *Renewable and Sustainable Energy Reviews,* vol. 28, pp. 191-195., 2013

[156] H. Li, J. B. Song, and Q. Zeng, "Adaptive modulation in networked control systems with application in smart grids," *IEEE communications letters,* vol. 17, no. 7, pp. 1305–1309, 2013.

[157] H. Huang, and Y. C. Chi, "Adaptive neuro-fuzzy controller for static VAR compensator to damp out wind energy conversion system oscillation," *Generation, Transmission and Distribution, IET,* vol. 7.2 , pp. 200-207, 2013.

[158] M.S. Mahmoud, and S.A. Hussain,"Adaptive PI secondary control for smart autonomous microgrid systems," *International Journal of Adaptive Control and Signal Processing,* vol. 29, no. 11, pp.1442–1458, 2015.

[159] X.X. Yin, Y. G. Lin, W. Li, H. W. Liu, and Y. J. Gu,"Adaptive sliding mode back-stepping pitch angle control of a variable-displacement pump controlled pitch system for wind turbines,"*ISA trans.,* vol. 58, pp.629-634, 2015.

[160] Y. Liu, Q. Zhang, C. Wang, and N. Wang,"A control strategy for microgrid inverters based on adaptive three-order sliding mode and optimized droop controls," *Electric Power Systems Research,* 117, pp.192-201, 2014.

[161] S. Rahme, and N. Meskin,"Adaptive sliding mode observer for sensor fault diagnosis of an industrial gas turbine," *Control Engineering Practice,* vol. 38, pp.57-74, 2015.

[162] Z. Chen, A. Luo, H. Wang, Y. Chen, M. Li, and Y. Huang, " Adaptive sliding-mode voltage control for inverter operating in islanded mode in microgrid," *International Journal of Electrical Power and Energy Systems,* vol. 66, pp.133-143, 2015.

[163] H. El Fadil, F. Giri, and J. M. Guerrero, "Adaptive sliding mode control of interleaved parallel boost converter for fuel cell energy generation system," *Mathematics and Computers in Simulation,* vol. 91, pp.193-210, 2013.

[164] M.I. Abouheaf, M. S. Mahmoud, and S. A. Hussain,"A novel approach to control of autonomous microgrid systems,"*International Journal of Energy Engineering,* vol. 5, no. 5, pp. 125-136, 2015.

[165] F.D. Li, M. Wu, Y. He, and X. Chen,"Optimal control in microgrid using multi-agent reinforcement learning, "*ISA trans.,* vol. 51(6), pp.743-751, 2012.

[166] E. Kuznetsova, Elizaveta, et al,"Reinforcement learning for microgrid energy management,"*Energy,* vol. 59, pp. 133-146, 2013.

[167] Y. Tao, and W. G. Zhen,"A reinforcement learning approach to power system stabilizer,"*Power and Energy Society General Meeting, 2009. PES'09. IEEE. IEEE,* 2009.

[168] M . S. Branicky, S. M. Phillips, W. Zhang, "Stability of networked control systems: explicit analysis of delay",*Proc. American Control Conference, Chicago,* vol. 4, pp. 2352–2357, 2000.

[169] Q. Shafiee, C. Stefanovic, T. Dragicevic, P. Popovski, J. C. Vasquez, and J. M. Guerrero, "Robust networked control scheme for distributed secondary control of islanded microgrids,"*Industrial Electronics, IEEE Trans.,* vol. 61, no. 10, pp. 5363–5374, 2014.

[170] A. K. Singh, R. Singh, and B. C. Pal, "Stability analysis of networked control in smart grids," *IEEE Trans. Smart Grid*, vol. 6, no. 1, pp. 1–10, 2015.

[171] G. Walsh, H. Ye, and L. Bushnell, "Stability analysis of networked control systems," *IEEE Trans. Control Systems Technology*, vol. 10, no. 3, pp. 438–446, 2002.

[172] W. Zhang, M. S. Branicky, and S. M. Phillips, "Stability of networked control systems," *IEEE Control Systems Magazine*, vol. 21, no. 1, pp. 84–99, 2001.

[173] D. Wu, J. Wu and S. Chen, "Separation principle for networked control systems with multiple-packet transmission," *IET Control Theory and Application,* vol. 5, no. 3, pp. 507–513, 2010.

[174] L. Schenato,"To zero or to hold control inputs with lossy links," *IEEE Trans. Automatic and Control,* vol. 54, no. 5, pp.1093–1099, 2009.

[175] M. S. Mahmoud, N. M. Alyazidi, A.W.A. Saif, "Dynamic feedback control over unreliable communication channels," *Journal off Mathematical Control and Information Advance Access IMI,* vol. 31, pp. 195–216, 2014.

[176] M.S. Mahmoud, N. M. Alyazidi, and A.W.A. Saif, "LQG control design over lossy communication links," *International Journal of Systems Science,* vol. 45, no. 11, pp.2309–2326. 2014.

[177] M. S. Mahmoud, M. S. U. Rahman, and F. M. AL-Sunni, "Networked control of microgrid system of systems," *International Journal of Systems Science* vol. 47, no. 11, pp.2607–2619, 2016.

[178] M. Babazadeh and H. Karimi," Robust decentralized control for islanded operation of a microgrid", *Proc. IEEE Power and Energy Society General Meeting*, pp. 1-8, 2011.

[179] M. S. Mahmoud, "Estimator design for networked control systems with nonstationary packet dropouts," *Journal of Mathematical Control and Information Advance Access IMI,* vol. 30, no. 3, pp. 395–405, 2013.

[180] M. S. Mahmoud, S.Z. Selim, M. H. Baig, "New results on networked control systems with non-stationary packet dropouts," *IET Control Theory and Applications,* vol. 6, no. 15, pp.2442–2452, 2012.

[181] L. Sheng, Z. Wang, W. Wang, and F. E. Alsaadi, "Output-feedback control for nonlinear stochastic systems with successive packet dropouts and uniform quantization effects," *IEEE Trans. Systems, Man, and Cybernetics: Systems*, pp. 1–11, 2016.

[182] J. Dong, and G.H. Yang, "H_∞ filtering for continuous-time TS fuzzy systems with partly immeasurable premise variables," *IEEE Trans. Systems, Man, and Cybernetics: Systems*, pp. 1–10, 2016.

[183] D. Zhang, H. Song, and L. Yu, "Robust fuzzy-model-based filtering for nonlinear cyber-physical systems with multiple stochastic incomplete measurements," *IEEE Trans. Systems, Man, and Cybernetics: Systems*, pp. 1–13, 2016.

[184] M.S. Mahmoud, and M.S.U. Rahman, "Event triggered of microgrid control with communication and control optimization," *Journal of the Franklin Institute,* vol. 353, no. 16, pp.4114–4132, 2016.

[185] I. Patrao, E. Figueres, G. Garcer, and R. Gonzlez-Medina,"Microgrid architectures for low voltage distributed generation," *Renewable and Sustainable Energy Reviews,* no. 43, pp. 415-424, 2015.

[186] J. A. McDowall, "Opportunities for electricity storage in distributed generation and renewables," *in Proc. IEEE/PES Transmission and Distribution Conference and Exposition,* pp. 1165-1168, 2001.

[187] J.C. Vasquez Quintero," Decentralized control techniques applied to electric power distributed generation in microgrids," *Universitat Politcnica de Catalunya, Doctoral thesis,* 2009.

[188] D.E. Olivares, A. Mehrizi-Sani, A.H. Etemadi, C.A. Canizares, R. Iravani, M. Kazerani, A.H. Hajimiragha, O. Gomis-Bellmunt, M. Saeedifard, R. Palma-Behnke, and G.A. Jimenez-Estevez,"Trends in microgrid control," Smart Grid, IEEE Trans. vol. 5, no. 4, pp.1905-1919, 2014.

[189] J. A. P. Lopes, C. L. Moreira, and A. G. Madureira, "Defining control strategies for microgrids islanded operation," *IEEE Trans. Power Syst.*, vol. 21, no. 2, pp. 916-924, May 2006.

[190] S. N. Bhaskara, M. Rasheduzzaman and B. H. Chowdhury, "Laboratory-based microgrid setup for validating frequency and voltage control in islanded and grid-connected modes", *IEEE Green Technologies Conference,* pp. 1–6, 2012.

[191] W. Xuehua, R. Xinbo, B. Chenlei, P. Donghua, and X. Lin, "Design of the PI regulator and feedback coefficient of capacitor current for grid-connected inverter with an LCL filter in discrete-time domain," *in Energy Conversion Congress and Exposition (ECCE), 2012 IEEE* , pp. 1657–1662, 2012.

[192] P. Peltoniemi, P. Nuutinen, M. Niemela, and J. Pyrhonen, "LQG-based voltage control of the single-phase inverter for noisy environment," *in Power Electronics*

and Applications, 2009. EPE '09. 13th European Conference on, pp. 1–10,2009.

[193] D. Shi, R. Sharma, and Y. Yanzhu, "Adaptive control of distributed generation for microgrid islanding," *Innovative Smart Grid Technologies Europe (ISGT EUROPE), 2013 4th IEEE/PES. IEEE,* 2013.

[194] T. Hornik and Q. C. Zhong, "H_∞ repetitive current controller for grid-connected inverters," *in Industrial Electronics. IECON '09. 35th Annual Conference of IEEE,* pp. 554-559, 2009.

[195] Y. Baek, K. J. Lee, and D. S. Hyun , "Improved predictive current control for grid connected inverter applications with parameter estimation,"*in Industry Applications Society Annual Meeting, 2009. IAS 2009. IEEE,* pp. 1–6, 2009.

[196] S. Liu, X. Wang, and P. X. Liu,"Impact of communication delays on secondary frequency control in an islanded microgrid," *Industrial Electronics, IEEE Trans.* vol. 62, no. 4, pp. 2021–2031, 2015.

[197] J. W. Simpson-Porco, F. Drfler, and F. Bullo," Synchronization and power sharing for droop-controlled inverters in islanded microgrids," *Automatica,* vol. 49, no. 9, pp.2603-2611, 2013.

[198] S. Riverso, F. Sarzo, and G. Ferrari-Trecate," Plug-and-play voltage and frequency control of islanded microgrids with meshed topology," *Smart Grid, IEEE Trans.* vol. 6, no. 3, pp.1176-1184, 2015.

[199] H. Karimi, E. J. Davison, and R. Iravani,"Multivariable servomechanism controller for autonomous operation of a distributed generation unit: Design and per-

formance evaluation," *Power Systems, IEEE Trans.* vol. 25, no. 2, pp.853-865, 2010.

[200] G.C. Konstantopoulos, Q.C. Zhong, B. Ren, M. and Krstic," Bounded droop controller for parallel operation of inverters," *Automatica,* vol. 53, pp.320-328, 2015.

[201] J. Schiffer, R. Ortega, A. Astolfi, J. Raisch, T.and Sezi," Conditions for stability of droop-controlled inverter-based microgrids," *Automatica,* vol. 50, no. 10, pp.2457-2469, 2014.

[202] F. Dorfler, and F. Bullo," Synchronization and transient stability in power networks and nonuniform Kuramoto oscillators," *SIAM Journal on Control and Optimization,* vol. 50, no. 3, pp.1616-1642, 2012.

[203] I. Petros, B. Fidan, "Adaptive control tutorial," *SIAM Society for Industrial and Applied Mathematics,* 2006.

[204] B. Khorramdel, and M. Raoofat,"Optimal stochastic reactive power scheduling in a microgrid considering voltage droop scheme of DGs and uncertainty of wind farms," *Energy* , vol. 45, no. 1, pp. 994-1006, 2012.

[205] J. B. Pomet, and L. Praly,"Adaptive nonlinear regulation: estimation from the Lyapunov equation,"*Automatic Control, IEEE Transactions on* vol. 37, no. 6, pp. 729–740, 1992.

[206] N. Hovakimyan and C. Cao"L_1 adaptive control theory: guaranteed robustness with fast adaptation,"*Advances in Design and Control*, 2010.

[207] C. Cao, and N. Hovakimyan,"L_1 adaptive output feedback controller to systems of unknown dimension," *American Control Conference, 2007. ACC'07. IEEE,* pp. 1191–1196, 2007.

[208] H. Sun, N. Hovakimyan, and T. Basar,"L_1 adaptive controller for systems with input quantization," *American Control Conference (ACC), 2010. IEEE,* pp. 253–258, 2010.

[209] H. Sun," L_1 adaptive control with quantization and delay, " *Doctoral dissertation, University of Illinois at Urbana-Champaign*, 2014.

[210] X. Wang, and N. Hovakimyan,"Performance prediction in uncertain networked control systems using L_1 -adaptation-based distributed event-triggering," *In 49th IEEE Conference on Decision and Control (CDC)*, pp. 7570–7575, 2010.

[211] A. Bryson," Optimal control-1950 to 1985,"*IEEE Control Systems,* vol. 16, no. 3, pp. 26–33, 1996.

[212] M. Abouheaf, F. Lewis, K. Vamvoudakis, S. Haesaert, and R. Babuska," Multi-agent discrete-time graphical games and reinforcement learning solutions,"*Automatica,* vol. 50, no. 12, pp. 3038–3053, 2014.

[213] M. Abouheaf, F. Lewis, S. Haesaert, R. Babuska, and K. Vamvoudakis," Multi-agent discrete-time graphical games: interactive Nash equilibrium and value iteration solution,"*In American Control Conference (ACC), IEEE 2013,* pp. 4189-4195, 2013.

[214] L. Busoniu, R. Babuska, and B. De Schutter," A comprehensive survey of multi-agent reinforcement learning," *IEEE Trans. Systems, Man, and Cybernetics, Part C: Applications and Reviews,* vol. 38, no. , pp.156-172, 2008.

[215] F. Lewis, D. Vrabie, V. Syrmos," Optimal Control,"*3rd edition, John Wiley: New York,* 2012.

[216] S. Lall and M. West," Discrete variational Hamiltonian mechanics," *Jrnl of Phys A: Math and Gen,* vol. 39, no.19 pp. 5509-5519, 2006.

[217] R. Beard and V. Stepanyan," Synchronization of information in distributed multiple vehicle coordination control," *Proc. IEEE Conf Dec and Conf., Maui, HI,* pp. 2029–2034, 2003.

[218] W. Ren, R. Beard, and E. Atkins," A survey of consensus problems in multi-agent coordination," *Proc. Amr. Con. Conf,* pp. 1859–1864, 2005.

[219] J. Tsitsiklis," Problems in Decentralized Decision Making and Computation," *Ph.D. dissertation. Dept. Elect. Eng. and Comput. Sci., MIT, Cambridge, MA,* 1984.

[220] Z. Li, Z. Duan, G. Chen, and L. Huang, "Consensus of multi-agent systems and synchronization of complex networks: A unified viewpoint," IEEE Trans Circ. and Syst, vol. 57, no. 1, pp. 213–224, 2010.

[221] F. A., Yaghmaie, F. L., Lewis, and R. Su, "Output Regulation of Heterogeneous Linear Multi-Agent Systems with Differential Graphical Game", 2015.

[222] Q., Wang, H., Gao, F., Alsaadi, and T. Hayat, " An overview of consensus problems in constrained multi-agent coordination," Systems Science and Control Engineering: An Open Access Journal," vol. 2 no. 1. pp. 275-284, 2014.

[223] Q. Wei, and D. Liu," Adaptive dynamic programming for optimal tracking control of unknown nonlinear systems with application to coal gasification," *IEEE Trans. Automation Science and Engineering,* vol. 11, no. 4, pp. 1020-1036, 2014.

[224] A. Al-Tamimi, F. L. Lewis and M. Abu-Khalaf, "Discrete-time nonlinear HJB solution using approximate dynamic programming: convergence proof", *IEEE Trans. Systems, Man and Cybernetics,* vol. 38(4), pp. 943-949, 2008.

[225] P. J. Werbos, "Approximate dynamic programming for real-time control and neural modelling", *Handbook of intelligent control Neural, fuzzy, and adaptive approaches,* pp. 493-525, 1992.

[226] T. Dierks and S. Jagannathan, "Online optimal control of affine nonlinear discrete-time systems with unknown internal dynamics by using time based policy update,"*IEEE Trans. Neurl Netw. Learn. Syst.,* vol. 23, no. 7, pp. 1118–1129, Jul. 2012.

[227] Y. Jiang and Z. P. Jiang, "Robust adaptive dynamic programming with an application to power systems,"*IEEE Trans. Neural Netw. Learn. Syst.,* vol. 24, no. 7, pp. 1150–1156, Jul. 2013.

[228] Z. Ni, H. He, and J. Wen, "Adaptive learning in tracking control based on the dual critic network design," *IEEE Trans. Neural Netw. Learn. Syst.,* vol. 24, no. 6, pp. 913–928, Jun. 2013.

[229] D. Wang, D. Liu, D. Zhao, Y. Huang, and D. Zhang, "A neural network-based iterative GDHP approach for solving a class of nonlinear optimal control problems with control constraints,"*Neural Comput. Appl.,* vol. 22, no. 2, pp. 219–227, Feb. 2013.

[230] H. Xu, S. Jagannathan, and F. L. Lewis, "Stochastic optimal control of unknown linear networked control system in the presence of random delays and packet losses,"*Automatica,* vol. 48, no. 6, pp. 1017–1030, Jun. 2012.

[231] R. Sutton and A. Barto," Reinforcement Learning: An Introduction," *MIT Press: Cambridge, Massachusetts,* 1998.

[232] J. Morimoto, G. Zeglin, and C. Atkeson, "Minmax Differential Dynamic Programming: Application to a Biped Walking Robot," *IEEE Int Conf on Intel Rob and Sys, Las Vegas, USA,* 2003.

[233] F. L. Lewis and D. Vrabie, "Reinforcement learning and adaptive dynamic programming for feedback control," *IEEE Circuits Syst. Mag.,* vol. 9, no. 3, pp. 32–50, Jul. 2009.

[234] F. L. Lewis, D. Vrabie, and K. G. Vamvoudakis, "Reinforcement learning and feedback control: Using natural decision methods to design optimal adaptive controllers," *IEEE Control Syst.,* vol. 32, no. 6, pp. 76–105, Dec. 2012.

[235] R. Gopalakrishnan, J. Marden, and A. Wierman, "An architectural view of game theoretic control," *ACM SIGMETRICS Perform Eval Rev,* vol. 38, no. 3, pp. 31–36, 2011.

[236] K. Vamvoudakis, F. Lewis, and G. Hudas, "Multi-agent differential graphical games: online adaptive learning solution for synchronization with optimality," *Automatica,* vol. 48, no. 8 pp. 1598–1611, 2012.

[237] D. P. Bertsekas and J. N. Tsitsiklis, "Neuro-dynamic programming", *Athena Scientific, Massachusetts,* 1996.

[238] D. P. Bertsekas and J. N. Tsitsiklis, "Neuro-dynamic programming: an overview",*IEEE Proc. Decision and Control,* vol. 1, pp. 560–564, 1989.

[239] X. Li, X. Wang, and G. Chen, "Pinning a complex dynamical network to its equilibrium," *IEEE Trans. Circuits Syst.,* vol. 51, no. 10, pp. 2074–2087, 2004.

[240] W. Ren, K. Moore, and Y. Chen, "High-order and model reference consensus algorithms in cooperative control of multivehicle systems," *J. Dynam. Syst., Meas., Control,* vol. 129, no. 5, pp. 678–688, 2007.

[241] P. J. Werbos, "Neural networks for control and system identification," *IEEE Proc. CDC, 1989,* pp. 260-265, 1989.

[242] D. Vrabie, D., et al, "Adaptive optimal control for continuous-time linear systems based on policy iteration", *Automatica,* vol. 45 (2), pp. 477-484, 2009.

[243] K. G. Vamvoudakis and F. L. Lewis, "Online actor-critic algorithm to solve the continuous-time infinite horizon optimal control problem", *Automatica,* vol. 46 (5), pp. 878–888, 2010.

[244] H. Modares, F. L. Lewis, and M. B. Naghibi-Sistani, "Adaptive optimal control of unknown constrained-input systems using policy iteration and neural networks,"*IEEE Trans. Neural Netw. Learn. Syst.,* Aug. 2013.

[245] B. B. Doll, K. G. Bath, N. D. Daw, and M.J. Frank," Variability in dopamine genes dissociates model-based and model-free reinforcement learning," *The Journal of Neuroscience,* vol. 36, no. 4, pp. 1211–1222, 2016.

[246] A. Al-Tamimi, F.L. Lewis, and M. Abu-Khalaf, "Model-free Q-learning designs for linear discrete-time zero-sum games with application to H_∞ control," *Automatica,* vol. 43, no. 3, pp. 473–481, 2007.

[247] J. M. D. Muoz, and E. F. Camacho, "Distributed model predictive control based on a cooperative game," *Opt. Control Appl. Methods,* vol. 32, no. 2, pp. 153–176, 2010.

[248] S. Skogestad, M. Morari, and J. C. Doyle, "Robust control of ill-conditioned plants: High-purity distillation," *IEEE Trans. Autom. Control,* vol. 33, no. 12, pp. 1092–1105, Dec. 1988.

[249] K. Menighed and J. Yam, "Distributed state estimation and model predictive control: Application to fault tolerant control," *Proc. IEEE Int. Conf. Control Autom.,* pp. 936–941. 2009

[250] J. M. Pak, C.K. Ahn, P. Shi, and M.T. Lim, "Self-recovering extended Kalman filtering algorithm based on model-based diagnosis and resetting using an assisting FIR filter," *Neurocomputing,* vol. 173, pp. 645–658. 2016.

[251] M.G. Villalva, J.R. Gazoli, and Filho, E. Ruppert, "Comprehensive approach to modeling and simulation of photovoltaic arrays," *IEEE Trans. power electronics,* vol. 24(5), pp.1198–1208, 2009.

Vitae

- Name: Nezar Mohammed AbdulRab Al-Yazidi
- Nationality: Yemen
- Date of Birth: 06/09/1980
- Emails: *nalyazidi@kfupm.edu.sa; nmz2009@gmail.com*
- Permenant Address: Yemen, Hadramout, AlHami.